C.P. No. 896

C.P. No. 896

MINISTRY OF AVIATION

AERONAUTICAL RESEARCH COUNCIL

CURRENT PAPERS

Crack Propagation in Fatigue. Some Experiments with DTD 5070A Aluminium Alloy Sheet

by

D. P. Rooke, N. J. F. Gunn, J. T. Ballett and F. J. Bradshaw

LONDON: HER MAJESTY'S STATIONERY OFFICE

1967

PRICE 16s 0d NET

U.D.C. No. 539.219.2 : 620.178.3 : 669.715 : 621-415

C.P. No. 896
October 1964

CRACK PROPAGATION IN FATIGUE. SOME EXPERIMENTS WITH DTD 5070A ALUMINIUM ALLOY SHEET

by

D. P. Rooke, N. J. F. Gunn,
J. T. Ballett, F. J. Bradshaw

SUMMARY

Fatigue crack propagation rates have been measured in 16 swg sheets of this aluminium alloy using stress levels of 8800 ±7200 psi, 4400 ±3600 psi and 13,200 ±10,800 psi. The scatters in crack initiation times and crack rates were determined. Varying the panel length/width ratio from 1.2 to 4.75 was found to have little effect on crack rate. A major study was made on the effect of varying panel width from 3" to 20" and various parameters were used to correlate all the results at all the three stress levels. The stress intensity factor, K, was preferred on grounds of simplicity and effectiveness, though all parameters failed to correlate stress differences adequately. Crack propagation rates in two directions at right-angles were little different. Buckling, which occurred in a few of the large panels, had little effect on crack rate. Tests on panels at the same stresses as above, with the cladding removed, showed negligible change in crack rate. Macroscopic fracture mode transitions were correlated with K values and crack rates.

Replaces R.A.E. Tech. Report No. 64025 - A.R.C. 27350

CONTENTS

		Page
1	INTRODUCTION	5
2	EXPERIMENTAL METHODS	7
	2.1 Material	7
	2.2 Test specimens	8
	2.3 End grips	8
	2.4 Testing machines	9
	2.5 Load measurement	9
	2.6 Crack measurement	10
	2.7 $1\frac{1}{4}$" wide specimens	10
3	ANALYSIS OF RESULTS	10
	3.1 Curve fitting	10
	3.2 Correlation by the stress intensity factor	13
	3.3 Other correlation methods	15
	3.3.1 The critical strain method	15
	3.3.2 The stress concentration method	19
4	SCATTER IN INCUBATION TIME AND CRACK PROPAGATION RATE	21
	4.1 Results	21
	4.2 Discussion	23
5	EFFECT OF PANEL LENGTH/WIDTH RATIO	24
	5.1 Results	24
	5.2 Discussion	24
6	EFFECT OF PANEL SIZE AND STRESS AMPLITUDE: CORRELATION ANALYSIS	25
	6.1 Results	25
	6.2 Discussion	25
7	EFFECT OF DIRECTION OF CRACK PROPAGATION	26
8	EFFECT OF BUCKLING	27
9	EFFECT OF REMOVING THE CLADDING	28
	9.1 Results	28
	9.2 Discussion	28
10	FRACTURE MODE TRANSITIONS	29
	10.1 Results	29
	10.2 Discussion	30
11	GENERAL DISCUSSION AND CONCLUSIONS	31
Table 1	Scatter in cycles to crack initiation and cycles to failure	34
Table 2	Results of crack propagation tests on 3" wide panels for scatter investigation. Alternating stress 3600 psi	35
Table 3	Results of crack propagation tests on 3" wide panels for scatter investigation. Alternating stress 7200 psi	36

CONTENTS (CONTD)

		Page
Table 4	Results of crack propagation tests on 3" wide panels for scatter investigation. Alternating stress 10,800 psi	37
Table 5	Results of crack propagation tests on 10" wide panels for scatter investigation. Alternating stress 3600 psi	39
Table 6	Effect of d/b on the crack propagation rate of 3" wide panels - d/b = 1·2	40
Table 7	Effect of d/b on the crack propagation rate of 3" wide panels - d/b = 1·6	41
Table 8	Effect of d/b on the crack propagation rate of 3" wide panels - d/b = 2·1	42
Table 9	Effect of d/b on the crack propagation rate of 3" wide panels - d/b = 3·2	43
Table 10	Effect of d/b on the crack propagation rate of 3" wide panels - d/b = 4·75	44
Table 11	Effect of panel width on the crack propagation rate - width $1\frac{1}{4}$"	45
Table 12	Effect of panel width on the crack propagation rate - width 3"	46
Table 13	Effect of panel width on the crack propagation rate - width $4\frac{1}{2}$"	47
Table 14	Effect of panel width on the crack propagation rate - width $6\frac{1}{2}$"	48
Table 15	Effect of panel width on the crack propagation rate - width 10"	49
Table 16	Effect of panel width on the crack propagation rate - width 20"	50
Table 17	Effect of rolling direction on the crack propagation rate of $4\frac{1}{2}$" wide panels (σ_a = 3600 psi)	51
Table 18	Effect of rolling direction on the crack propagation rate of $4\frac{1}{2}$" wide panels (σ_a = 7200 psi)	52
Table 19	Effect of "anti-buckling"bars on the crack propagation of 20" wide panels	53
Table 20	Crack propagation rates of 3" wide panels with cladding removed	54
Symbols		55
References		57
Illustrations		Figures 1-29
Detachable abstract cards		-

1 INTRODUCTION

In recent years there has been an increasing need for data on the rates of fatigue crack propagation in alloys of interest to the aircraft industry. In general, alloys showing slow crack propagation characteristics have an obvious advantage over those with faster rates as there is a greater likelihood of detecting the fatigue crack before failure. There is also the hope that in the future quantitative crack propagation data can be used as a basis for more accurate methods of estimating the safe life of a structure. Though the fatigue failure of metals in thick sections and sheets are both serious problems most measurements have been made on materials in sheet form as these are the easiest to study and analyse. It is relatively simple to compare the crack propagation characteristics of two different alloys in any one laboratory using one test procedure; but there is a need to be able to compare tests in different laboratories on different sizes of specimen at different stress levels and frequencies. Only a limited amount of work has been done in this country on the problem and this Report describes some experiments carried out to see how far variation of a few of the simplest factors can be rationalised to a common basis.

Rectangular sheets of one type of clad aluminium alloy of one thickness were subjected to fatigue in fluctuating tension at stress levels of 13,200 ±10,800 psi or 8800 ±7200 psi or 4400 ±3600 psi (gross area). The stress ratio, R, (ratio of minimum to maximum stress) was thus 0·1 for all levels and corresponds roughly to the type of fatigue stressing of components in an aircraft fuselage. The simpler stress ratio of R ~ 0 was not attainable owing to machine limitations. A slot was made in the centre of each sheet or panel to provide a starting notch from which two fatigue cracks could run. The crack lengths and number of fatigue cycles were measured at suitable intervals.

The following points were investigated:-

(1) The scatter in the time to initiate a crack and in the rates of crack propagation.

It is necessary to know the scatter in crack rate in order to know whether the factor being studied is having a significant effect, particularly when one comes to compare the different methods of crack analysis (see (3)). Further, it is often stated that the scatter in the total fatigue life of a test piece is due mainly to the variability in the early stages, i.e. in the time to initiate the crack, rather than in the crack propagation phase. Accordingly measurements were made of the time taken before the fatigue crack started to run.

(2) The effect of altering the ratio of panel length to width.

Given a certain width of test piece it is obviously economical to choose the shortest length possible; the fatigue machine may also limit the length of the test piece which can be used. However with the grips holding the panel too close to the running crack, the stress distribution round the crack will be affected by the restraint of the rigid grips. The restraint will depend on the detailed grip design but here we have investigated the effects on crack propagation of reducing the ratio (length/width) of the panel from 4·75 to 1·2. The length here is that part of the panel free of the grips. This work was done on material 3" wide. A commonly accepted minimum ratio is 2·0 but we have found no detailed report which justifies this value.

(3) The effect of panel size and stress amplitude.

It is well known that the scaling factors for crack propagation rates in specimens of different sizes under different stresses are not simple. Much work has been done with various approaches, empirical and otherwise, to correlate results. Schijve, Brock and Rijk[1] and Barrois[2] have made valuable summaries of some of the methods. Most work has been done in the U.S.A. and the two most common methods used are those based on the "stress intensity factor"[3,4] and those using developments of the original Neuber stress concentration ideas[5,6,7]. Our aim here has not been to test one method to its limits but rather to test, at three stress levels, a range of commonly used specimen sizes to see how well the various methods correlate the results. It is hoped in later work to explore these limitations further.

Sheets of widths 3" to 20" were tested at the two lower stress levels and the results, together with those from specimens $1\frac{1}{4}$" wide used for another investigation[8] have been analysed. Results from all the experiments are presented mainly in terms of "stress intensities" since, to anticipate, this parameter turned out to be the most convenient. This investigation occupied the major part of the time.

(4) The effect of direction of crack propagation.

In all the other tests the direction of crack propagation was at right angles to the rolling direction of the sheet i.e. the tensile load axis and rolling directions were the same. In aircraft structures this is not always the case and so a limited study was made of crack propagation in panels $4\frac{1}{2}$" wide with the tensile axis at right angles to the rolling direction.

(5) The effect of buckling.

When the ratio of total crack length to sheet thickness becomes too great, there will be a tendency for the sheet to buckle. It can be shown that there are compressive stresses in the sheet on either side of the central crack approximately equal to the applied tensile stress and that above a critical stress level buckling should occur[9]. If this happens the stresses round the crack tip will be affected thereby altering the crack propagation rate. Attempts were made to measure the amount of buckling and the effect on crack rate of stiffening the larger sheets with bars to prevent buckling.

(6) The effect of removing the cladding.

It is usually held that cladding a material has a detrimental effect on the fatigue life. There is little data on its effect on crack propagation. Panels 3" wide were prepared and tested as normal except that the cladding on both sides was machined off before test. This left a somewhat thinner sheet consisting of core material only.

(7) The mode of fatigue failure in sheet specimens is known to depend on the material, thickness, alternating and mean stress levels, environment etc. We have related the macroscopic characteristics of the fracture surfaces with the stress situation.

2 EXPERIMENTAL METHODS

2.1 Material

The material used for all the tests was a 16 swg clad artificially aged aluminium alloy (Al-2·5Cu-1·5Mg-1·2Ni-1·0Fe) to Specification DTD 5070A. The cladding consisted of 5% of the thickness on each side of Al +0.8 -1.2% Zn. All test specimens including those for tensile testing were cut from 6' × 3' sheets. With the exception of those used to determine the effects of rolling direction, specimens were cut so that their longitudinal axes were parallel to the direction of final rolling. Sheets from two casts of material were used, the mechanical properties of each were measured and are tabulated below.

R.A.E. designation	Cast No.	H.T. batch No.	0·2% ps tsi	T.S. tsi	Elong % on 2"
A	26 WG1	19B26	26·0 ±0·1	27·7 ±0·1	6·5
B longitudinal	4WK1	8838/2	26·7 ±0·4	28·0 ±0·4	6·4
B transverse		25A11	25·7 ±0·1	27·8 ±0·1	5·5

Cast analyses supplied by the manufacturer were as follows:

Content % / Cast	Cu	Mg	Ni	Fe	Mn	Si	Zn	Ti	Al
26 WG1	2·55	1·54	1·12	1·06	0·025	0·20	0·04	0·08	remainder
4 WK1	2·52	1·63	1·14	1·03	0·03	0·20	0·10	0·07	remainder

Figures 1 and 2 show how the sheets from the two casts of material were cut for test specimen selection. Two sheets of cast A material and twelve sheets of cast B material were used. The test specimens were selected from random positions in any one sheet and it will be seen that in both the scatter and the effect of panel width experiments specimens were selected from both material casts. It will also be seen that only one 20" panel could be cut from any one sheet.

2.2 Test specimens

To determine the tensile properties of the material, test pieces as illustrated in Fig.3 were used, with a Lamb extensometer used for determining the proof stresses. The crack propagation panels used are illustrated in Fig.3; all had central slots $\frac{1}{2}$" in length except for the 3" wide panels which had slots 1/3" long. The slots were made with a jewellers saw and were about 0·008" wide. For the study of scatter the slots in the 3" panels were terminated in holes 0·020" diameter so as to provide more reproducible crack starting conditions. The free lengths of the panels were always equal to twice panel width ($d/b = 2$), except for those used in the experiments to determine the effect of d/b. The surfaces of the panels were not prepared in any way except for an initial thorough degreasing. In the case of the experiments to determine the effect of cladding removal however, both sides of the panels were scalped on a milling machine using a flycutter to remove about 0·004" per side. This amount is a little more than the 5% of cladding per side and so ensured that only core material remained. A central transverse band approximately 2" wide was then polished on each side of each panel to remove all machining marks that might influence crack growth. A final degreasing was then carried out.

2.3 End grips

Three sizes of end grips were made and used for testing the range of panel widths 3" - 20". They were identical in design, only overall dimensions and bolt sizes varying. These have been described in Ref.10. Except for the 10" and 20" wide panels, gripping was effected by friction only and this was done by transverse

serrations machined into the inner faces of the grips. The 10" and 20" panels were secured into the end grips by a row of bolts.

To examine the effect of buckling on the crack propagation rates in 20" wide panels, restraints were fitted across some of the panels to minimise the tendency to buckle as the crack progressed. These "anti-buckle" bars were channel section members made of aluminium alloy with a length of $\frac{1}{2}$" thick sponge rubber cemented to the lower faces of the "channel" and having a hole at each end. Four of these bars were bolted together in pairs 'sandwiching' the panel on each side of the crack line.

2.4 Testing machines

All crack propagation tests were made in Schenck Pulsators except for the tests made on the $1\frac{1}{4}$" panels. Panels up to $6\frac{1}{2}$" in width were tested in a 6 ton pulsator operating at approximately 2500 cpm. This machine has been described in Ref.10. For the 10" and 20" wide panel, a 20 ton long bed Schenck Pulsator was necessary to accommodate the overall dimensions of these large panels. The operating speed of this machine was slightly lower than the 6 ton machine, namely 2000 cpm.

During the period of the tests the average temperature was 20°C and the relative humidity 50%.

2.5 Load measurement

All tests were at one of three stress levels, calculated on gross area, - fluctuating peak tension stresses of 24,000 psi, 16,000 psi and 8000 psi. These stresses were made up such that the ratio of minimum stress to maximum stress per cycle was 0·1.

The loads (mean and alternating) were measured by a Peekel strain bridge (reading in microstrain) and a cathode ray oscilloscope from strain gauges cemented onto the ring dynamometer of the pulsator. On the 6 ton machine the calibration of the dynamometer was 10·8 lb/microstrain and on the 20 ton pulsator 14·9 lb/microstrain. The calibrations were arrived at by inserting a specially calibrated strain gauged load cell into the machines and loading statically. The strain in the dynamometer could be read to an accuracy of ±2 microstrain, which for the 6 ton pulsator corresponds to ±22 lb load or on a 3" wide panel ±117 psi. This corresponds to ±3.2%, ±1·6% and ±1·1% of the three alternating stresses ±3600, ±7200 and ±10,800 psi used. Load measurement in the 20 ton machine was made in the same way. With this machine ±2 microstrain was equivalent to ±29.8 lb load or on a 10" wide panel ±46·5 psi. This

corresponds to ±1·3% and ±0·6% of the two alternating stresses ±3600 and ±7200 psi used.

2.6 Crack measurement

After final cleaning of the panels, scales were photo printed onto them so that when photographed at selected intervals the crack progression could be measured (see Ref.10 for details). The scale was graduated in inches with 1/20" sub-divisions as shown in Fig.3. The stress cycle counter was mounted near the panel so that it and the panel were photographed together by a Shackman Auto-camera Mk.III. Twenty to thirty photographs were taken during each test with an exposure time of 1/200 second. Using a field of view appropriate for the panel size, this technique resulted in the following estimated errors in crack tip position:-

3" wide panels ±0·013"
$4\frac{1}{2}$" and $6\frac{1}{2}$" wide panels ±0·025"
10" and 20" wide panels ±0·035"

2.7 $1\frac{1}{4}$" wide specimens

These were from one sheet of cast A, but being the subject of a separate research were tested slightly differently. The free length was 3·025" and the grips were in the form of sideplates bolted onto the specimen ends. The total length of the central slot was 0·16", the width 0·008". A Haigh fatigue machine was used, operating at 6000 cpm. Loads were measured by a load cell with strain gauges in series with the specimen. The accuracy of load measurement was ~ ±2%. The progress of the fatigue cracks was measured by means of a microscope with a calibrated eyepiece relative to reference lines lightly scribed on the specimen. The estimated accuracy of this method was ~ ±0·004" (for further details see Ref.8).

3 ANALYSIS OF RESULTS

3.1 Curve fitting

The experimental measurements resulted in values of crack half-length, a, at given numbers of cycles, N. Curves of a vs.N could then be drawn and tangents (da/dN) obtained at various values of a. This method is lengthy, laborious and inaccurate if done by hand; the data was therefore processed with the aid of a Mercury computer. A curve was fitted using a least squares procedure and the slopes (da/dN) obtained from the equation of the fitted curve. It was convenient to choose certain fixed values of da/dN and to obtain the corresponding values a and N using an iteration procedure.

Several authors have suggested functional relationships between a and N; three were chosen and tested to see which best fitted the experimental points. None of the suggested relationships was capable of giving a good fit over the whole range. However the fit was much improved by using a polynomial expansion based on the functional forms.

The first relationship tried was that suggested by both Frost and Dugdale[11] and Liu[12] They said that the rate of growth was given by

$$\frac{da}{dN} = C_1 a \quad , \tag{1}$$

where C_1 is a constant. This equation was only expected to be valid for crack lengths much less than the width of the sheet (2b). Integrating (1) we have

$$\ell n \left(\frac{a}{a_o}\right) = C_1 (N - N_o) \quad , \tag{2}$$

where a_o is the value of the crack half-length at $N = N_o$, i.e., the crack half-length is of the form

$$a = A\, e^{C_1 N} \quad , \tag{3}$$

where

$$A = a_o\, e^{-C_1 N_o} \quad . \tag{4}$$

It was not possible to choose values of A and C_1 to obtain a good fit over the whole experimental range since in the smaller test panels $a \leq 0.8b$. A much better fit was obtained with a third-order polynomial, i.e.,

$$a = \sum_{j=0}^{3} A_j X^j \quad , \tag{5}$$

where $X^j = [e^{C_1 N}]^j$ and A_j are constant coefficients. The A_j's were determined by the least squares fit procedure.

Another suggested relationship tried was that due to Head[13], which states that the crack growth rate is given by

$$\frac{da}{dN} = C_2 a^{3/2} \quad , \tag{6}$$

where C_2 is a constant. Integrating (6) gives

$$a^{-\frac{1}{2}} = A + BN \tag{7}$$

where A and B are constants. To obtain a good fit over the whole range it was found necessary to expand (7) as a polynomial in N, i.e.,

$$a^{-\frac{1}{2}} = \sum_{j=0}^{3} A_j N^j \quad , \tag{8}$$

where the A_j's are again determined by the least squares procedure.

The third functional relationship tried was that due to Weibull[14], who suggested that the rate of crack growth was given by

$$\frac{da}{dN} = C_3 \sigma_n^s \quad , \tag{9}$$

where C_3 is a constant, σ_n is the average stress on the net section and s is a constant exponent. σ_n may be written as a function of the crack half-length, i.e.,

$$\sigma_n = \frac{\sigma_p}{1 - a/b} \quad , \tag{10}$$

where σ_p is the constant nominal stress on the gross section. Substituting for σ_n in (9) and integrating we obtain

$$N = A + BY \quad , \tag{11}$$

where A and B are constants and

$$Y = (1 - a/b)^{s+1} \quad . \tag{12}$$

Again a much better fit with the experimental points could be obtained with a polynomial expansion, i.e.,

$$N = \sum_{j=0}^{3} A_j Y^j \quad ; \qquad (13)$$

the A_j's were determined as before.

Curves of a vs. N were computed using the three equations (5), (8) and (13) for several specimens and then compared with the experimental points. It was found that equation (13) gave the best fit over the whole range of experimental values and was therefore used to analyse the data obtained in all the tests.

3.2 Correlation by the stress intensity factor

It has been suggested by Paris[3] that the stress intensity factor, K, is a good parameter for correlating crack growth rates, under various conditions, due to cyclic loading. This follows from the work of Irwin[15] who showed that the elastic stresses at a point near the root of a crack always have the following form:

$$\sigma = \frac{K}{\sqrt{2r}} f(\theta) \quad , \qquad (14)$$

where r and θ are polar co-ordinates, with the origin at the crack tip, of the point under consideration. This expression is only valid if $r \ll a$ (the crack half-length). $f(\theta)$ is a function of θ only, determined by which component of stress is being considered. K is a function of crack length and loading. For a crack in an infinite plate with a uniform stress (σ_∞) applied perpendicular to the crack, at infinity, we have

$$K = \sigma_\infty \sqrt{a} \quad . \qquad (15)$$

The exact stress analysis cannot be done analytically for a sheet of finite width. However, Irwin[16] has suggested that a good approximation to K may be obtained for a finite sheet of width 2b by taking the expression obtained by Westergaard[17] for a series of co-linear cracks of length 2a separated by a distance 2b. Thus, we have,

$$K = \sigma_\infty \sqrt{a}\, \alpha_W = \sigma_\infty \sqrt{a} \left[\frac{2b}{\pi a} \tan \frac{\pi a}{2b} \right]^{\frac{1}{2}} , \qquad (16)$$

where α_W is the Westergaard finite width correction used in the present work.

Another type of finite sheet correction (α_G) has been used by Irwin and Kies[18,19]. They calculate the correction to the strain energy release rate ($= \pi K^2/E$, where E is Young's Modulus) due to the finiteness of the sheet. The correction is based on the work of Greenspan[20] who calculated the effect of various shaped perforations on the axial rigidity of a sheet finite in both directions. Within the approximations of the method the correction to K turns out to be independent of the length of the sheet[19], and is given by

$$K = \sigma_\infty \sqrt{a}\, \alpha_G = \sigma_\infty \sqrt{a}\, \frac{\sqrt{4 + 2\left(\frac{a}{b}\right)^4}}{2 - \left(\frac{a}{b}\right)^2 - \left(\frac{a}{b}\right)^4} . \qquad (17)$$

In order to compare α_W and α_G a plot of α_G/α_W vs. a/b is shown in Fig.4.

There is a third finite width correction (α_D) due to Dixon[21], it is an empirical correction based on results using photoelastic techniques. It is given by

$$\alpha_D = \left[1 - \left(\frac{a}{b}\right)^2 \right]^{-\frac{1}{2}} . \qquad (18)$$

A comparison of α_D and α_W is also shown in Fig.4.

The elastic solutions predict infinite stresses at the crack tip, (see (14)); in reality plastic flow occurs thereby ensuring that the stresses are everywhere finite. In order to make allowance for the effect of plasticity it has been suggested[22] that the crack should be regarded as being increased in length by an amount equal to the radius of the plastic zone (r_o) ahead of the crack tip; thus

$$K = \sigma_\infty \left[\frac{2b}{\pi} \tan \frac{\pi a_1}{2b} \right]^{\frac{1}{2}} , \qquad (19)$$

where $a_1 = a + r_o$. Graphs of $R_o(r_o/a)$ vs. $Z(\sigma/\sigma_Y)$ have been plotted by Rooke[23] for various yield criteria, using these graphs and the finite sheet relation

$$Z = \frac{\sigma_\infty}{\sigma_Y}\left[\frac{2b}{\pi a}\tan\frac{\pi a}{2b}\right]^{\frac{1}{2}} , \qquad (20)$$

we can obtain R_o as a function of a/b for the experiments under consideration. Fig.5 shows a plot of R_o vs. a/b for the three stress levels.

The effect of this correction on K can be estimated from (16); differentiating with respect to a, we have,

$$\frac{dK}{da} = \frac{\sigma_\infty}{2}\left[\frac{2b}{\pi}\tan\frac{\pi a}{2b}\right]^{-\frac{1}{2}}\sec^2\frac{\pi a}{2b} . \qquad (21)$$

Re-arranging (21) we obtain

$$\frac{dK}{K} = \frac{\pi a}{2b\sin\left(\frac{\pi a}{b}\right)} \times \frac{da}{a} . \qquad (22)$$

Since $r_o \ll a$ we may replace da/a by R_o in (22), giving

$$\frac{dK}{K} = \frac{\pi a\, R_o}{2b\sin\left(\frac{\pi a}{b}\right)} . \qquad (23)$$

Since R_o is known as a function of a/b (see Fig.4) we have the correction to K due to plasticity as a function of a/b; this is plotted in Fig.6.

The values of K were calculated, using (19) as part of the computer curve-fitting programme, with σ_∞ equal to the amplitude of the alternating stress (σ_a). In this respect it differs from that in Ref.4 where K is based on the peak stress.

3.3 Other correlation methods

3.3.1 The critical strain method

It has been suggested[24] that there exists a critical strain (ε_o) which characterizes the rate of crack propagation. This strain is given by

$$\varepsilon_c = k\,\varepsilon_n \tag{24}$$

where ε_n is the average strain corresponding to the peak stress on the net section of the cracked sheet and k is a strain concentration factor. The explicit form of k is

$$k = \left[1 + 2\sqrt{\frac{a}{\rho'}}\right]\sqrt{\frac{1 - a/b}{1 + a/b}} \quad , \tag{25}$$

where ρ' is a material constant. The form of k is based on the theoretical stress concentration in notched sheets, due to Neuber[25], modified for finiteness of plate in the manner of Dixon[21]. It is assumed[24] that k is given by (25) if $a/b \leq 0{\cdot}4$; for larger values of a/b k is a constant at the value it has when $a/b = 0{\cdot}4$.

Since the strain (ε_n) may be expressed in terms of stress thus,

$$\varepsilon_n = \frac{\sigma_n}{E_s} = \frac{\sigma_p}{\left(1 - \frac{a}{b}\right)E_s} \quad , \tag{26}$$

where σ_n ard σ_p are respectively the average net and gross stresses and E_s is the secant modulus, we have

$$\varepsilon_c = \frac{\sigma_p}{E_s}\left[1 + 2\sqrt{\frac{a}{\rho'}}\right]\alpha_D \quad . \tag{27}$$

Since

$$K = \sigma_a \sqrt{a}\,\alpha_W = \frac{(1 - R)}{2}\,\sigma_p \sqrt{a}\,\alpha_W \quad , \tag{28}$$

where R is the ratio of minimum stress applied to maximum stress, i.e.,

$$R = \frac{\sigma_p - 2\,\sigma_a}{\sigma_p} \quad , \tag{29}$$

we have, for $a/b \leq 0{\cdot}4$,

$$\frac{\varepsilon_c}{K} = \frac{2}{E_s(1 - R)} \left[\frac{1}{\sqrt{a}} + \frac{2}{\sqrt{\rho'}} \right] \frac{a_D}{a_W} \quad . \tag{30}$$

The above can be simplified by putting

$$a_D = a_W \quad ; \tag{31}$$

this is valid to within 1·5% for $a/b \leq 0{\cdot}4$ (see Fig.4). Thus

$$\frac{\varepsilon_c}{K} = \frac{2}{E_s(1 - R)} \left[\frac{1}{\sqrt{a}} + \frac{2}{\sqrt{\rho'}} \right] \quad . \tag{32}$$

It is convenient to define the dimensionless parameter β by

$$\beta = \frac{E(1 - R)\sqrt{\rho'}\,\varepsilon_c}{4K} = \frac{E}{E_s} \left[1 + \frac{1}{2}\sqrt{\frac{\rho'}{a}} \right] \quad . \tag{33}$$

In the present series of experiments the average net-section stresses were below the elastic limit, for $a/b \leq 0{\cdot}4$, in all but the tests at the highest stress level. However the change in modulus is less than 1%, therefore we put

$$E_s = E \quad , \tag{34}$$

and therefore,

$$\beta = 1 + \frac{1}{2}\sqrt{\frac{\rho'}{a}} \quad . \tag{35}$$

For $a/b > 0{\cdot}4$, k is a constant which is given by

$$k = 0{\cdot}655 \left(1 + 1{\cdot}26\sqrt{\frac{b}{\rho'}} \right) \quad . \tag{36}$$

Thus

$$\varepsilon_c = 0{\cdot}655\left(1 + 1{\cdot}26\sqrt{\frac{b}{\rho'}}\right)\left(1 - \frac{a}{b}\right)^{-1}\frac{\sigma_p}{E_s} \tag{37}$$

and

$$\frac{\varepsilon_c}{K} = \frac{1{\cdot}31\left(1{\cdot}26 + \sqrt{\frac{\rho'}{b}}\right)}{\alpha_w E_s \sqrt{\rho'}\left(1 - R\right)}\left[\sqrt{\frac{a}{b}}\left(1 - \frac{a}{b}\right)\right]^{-1} . \tag{38}$$

Therefore the parameter β is given by

$$\beta = \frac{0{\cdot}328\, E}{\alpha_w E_s}\left(1{\cdot}26 + \sqrt{\frac{\rho'}{b}}\right)\left[\sqrt{\frac{a}{b}}\left(1 - \frac{a}{b}\right)\right]^{-1} . \tag{39}$$

Since, for large cracks, the average stress on the net section exceeds the elastic limit, it follows that

$$E_s \neq E . \tag{40}$$

In order to obtain E_s an empirical stress-strain law suggested in the Royal Aeronautical Society Data Sheets[26] was used; the law states that

$$\frac{\sigma}{E_s} = \frac{\sigma}{E} + \varepsilon_o\left(\frac{\sigma}{\sigma_o}\right)^m , \tag{41}$$

where ε_o and σ_o are co-ordinates of a reference point on the stress-strain curve. The exponent (m) is given by

$$m = \log\left[1 + \frac{\varepsilon_o - \varepsilon'_o}{\varepsilon'_o}\right] \Big/ \log\left[1 + \frac{\sigma_o - \sigma'_o}{\sigma'_o}\right] , \tag{42}$$

where $(\varepsilon'_o, \sigma'_o)$ is another reference point. Using an experimentally determined stress-strain curve it was found that

$$m = 7{\cdot}1 \tag{43}$$

for the range of stress used. Finally we have

$$\frac{E}{E_s} = 1 + 5{\cdot}4 \times 10^{-7}\left(1 - \frac{a}{b}\right)^{-6{\cdot}1} \quad \text{for } \sigma_p = 8000 \text{ psi} , \tag{44}$$

$$\frac{E}{E_s} = 1 + 3{\cdot}7 \times 10^{-5}\left(1 - \frac{a}{b}\right)^{-6{\cdot}1} \quad \text{for } \sigma_p = 16{,}000 \text{ psi} , \tag{45}$$

and

$$\frac{E}{E_s} = 1 + 4{\cdot}3 \times 10^{-4}\left(1 - \frac{a}{b}\right)^{-6{\cdot}1} \quad \text{for } \sigma_p = 24{,}000 \text{ psi} . \tag{46}$$

Using (44) to (46) in (39) together with (35) β was plotted for all values of a/b, in Fig.7, for both 3" and 10" sheets, with $\rho' = 0{\cdot}0025"$.

3.3.2 The stress concentration method

Two other very similar methods have been suggested for correlating crack growth data by Hardrath and McEvily[5] and by Kuhn and Figge[6]. Both methods use semi-empirical means of calculating stress concentration factors at the tips of cracks. They start with the theoretical elastic stress concentration for a hole in a finite sheet (K_c) calculated by Howland[27]. This is modified in the manner of Neuber to obtain the theoretical factor (K_T) for an elliptical hole with the major axis of the ellipse equal to the crack-length. The explicit form of K_T is

$$K_T = 1 + (K_c - 1)\sqrt{\frac{a}{\rho}} , \tag{47}$$

where ρ is the radius of the crack-tip. K_T is then modified to take into account the Neuber size-effect parameter; this gives, for a fatigue crack, a new factor (K_N) which is

$$K_N = 1 + \frac{K_T - 1}{1 + \sqrt{\frac{\rho'}{\rho}}} , \tag{48}$$

where ρ' is the Neuber material constant. Since ρ is very small and difficult to measure for a fatigue crack Hardrath and McEvily assume that $\rho = \rho'$. Thus (47) becomes

$$K_N = 1 + \frac{1}{2}(K_c - 1) \sqrt{\frac{a}{\rho'}} \quad . \tag{49}$$

Kuhn and Figge, however, take the limit of $\rho \to 0$ and obtain

$$\lim_{\rho \to 0} \{K_N\} \equiv K_{TN} = 1 + (K_c - 1) \sqrt{\frac{a}{\rho'}} \quad . \tag{50}$$

Since the constant ρ' is determined such that the best fit with experimental data is obtained it follows from (49) and (50) that ρ' as determined by Kuhn and Figge should be four times that determined by Hardrath and McEvily. A comparison of results given by Hardrath and McEvily[5] for an Al-Zn-Mg alloy (7075-T6), $\rho' = 0{\cdot}002"$, and for an Al-Cu alloy (2024-T3), $\rho' = 0{\cdot}003"$, with the curve given by Kuhn and Figge[6] show this to be approximately true. Thus for the purposes of correlation both methods will give similar results. The Royal Aeronautical Society Data Sheet[28] value of $\rho' = 0{\cdot}0025"$ for aluminium alloys is comparable with that of Hardrath and McEvily.

It is assumed that a crack will propagate when K_{TN} times the average net section stress reaches a certain value for a given crack length. Now

$$K_{TN}\, \sigma_n = \frac{K_{TN}\, \sigma_p}{1 - a/b} \quad , \tag{51}$$

and so, from (28), (50) and (51) we have

$$\frac{K_{TN}\, \sigma_n}{K} = \frac{2\left[1 + (K_c - 1)\sqrt{\frac{a}{\rho'}}\right]}{(1 - R)\sqrt{a}\left(1 - \frac{a}{b}\right) a_W} \quad . \tag{52}$$

It is convenient to define a parameter (γ) in the following manner:

$$\gamma \equiv \frac{(1 - R)\sqrt{\rho'}\, K_{TN}\, \sigma_n}{4K} = \frac{\sqrt{\frac{\rho'}{a}} + K_c - 1}{2\left(1 - \frac{a}{b}\right)\alpha_W} \quad . \tag{53}$$

From the curve given by Kuhn and Figge we obtain, for DTD 5070A (σ_u = 62,000 psi), $\sqrt{\rho'}$ = 0·15 $\sqrt{\text{in}}$ A plot of γ vs.a/b is given in Fig.8.

Recently Kuhn[29] has suggested a stress concentration factor modified for finite width of sheet according to Dixon[21]. The new K_{TN} is given by

$$(K_{TN})_{new} \equiv K_F = 1 + 2\, K_W \sqrt{\frac{a}{\rho'}} \quad , \tag{54}$$

where

$$K_W = \sqrt{\frac{1 - a/b}{1 + a/b}} = \left(1 - \frac{a}{b}\right)\alpha_D \quad . \tag{55}$$

The same criterion for crack propagation is adopted as above. The parameter γ, defined above, is now replaced by γ_F, defined by

$$\gamma_F \equiv \frac{(1 - R)\sqrt{\rho'}\, K_F\, \sigma_n}{2K} = \frac{\sqrt{\frac{\rho'}{a}} + 2\, K_W}{\left(1 - \frac{a}{b}\right)\alpha_W} \quad . \tag{56}$$

A plot of γ_F vs. a/b is given in Fig.8.

4 SCATTER IN INCUBATION TIME AND CRACK PROPAGATION RATE

4.1 Results

A number of 3" wide panels were tested at the three different stress levels (4400 ±3600, 8800 ±7200 and 13,200 ±10,800 psi) and 10" wide panels at 4400 ±3600 psi. Approximately 10 panels were tested in each of the three cases. For the 10" wide panels, the cracks were made to run from the standard saw cuts. For the 3" wide panels, each saw cut terminated in a drilled hole 0·020" diameter and care was taken not to damage the internal surface of the hole when the saw blade broke through the hole. In this way it was hoped to provide a rather more reproducible stress concentration to start the crack. The total slot length was 1/3".

"Initiation times" were measured by observing the number of cycles (N) necessary for the crack to reach a new total length, as small as possible yet clearly different from the original length. Table 1 shows the mean and standard deviations of log N as measured. Two values of crack length, 0·5" and 0·6" in the 3" panels and 0·7" and 0·8" in the 10" panels, were taken to ensure that the observations of N were reliable. Although the measurement accuracy of the running crack would have allowed shorter lengths to be taken, the surface disturbance near the sawn slots made it inadvisable. During the other experiments at the two lower stress levels further data was obtained for the 3" panels under what should have been identical conditions except that cracks in these cases started from standard saw cuts and the specimens were not necessarily from the same sheet (see also Table 1). Corresponding figures for total cycles to complete specimen failure are also given.

Crack propagation observations were analysed by the methods described in section 3 and are summarized in Tables 2, 3, 4 and 5. The computer programme was arranged to yield values of K appropriate to selected values of da/dN. Since all the data for da/dN is based on total length of crack all the scatter results are based on the average progression of two cracks. Fig.9 shows the coefficient of variation of K, v(K), for different values of da/dN for the four tests, with and without the inclusion of the additional 3" panel data (S = scatter tests only, A = all tests). We can convert these results into variations in da/dN at fixed values of K by noting in Figs.12, 13 and 14 (section 6) that sufficiently accurately for our purpose $da/dN = Ae^{BK}$ where $B = \frac{1}{1000}\ lb^{-1}\ in^{3/2}$. Since the standard deviations are small, then $\sigma\left(\log \frac{da}{dN}\right) \simeq B/2{\cdot}3\ \sigma(K) = \frac{BK}{2{\cdot}3} v(K)$. Using Fig.14 to obtain values of K we may tabulate values of $\sigma\left(\log \frac{da}{dN}\right)$, σ_1 and σ_2 corresponding to v(K) = 0·02 and 0·04. These values are, respectively, that found for the 3" panels at ±7200 psi, scatter tests only, and a rough average of all the other runs.

$\frac{da}{dN}$ (in per cycle)	BK	$\sigma_1\left(\log \frac{da}{dN}\right)$	$\sigma_2\left(\log \frac{da}{dN}\right)$
10^{-6}	1·3	0·01	0·02
10^{-5}	3·5	0·03	0·06
10^{-4}	6·0	0·05	0·10
10^{-3}	8·5	0·07	0·14

Finally, values of $\sigma\left(\log \frac{da}{dN}\right)$ can be compared directly with initiation times or cycles to failure by noting that if a crack takes N cycles to traverse a fixed distance ℓ at a constant rate $\frac{da}{dN} = \frac{\ell}{N}$; whence for small deviations $\sigma\left(\log \frac{da}{dN}\right) = \sigma\ (\log N)$.

4.2 Discussion

These results can form a basis for testing the significance of small differences in subsequent experiments. It is interesting however to see how far the scatter observed is due to the intrinsic material variations rather than errors in testing technique. Our estimated uncertainty in each crack tip position was ±0·013" (3" panels) and ±0·035" (10" panels) as given in section 2.6. Assume errors in a are $\frac{1}{\sqrt{2}}$ of these i.e. 0·009" (3" panels) and 0·025" (10" panels). Measurements of N to sufficient accuracy presented no problem; stressing errors were given in Section 2.5.

Considering the initiation times first, calculations of the effect of these errors on the observed scatter show that for the 3" panels at ±3600 psi, all the measurement errors were smaller than the observed scatter; for the 3" panels at ±7200 and ±10,800 psi the stressing errors and to a lesser extent the crack tip position errors could well have been a major source of scatter; for the 10" panels the crack tip position error was sufficient to account for the observed scatter. Accordingly we can only regard the last three sets of observations as upper limits for material variations. On the very limited data available, the scatter of the panels with holed ends to the saw cuts were little different from those without.

The effects of experimental errors on crack propagation rates are more involved. Our estimated stressing errors were ~3·2%, 1·6%, 1·1% and 1·3% for 3" at σ_a = ±3600 psi, ±7200 psi, ±10,800 psi and 10" at σ_a = ±3600 psi respectively and bearing in mind that K is proportional to stress it is obvious that we cannot, especially for the 3", ±7200 psi scatter tests, expect results much better than those observed. In general the errors in crack position should only have a significant effect at the lower crack propagation rates, ($\sim 10^{-5}$ in/cycle or less) and could here account for some of the observed increase in v(K) in Fig. 9.

But in view of the low values of v(K) of ~0·02 for 3", ±7200 psi scatter tests, it is reasonable to assume that the higher scatters of the other runs are due to other undetermined experimental errors and that this value of v(K)

only is the best upper limit for material variations of specimens taken from one sheet. Comparing our results with Barrois[2], he found for an aluminium alloy Au4G1 (Similar to 24ST Al clad) values of crack propagation rate leading, if we have interpreted them correctly, to $\sigma\left(\log \frac{da}{dN}\right) \approx 0{\cdot}2$ for values of da/dN between 10^{-3} and 10^{-2}. This is a larger scatter, but Barrois does not consider experimental errors.

Because of our experimental errors we cannot compare material induced scatter initiation time and crack propagation in much detail but as Table 1 shows, at the lowest stress and shortest crack length (1/3") the initiation time scatter is greater. Higher stresses and longer starting cracks reduce it to the same order as propagation rate scatter. The low scatter in total life from our high K_t specimens may be compared with typical values given by Ford, Graff and Payne[30] of $\sigma(\log N)$ for a notched (K_t ~5) Al alloy of ~0·18.

5 EFFECT OF PANEL LENGTH/WIDTH RATIO

5.1 Results

To determine the effect of panel free length/panel width, (d/b), on the crack propagation characteristics, duplicate tests were made at two stress levels (8000 and 16,000 psi peak) on 3" wide panels having the following d/b ratios - 1·2, 1·6, 2·1, 3·2 and 4·75. The free length of the panel, i.e. the ungripped length, was determined by measuring the length of the specimen between the serration marks made by the grips. Since the panel was probably not fully constrained by the grips at these points the values of d/b quoted may be slightly too low. The results of the tests are shown in Tables 6 - 10 and Figs.10 and 11. Each curve in each figure represents the mean value for two tests and although there is some scatter at the lower stress level these curves are reasonably close together in spite of the different geometry of the panels. More important, there is no trend in the results for the different values of d/b at either stress level.

5.2 Discussion

Comparison of the two sets of curves shows that for a given rate the values of K are slightly higher for the higher stress level. This trend will be discussed in more detail in the next section.

Since all the panels were of the same width, using a different width correction (e.g. α_D or α_G) would only change the K-scale at any one stress level and would not affect the relative positions of the curves. Thus the conclusion that the rates are virtually independent of length of panel remains valid.

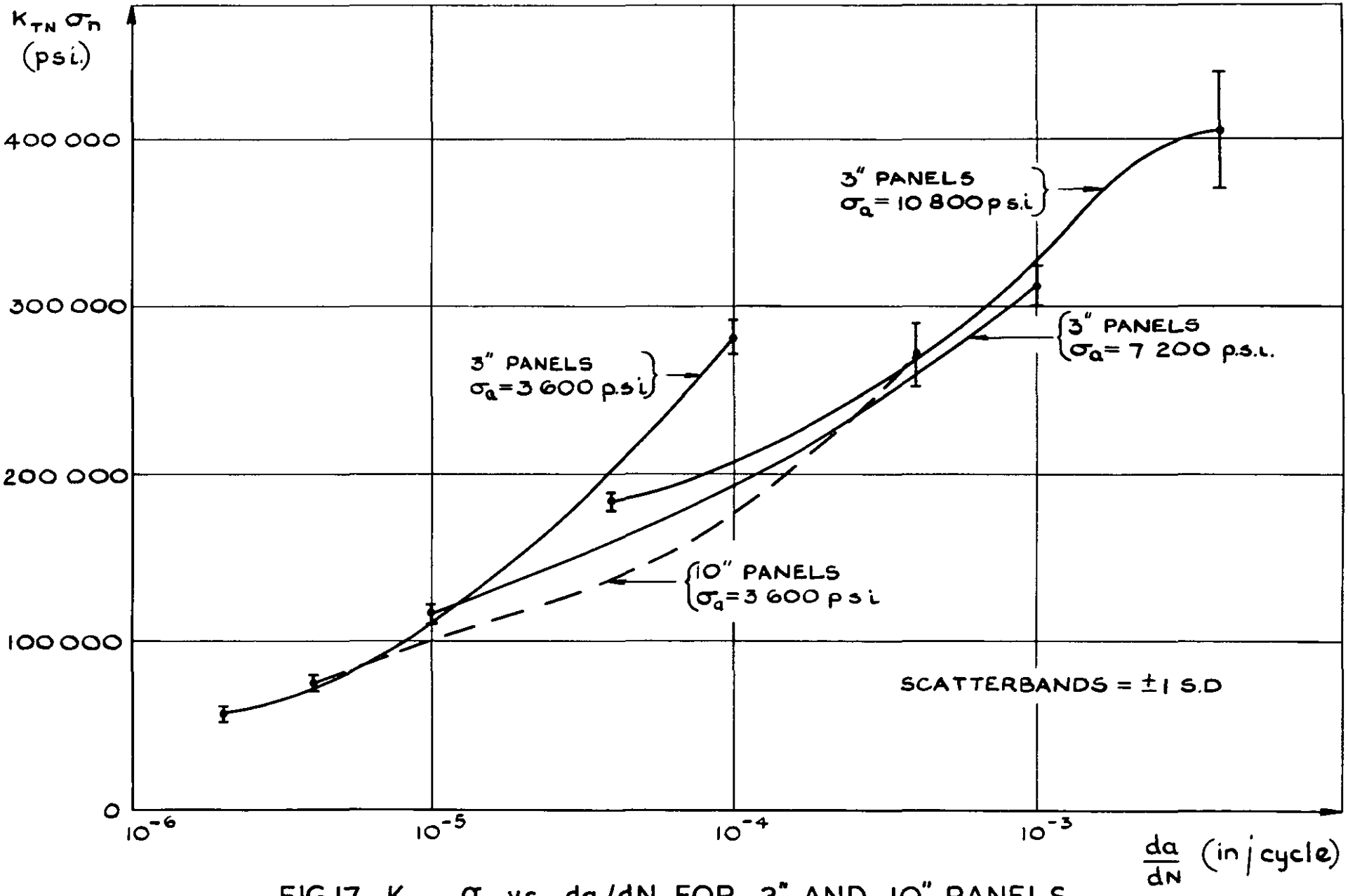

FIG.17. $K_{TN}\,\sigma_n$ vs. da/dN FOR 3" AND 10" PANELS

and the constant unity may be neglected. Thus $K_F \sigma_n / K \propto a_D / a_W$, which is of order unity for most values of a/b. Summarising, K or $K_F \sigma_n$ provided the best width correlation up to the surprisingly high values of a/b ~ 0·8.

The effect of stress level may be seen in comparing Figs.12 and 13. Correlation on a K basis shows differences between the two lower stress levels which are clearly significant in the 3" panel results of Fig.14. The additional stress level of σ_a = 10,800 psi confirms the trend. Use of a_G, ε_c, $K_{TN} \sigma_n$ or $K_F \sigma_n$ as in Figs.15, 16, 17 and 18 does not improve matters. In this respect all methods of correlation have failed to allow exactly for the variation in stress level.

In general we have preferred to use K since it is a simple analytical function which correlates width well and is easily calculated. Although $K_F \sigma_n$ gives similar results it requires a knowledge of an empirical parameter ρ' which must be found for each material such that a best fit is obtained. The physical interpretation of ρ' is not clear, since although it is called "Neubers material constant" its value depends on the manner in which K_F (or K_{TN}) is calculated (see section 3). K, on the other hand, is based on an exact elastic analysis with reasonably known approximations. The complications introduced with ρ' do not improve the correlation in stress nor make it easier to understand the sources of error.

Taking the analysis based on K, a possible source of error may lie in the fact that the use of K to describe the stress field is only valid near the crack tip. Taking for instance a distance from the tip equal to the size of the plastic-zone then here the elastic stress given by the K approximation can differ from the exact elastic stress by up to several per cent. For the stresses and crack lengths used here, the difference in exact elastic stresses with cracks of the same K only differ by 1 - 2%, but taking into account the plastic relaxation which will occur this difference may increase and if we are interested in the volume of material over which a certain stress is exceeded the effect of such differences may be increased further. The problem requires more investigation; factors such as the differences in the strain distribution round cracks with the same K should also be considered. Despite these points however, the value of fatigue crack propagation correlation on the basis of K is clearly established.

7 EFFECT OF DIRECTION OF CRACK PROPAGATION

A small number of tests were made on $4\frac{1}{2}$" wide panels (with d/b = 2) which were cut transversely to the final direction of rolling. As will be seen from

Tables 17 and 18 three tests were made at each of the two peak stress levels, 8000 and 16,000 psi. The results from these panels are compared with those obtained for the $4\frac{1}{2}$" panels in the size effect tests - see Figs.19 and 20. The mean values for these tests at each level are plotted and show that there is very little difference whether the crack and rolling direction are the same or at right angles. The tensile properties may be compared in the two directions at right angles by reference to the table in section 2.1.

8 EFFECT OF BUCKLING

In the final stages of a panel's life, just before it fails catastrophically, the fatigue crack may be sufficiently large for buckling of the panel to occur (due to the lateral compressive stresses at the edges of the crack). Mansfield[9] has suggested for the buckling stress, $\sigma_b \simeq \lambda E^2 t^2/A a^2$ where t is the sheet thickness and λ is a constant ($\simeq 10$). Taking our two peak stresses of 8000 and 16,000 psi and working out the critical values of a for the onset of buckling with these stresses, they are respectivcly 2·5" and 3·5". On this basis we should only expect buckling in the 20" panels as only here were such values of a reached. In practice this was found to be so. Since buckling will affect the stress field round the crack tip (see Ref.9) and hence presumably crack growth rate a number of 20" wide panels having a d/b ratio of 2 were tested at the peak stress of 8000 psi to determine the effect of buckling restraint. 20" wide panels at σ_p = 16,000 psi failed before the crack length was great enough to induce any substantial buckling. Two panels were tested with "anti-buckle" bars (described in section 2.3) strapped across the width, the centre line of the bars being 2" from the crack line. These were compared with results for unrestrained panels tested during the investigation on size effects. All five panels had four strain gauges, cemented on to them in the positions shown by Fig.21, to measure the transverse strain due to buckling throughout the test. Figs.22 to 24 show plots of transverse strain due to buckling. Ends A and B refer respectively to the ends of the panels further from and nearer to the fixed head of the pulsator. Fig.22 shows a typical result of a test without "anti-buckle" bars and Figs.23 and 24 show the two tests with bars. It will be seen in Fig.22 as predicted by Mansfield that until a $\simeq$ 2", the strains due to buckling in an unsupported panel were fairly small and only for a $\geqslant$ 2" did these strains mount rapidly. A strain difference between top and bottom gauges of 2×10^{-3} would correspond to a panel radius of curvature of ~ 30". Figs.23 and 24 show that the "anti-buckle" bars effectively reduced the strains. Fig.22 indicates, that because the tension and compression gauges were showing tensile stresses of two different magnitudes the panel was in fact pulsating to

produce tension on each side. Figs.23 and 24 show that the panels were buckling in one direction only. The crack propagation results of these tests are shown in Table 19 and the average plotted in Fig.25.

Bearing in mind that a has reached the value of 2" by the time $\frac{da}{dN} \simeq 6 \times 10^{-5}$ in/cycle we might expect the crack growth curves to begin to differ at this point. In fact they do not do so significantly even up to complete fracture (the last dotted part of the curve is based on one sample only). Accordingly we can conclude that at no time did buckling have much effect on crack propagation, even though when $a \simeq 3"$ and da/dN reached 2×10^{-4} in/cycle appreciable buckling strains were recorded.

9 EFFECT OF REMOVING THE CLADDING

9.1 Results

Tests in triplicate were made on 3" wide panels from which the cladding on each side had been removed, at each of the two peak stresses 8000 and 16,000 psi. The cladding on each face is nominally 5% of the total thickness. To ensure complete removal of the cladding, 0·004" was machined from each side leaving the specimen nominally 0·056". The results of these tests are shown in Table 20 and Figs.26 and 27. Also shown in these figures are the results of all the clad 3" panels; the difference is seen to be negligible.

9.2 Discussion

It is known that in general crack propagation depends on sheet thickness; but we can assume that the 12½% thickness reduction which we have made will have a negligible effect on its own. Accordingly since the values of K are based on gross area stress in both cases, we must conclude that the cladding was effectively behaving in just the same way as the core material. If it had been playing no part there would have been a readily detectable change (~10%) in K for the same value of da/dN. Alternatively one could regard the cladding as taking no fatigue load directly, but acting as a brake on the progression of the crack front. However if this were so one would expect evidence of this in the clad material such as a pronounced curvature in the crack front. This was not observed and since in any case it is known from other work[8] that the crack propagation characteristics of pure aluminium are little worse if at all, than that of DTD 5070A the first conclusion is tentatively preferred.

10 FRACTURE MODE TRANSITIONS

10.1 Results

As the cracks traversed the sheets the mode of failure changed in a systematic way. In terms of the two stages of crack growth as described by Forsyth[31], it is worth mentioning that the Stage 1 shear mode was virtually undetectable. Under the biaxial stress situation at the crack tip we always had the Stage 2 mode with the subsequent modifications of it. The general sequence of modes and the associated macroscopic appearance of the fracture surfaces could be classified as follows (see Fig.28):

(1) Failure in a tensile mode with a nominally flat fracture surface perpendicular to the panel surface plus small shear lips, complicated by the cladding, at the free surface.

(2) Failure in multiple shear leading to a chevron fatigue fracture surface with shear lips on a comparable scale at the free surface.

(3) Failure in double shear on two planes at right angles to each other and inclined at 45° to the panel surface (the shear lips are now fully incorporated in the double shear).

(4) Failure in single shear on a plane inclined at 45° to the panel surface.

The entire sequence was not always observed. It depended on the stress level and the sheet width. For instance at the stress level of 8800 ±7200 psi the crack started in the multiple shear mode with virtually no flat mode; at 4400 ±3600 psi the 20" panels showed no region with double shear failure; the failure mode in the 3" panels at 13,200 ±10,800 was all double or single shear. At no time did we observe substantial crack tunnelling in the centre of the sheet such as can occur in thicker sheets, or in more brittle Al-Sn-Mg alloys. These modes are similar to those described by Lipsitt, Forbes and Baird[32]. The position of our cracks was not observed frequently enough to confirm the arrests which they reported before a new mode started, but since we had the additional multiple shear mode, not reported by them, with no sudden transitions into and out of it we would not expect such arrests here.

The values of K at which the fracture mode transitions occurred were calculated and are plotted for the two principal stress levels in Fig.29 for the panel widths tested. Although there was a fairly large spread in individual K values it can be seen that any one transition occurs at approximately the same average K-value for all widths. Fig.28 relates the fracture mode observed,

at the two stress levels, to the mean values of K for the two stress levels. Let $K = K_1$ at the start of the multiple-shear mode, $K = K_2$ at the start of the double-shear mode and $K = K_3$ at the start of the single-shear mode; from Fig.28 we find that

$$\frac{K_2(\sigma_p = 16{,}000 \text{ psi})}{K_2(\sigma_p = 8000 \text{ psi})} \approx 1{\cdot}2 \qquad (57)$$

and

$$\frac{K_3(\sigma_p = 16{,}000 \text{ psi})}{K_3(\sigma_p = 8000 \text{ psi})} \approx 1{\cdot}1 \ . \qquad (58)$$

The K_3 transition, for 3" panels only, at $\sigma_p = 24{,}000$ psi is about 20% higher than at $\sigma_p = 16{,}000$ psi.

10.2 Discussion

It has been suggested[33] that the fracture mode transition to double shear ($K = K_2$) should occur when the radius of the plastic zone, perpendicular to the crack ($r_p(90°)$), is equal to half the sheet thickness. Using Liu's formula[33] we have

$$r_p(90°) = \frac{5K_2^2(\text{peak})}{8\sigma_y^2} \ , \qquad (59)$$

where $K_2(\text{peak})$ is the value of K calculated using σ_p instead of σ_a and σ_y is the yield stress. Since K is a linear function of stress we have

$$K_2(\text{peak}) = \frac{\sigma_p}{\sigma_a} K_2 \qquad (60)$$

and therefore

$$r_p(90°) = \frac{5\sigma_p^2 K_2^2}{8\sigma_a^2 \sigma_y^2} \ . \qquad (61)$$

Thus for σ_p = 8000 psi, $r_p(90°) \approx 0{\cdot}014"$ and for σ_p = 16,000 psi, $r_p(90°) \approx 0{\cdot}021"$. The half-sheet thickness (t/2) is 0·032" and so the plastic zone radii, as calculated, do not agree with this figure. Moreover the value of $r_p(90°)$ is not a constant for the two stress levels.

The corresponding values of $r_p(90°)$ for the K_3 transition are 0·029" (σ_p = 8000 psi) and 0·036 (σ_p = 16,000 psi), so that on this data we might alter Liu's criterion to apply to the K_3 transition. This has been suggested by Liu himself[34], who analysed results obtained by Weibull[35]; Liu found that the transition to double shear occurred at $r_p(90°) \approx 0{\cdot}3t$ and the transition to single shear at $r_p(90°) \approx 0{\cdot}5t$. For the sheets used in these tests $0{\cdot}3t = 0.019"$ which lies between the two values, calculated above, for the K_2 transition. The K_3 transition at the highest stress (σ_p = 24,000 psi) however, corresponds to $r_p(90°) \approx 0{\cdot}054"$ which is appreciably larger than 0·5t. Other work[36] has shown that while the shear lip depth in fatigue is appreciably less than this theoretical r_p there is also a region of plastic strain extending some distance beyond r_p away from the crack in the surface of the sheet. Accordingly more data is needed before definite conclusions may be drawn. It is evident from the data in section 6 and Fig.14, on the difference between K-values for a given crack rate at different stresses, that fracture mode transitions are somewhat better correlated with crack rate.

11 GENERAL DISCUSSION AND CONCLUSIONS

(1) We have shown that the scatter in crack propagation rate in specimens taken from one sheet can be very low. Results could best be expressed as an equivalent S.D. in stress for a given crack rate. This S.D. could be as low as 2% though usually it was nearer twice this figure. Similarly the scatter in crack initiation times were, with the exception of the 3" ±3600 psi tests, low, having values of $\sigma(\log Ni) \sim 0{\cdot}04$. Bearing in mind that the experimental errors - primarily those in load application - were comparable with these scatters the figures only give upper limits of scatter due to material variations. More precise equipment would be needed to pursue the subject further.

(2) The directional effect in crack propagation rate was found to be very small in this material in contrast with Frost's relatively large effect in the aluminium (AlZnMgCu) alloy DTD 687A[37]. However, in his material crack propagation was accompanied by periodic 'unstable' tunnelling and he found that unstable fast fracture was also sensitive to direction: this is an added factor not present in our work.

(3) Although a panel length/width ratio of 2:1 was adopted for most of the work, it was found that even down to the smallest ratio of 1·2:1 used the crack propagation rate (in 3" wide panels) was insignificantly affected. This confirmed that Irwin's derivation of length independence based on Greenspan's work was valid for values of a/b and a/d beyond the suggested limits.

(4). Regarding the general crack growth dependence on stress and crack length, our results can be expressed over most of the range by $da/dN = Ae^{BK}$. Expressions of this form and modifications of it have been considered by previous workers[2,30] but although they are valuable as a means of summarising data they do not throw light on the physical processes involved. Similarly expressions of the form $da/dN \propto a^{\alpha} \sigma^{\beta}$ have been considered (see Ref.1 for a summary). Expressed in this form our results show that α lies between 1·5 and 3·0 and over most of the range is ~ 2. Similarly β is between 2·5 and 4·5.

Various arguments have been put forward to account for such parameters. Of those based on physical models all necessarily demand great simplifications. For example, Irwin[39] has suggested that β should be ~ 4 on the basis of Coffin's work on fatigue life at high strains. Coffin deduced that $N^{\frac{1}{2}}$ x (plastic strain amplitude) was a constant. However Coffin's empirical formula was based on tests on plain specimens under a constant plastic strain range; this is very different from the propagating crack case. In plain specimens much of the time is often spent initiating and propagating the crack along slip planes. In our type of test the crack is propagated by successive cycles of fracture at right angles to the principal tensile stress. It would be surprising also, if the crack rate did not vary with the fracture modes listed in section 10.

(5) In correlating results from panels of different widths, the stress intensity factor K (with the Westergaard width correction) and the stress concentration factor $K_F \sigma_n$ were the most successful of the parameters tried. In general, agreement was within the limits of scatter. In contrast, correlation of results at three different stress levels in 3" wide panels showed significant residual differences no matter which method was used. There is no obvious explanation for this.

In general the K factor was preferred because of its simplicity and clear basis. Here Irwin's method of regarding the crack as effectively longer by an amount equal to the plastic zone was followed, but at the fatigue stresses used the correction was for the most part negligible. It amounted to ~ 7% at most in the 3" panels with σ_p = 24,000 psi.

(6) A study of buckling in the 20" wide panels showed that it occurred roughly when expected, but that its effect on crack propagation rate, when compared with similar supported panels, was insignificant in these experiments.

(7) Tests made on panels with the cladding removed showed that if stresses are based on the gross area, including cladding if any, then crack propagation rates were the same with or without cladding.

(8) The macroscopic fracture modes in general progressed from normal tensile, through multiple shear, double shear and finally single shear. Transition from double to single shear could roughly be correlated with the point where the plastic zone was approximately half the sheet width. However, in that r_p is directly related to K and in view of the failure of K to correlate rates at different stress levels it is not surprising that the transitions could best be said to occur at definite values of crack growth rate.

Table 1

SCATTER IN CYCLES TO CRACK INITIATION AND CYCLES TO FAILURE

No. of tests		Scatter only			All		
Panel width and alternating stress level	Total crack length	No. of tests	Mean of log N	S.D. of log N	No. of tests	Mean of log N	S.D. of log N
3"	0·5"		5·18	0·17		5·13	0·17
	0·6"	9	5·25	0·13	14	5·21	0·13
3600 psi	failure		5·45	0·085		5·44	0·092
3"	0·5"		4·07	0·047		4·08	0·055
	0·6"	10	4·19	0·038	14	4·19	0.047
7200 psi	failure		4·43	0·020		4·43	0·048
3"	0·5"		3·76	0·038			
	0·6"	16	3·78	0·037			
10,800 psi	failure		3·79	0·039			
10"	0·7"		4·69	0·039			
	0·8"	10	4·82	0·044			
3600 psi	failure		5·29	0·030			

Table 2

RESULTS OF CRACK PROPAGATION TESTS ON 3" WIDE PANELS FOR SCATTER INVESTIGATION. ALTERNATING STRESS 3600 psi

Test No.	330		332		334		337		338		341		344		346		349	
$\frac{da}{dN}$ inches per cycle	a in	K x 10^{-3} psi $\sqrt{in}$	a in	K x 10^{-3} psi $\sqrt{in}$	a in	K x 10^{-3} psi $\sqrt{in}$	a in	K x 10^{-3} psi $\sqrt{in}$	a in	K x 10^{-3} psi $\sqrt{in}$	a in	K x 10^{-3} psi $\sqrt{in}$	a in	K x 10^{-3} psi $\sqrt{in}$	a in	K x 10^{-3} psi $\sqrt{in}$	a in	K x 10^{-3} psi $\sqrt{in}$
6×10^{-7}			0.19	1.58														
8×10^{-7}			0.22	1.70														
1×10^{-6}	0.24	1.79	0.24	1.78	0.21	1.68												
2×10^{-6}	0.31	2.05	0.31	2.04	0.29	1.99			0.27	1.90	0.31	2.03	0.26	1.86	0.27	1.91	0.28	1.96
4×10^{-6}	0.39	2.31	0.38	2.30	0.39	2.33			0.41	2.39	0.41	2.38	0.41	2.39	0.40	2.37	0.39	2.33
6×10^{-6}	0.44	2.50	0.45	2.51	0.46	2.65	0.57	2.93	0.55	2.85	0.53	2.77	0.52	2.76	0.53	2.77	0.50	2.67
8×10^{-6}	0.51	2.72	0.55	2.84	0.62	3.08	0.68	3.29	0.66	3.23	0.68	3.30	0.61	3.05	0.63	3.13	0.62	3.08
1×10^{-5}	0.63	3.11	0.72	3.44	0.72	3.43	0.75	3.53	0.74	3.49	0.77	3.62	0.68	3.28	0.71	3.39	0.71	3.40
2×10^{-5}	0.90	4.16	0.94	4.34	0.92	4.25	0.91	4.22	0.92	4.22	0.95	4.41	0.86	3.96	0.89	4.13	0.91	4.20
4×10^{-5}	1.04	4.90	1.07	5.07	1.05	4.95	1.04	4.89	1.04	4.91	1.07	5.12	0.99	4.62	1.03	4.81	1.04	4.91
6×10^{-5}	1.10	5.32	1.12	5.50	1.11	5.37	1.10	5.30	1.10	5.32	1.13	5.54	1.06	5.01	1.09	5.22	1.10	5.32
8×10^{-5}	1.14	5.63	1.16	5.81			1.13	5.59	1.14	5.62	1.16	5.85	1.10	5.30	1.13	5.52	1.14	5.62
1×10^{-4}	1.16	5.87	1.18	6.05			1.16	5.83					1.13	5.53	1.15	5.75	1.16	5.86
2×10^{-4}															1.22	6.53	1.23	6.65

Table 3

RESULTS OF CRACK PROPAGATION TESTS ON 3" WIDE PANELS FOR SCATTER INVESTIGATION. ALTERNATING STRESS 7200 psi

Test No.	331		333		335		336		339		342		343		345		347		348	
$\frac{da}{dN}$ inches per cycle	a in	$Kx10^{-3}$ psi $\sqrt{in}$	a in	$Kx10^{-3}$ psi $\sqrt{in}$	a in	$Kx10^{-3}$ psi $\sqrt{in}$	a in	$Kx10^{-3}$ psi $\sqrt{in}$	a in	$Kx10^{-3}$ psi $\sqrt{in}$	a in	$Kx10^{-3}$ psi $\sqrt{in}$	a in	$Kx10^{-3}$ psi $\sqrt{in}$	a in	$Kx10^{-3}$ psi $\sqrt{in}$	a in	$Kx10^{-3}$ psi $\sqrt{in}$	a in	$Kx10^{-3}$ psi $\sqrt{in}$
8×10^{-6}									0.22	3.49										
1×10^{-5}			0.27	3.83			0.24	3.64	0.26	3.76										
2×10^{-5}	0.38	4.67	0.38	4.63	0.37	4.58	0.34	4.38	0.36	4.52	0.38	4.65	0.37	4.55	0.38	4.67	0.38	4.62	0.37	4.57
4×10^{-5}	0.50	5.47	0.48	5.30	0.48	5.34	0.45	5.10	0.47	5.23	0.50	5.43	0.47	5.25	0.50	5.45	0.49	5.39	0.48	5.34
6×10^{-5}	0.57	5.89	0.53	5.68	0.55	5.76	0.51	5.52	0.53	5.64	0.56	5.85	0.53	5.62	0.56	5.86	0.55	5.79	0.54	5.74
8×10^{-5}	0.61	6.19	0.57	5.95	0.59	6.05	0.56	5.83	0.57	5.93	0.60	6.15	0.56	5.88	0.60	6.14	0.59	6.07	0.58	6.02
1×10^{-4}	0.64	6.41	0.61	6.16	0.62	6.27	0.59	6.06	0.61	6.16	0.64	6.38	0.59	6.09	0.64	6.36	0.62	6.28	0.62	6.23
2×10^{-4}	0.74	7.13	0.70	6.83	0.72	6.98	0.70	6.80	0.71	6.88	0.74	7.11	0.69	6.73	0.73	7.06	0.72	6.96	0.71	6.91
4×10^{-4}	0.83	7.88	0.79	7.53	0.81	7.71			0.80	7.62	0.83	7.85	0.78	7.40	0.82	7.78	0.81	7.67	0.80	7.62
6×10^{-4}	0.88	8.32	0.84	7.96	0.87	8.16			0.86	8.07	0.88	8.30	0.83	7.82	0.87	8.22	0.86	8.10	0.85	8.05
8×10^{-4}	0.92	8.64	0.88	8.28	0.90	8.47			0.89	8.39			0.86	8.12	0.91	8.54	0.89	8.42	0.89	8.36
1×10^{-3}	0.94	8.90	0.91	8.52					0.92	8.64			0.89	8.36	0.93	8.79			0.91	8.61

Table 4

RESULTS OF CRACK PROPAGATION TESTS ON 3" WIDE PANELS FOR SCATTER INVESTIGATION. ALTERNATING STRESS 10,800 psi

Test No.	413		415		416		417		419		420		421		422	
$\frac{da}{dN}$ inches per cycle	a in	K x 10^{-3} psi $\sqrt{in}$	a in	K x 10^{-3} psi $\sqrt{in}$	a in	K x 10^{-3} psi $\sqrt{in}$	a in	K x 10^{-3} psi $\sqrt{in}$	a in	K x 10^{-3} psi $\sqrt{in}$	a in	K x 10^{-3} psi $\sqrt{in}$	a in	K x 10^{-3} psi $\sqrt{in}$	a in	K x 10^{-3} psi $\sqrt{in}$
4×10^{-5}	0.28	6.09			0.26	5.76	0.27	5.91	0.29	6.14	0.27	5.90	0.27	5.94		
6×10^{-5}	0.32	6.52	0.26	5.79	0.29	6.12	0.30	6.27	0.32	6.52	0.31	6.42	0.31	6.33	0.30	6.22
8×10^{-5}	0.35	6.84	0.29	6.16	0.31	6.38	0.32	6.52	0.35	6.78	0.35	6.77	0.33	6.61	0.33	6.60
1×10^{-4}	0.45	7.87	0.32	6.45	0.33	6.59	0.34	6.71	0.37	6.98	0.37	7.02	0.35	6.83	0.36	6.88
2×10^{-4}	0.56	8.95	0.40	7.33	0.39	7.28	0.40	7.35	0.43	7.62	0.44	7.74	0.42	7.60	0.43	7.65
4×10^{-4}	0.62	9.60	0.49	8.25	0.48	8.21	0.48	8.13	0.49	8.32	0.50	8.40	0.52	8.58	0.50	8.33
6×10^{-4}	0.66	10.07	0.54	8.82	0.56	8.98	0.54	8.74	0.54	8.78	0.54	8.76	0.59	9.29	0.53	8.70
8×10^{-4}	0.69	10.44	0.58	9.24	0.62	9.60	0.59	9.27	0.57	9.13	0.56	9.00	0.64	9.83	0.56	8.95
1×10^{-3}			0.61	9.57	0.66	10.07	0.63	9.71	0.60	9.43	0.58	9.19	0.68	10.25	0.57	9.14
2×10^{-3}					0.78	11.46	0.75	11.09	0.70	10.46	0.63	9.74	0.79	11.55	0.63	9.70
4×10^{-3}									0.79	11.62	0.68	10.25			0.67	10.22

Table 4 (Contd)

Test No.	424		425		426		427		428		429		430		431	
inches $\frac{da}{dN}$ per cycles	a in	K x 10^{-3} psi $\sqrt{in}$	a in	K x 10^{-3} psi $\sqrt{in}$	a in	K x 10^{-3} psi $\sqrt{in}$	a in	K x 10^{-3} psi $\sqrt{in}$	a in	K x 10^{-3} psi $\sqrt{in}$	a in	K x 10^{-3} psi $\sqrt{in}$	a in	K x 10^{-3} psi $\sqrt{in}$	a in	K x 10^{-3} psi $\sqrt{in}$
4×10^{-5}	0.27	5.94	0.25	5.64			0.29	6.14	0.26	5.81			0.25	5.74		
6×10^{-5}	0.31	6.33	0.29	6.16	0.28	6.05	0.32	6.49	0.29	6.17	0.28	6.06	0.29	6.12	0.27	5.95
8×10^{-5}	0.33	6.60	0.32	6.54	0.30	6.31	0.34	6.75	0.31	6.42	0.32	6.54	0.31	6.40	0.32	6.45
1×10^{-4}	0.35	6.80	0.35	6.83	0.32	6.51	0.36	6.95	0.33	6.62	0.36	6.90	0.33	6.62	0.35	6.81
2×10^{-4}	0.41	7.46	0.45	7.82	0.38	7.18	0.43	7.67	0.40	7.30	0.47	8.05	0.40	7.34	0.45	7.86
4×10^{-4}	0.48	8.18	0.55	8.91	0.47	8.05	0.53	8.70	0.48	8.22	0.58	9.21	0.49	8.25	0.55	8.86
6×10^{-4}	0.53	8.65	0.62	9.59	0.54	8.76	0.61	9.52	0.56	9.00	0.64	9.89	0.55	8.93	0.60	9.45
8×10^{-4}	0.56	9.02	0.66	10.09	0.59	9.35	0.67	10.13	0.62	9.63	0.69	10.38	0.61	9.47	0.64	9.88
1×10^{-3}	0.59	9.33	0.70	10.47	0.64	9.82	0.71	10.59	0.66	10.11	0.72	10.77	0.65	9.90	0.67	10.22
2×10^{-3}	0.69	10.40	0.80	11.68	0.76	11.22	0.82	11.94					0.76	11.23	0.77	11.31
4×10^{-3}	0.79	11.58													0.86	12.47

Table 5

RESULTS OF CRACK PROPAGATION TESTS ON 10" WIDE PANELS FOR SCATTER INVESTIGATION. ALTERNATING STRESS 3600 psi

Test No.	382		383		384		394		395		396		397		398		399		400	
$\frac{da}{dN}$ inches per cycle	a in	$Kx10^{-3}$ psi$\sqrt{in}$	a in	$Kx10^{-3}$ psi$\sqrt{in}$	a in	$Kx10^{-3}$ psi$\sqrt{in}$	a in	$Kx10^{-3}$ psi$\sqrt{in}$	a in	$Kx10^{-3}$ psi$\sqrt{in}$	a in	$Kx10^{-3}$ psi$\sqrt{in}$	a in	$Kx10^{-3}$ psi$\sqrt{in}$	a in	$Kx10^{-3}$ psi$\sqrt{in}$	a in	$Kx10^{-3}$ psi$\sqrt{in}$	a in	$Kx10^{-3}$ psi$\sqrt{in}$
4×10^{-6}	0.42	2.35	0.33	2.08	0.43	2.37	0.44	2.40	0.47	2.48	0.44	2.40	0.47	2.49	0.39	2.27	0.41	2.32		
6×10^{-6}	0.58	2.77	0.55	2.70	0.60	2.83	0.63	2.89	0.67	2.97	0.63	2.89	0.66	2.96	0.61	2.85	0.62	2.87	0.61	2.85
8×10^{-6}	0.70	3.04	0.70	3.06	0.73	3.11	0.77	3.20	0.81	3.28	0.76	3.19	0.79	3.26	0.77	3.21	0.77	3.21	0.78	3.22
1×10^{-5}	0.78	3.24	0.82	3.32	0.83	3.32	0.88	3.43	0.92	3.51	0.87	3.41	0.90	3.48	0.89	3.46	0.89	3.46	0.91	3.49
2×10^{-5}	1.07	3.81	1.18	4.02	1.14	3.94	1.22	4.09	1.28	4.20	1.21	4.08	1.24	4.13	1.28	4.20	1.26	4.17	1.28	4.21
4×10^{-5}	1.41	4.45	1.53	4.66	1.48	4.57	1.59	4.77	1.67	4.91	1.59	4.77	1.60	4.78	1.67	4.91	1.65	4.87	1.63	4.85
6×10^{-5}	1.69	4.95	1.73	5.01	1.71	4.98	1.84	5.21	1.93	5.37	1.85	5.23	1.84	5.21	1.91	5.33	1.89	5.29	1.83	5.19
8×10^{-5}	1.97	5.46	1.86	5.26	1.89	5.31	2.03	5.55	2.12	5.73	2.05	5.59	2.02	5.53	2.08	5.65	2.06	5.61	1.96	5.44
1×10^{-4}	2.23	5.94	1.97	5.45	2.05	5.60	2.18	5.83	2.28	6.03	2.21	5.89	2.17	5.81	2.21	5.90	2.20	5.87	2.06	5.62
2×10^{-4}	2.92	7.38	2.30	6.06	2.60	6.67	2.67	6.82	2.77	7.04	2.73	6.94	2.65	6.77	2.64	6.74	2.63	6.73	2.37	6.19
4×10^{-4}			2.62	6.70	3.10	7.85	3.13	7.92	3.21	8.15	3.19	8.08	3.10	7.86	3.04	7.70	3.05	7.72	2.65	6.77
6×10^{-4}			2.80	7.11							3.42	8.78	3.34	8.53			3.28	8.35	2.81	7.13
8×10^{-4}			2.93	7.41							3.56	9.29							2.92	7.40
1×10^{-3}																			3.01	7.61
2×10^{-3}																			3.27	8.32

Table 6

EFFECT OF d/b ON THE CRACK PROPAGATION RATE OF 3" WIDE PANELS

(i) $d/b = 1 \cdot 2$

Alternating stress	3600 psi				7200 psi			
Test No.	299		300		301		302	
$\frac{da}{dN}$ inches per cycle	a in	$K \times 10^{-3}$ psi $\sqrt{in}$	a in	$K \times 10^{-3}$ psi $\sqrt{in}$	a in	$K \times 10^{-3}$ psi $\sqrt{in}$	a in	$K \times 10^{-3}$ psi $\sqrt{in}$
8×10^{-7}			0·22	1·71				
1×10^{-6}			0·24	1·80				
2×10^{-6}	0·34	2·15	0·31	2·06				
4×10^{-6}	0·58	2·95	0·41	2·39				
6×10^{-6}	0·73	3·48	0·63	3·13	0·23	3·57		
8×10^{-6}	0·82	3·80	0·79	3·68	0·28	3·92	0·22	3·47
1×10^{-5}	0·87	4·03	0·86	3·97	0·31	4·17	0·26	3·77
2×10^{-5}	1·01	4·72	1·01	4·72	0. 41	4·85	0·38	4·67
4×10^{-5}	1·11	5·42	1·12	5·43	0. 50	5·49	0. 52	5·55
6×10^{-5}	1·16	5·85	1·16	5·87	0·56	5·85	0·59	6·05
8×10^{-5}	1·19	6·17	1·20	6·19	0·60	6·12	0·64	6·39
1×10^{-4}	1·22	6·42	1·22	6·45	0. 63	6·32	0·68	6·65
2×10^{-4}			1·28	7·30	0·72	7·00	0·78	7·45
4×10^{-4}					0·81	7·70	0·87	8·24
6×10^{-4}					0·87	8·13		
8×10^{-4}					0·90	8·44		
1×10^{-3}					0·92	8·69		

Table 7

EFFECT OF d/b ON THE CRACK PROPAGATION RATE OF 3" WIDE PANELS

(ii) d/b = 1·6

Alternating stress	3600 psi				7200 psi			
Test No.	293		297		294		295	
$\frac{da}{dN}$ inches per cycle	a in	$K \times 10^{-3}$ psi $\sqrt{in}$	a in	$K \times 10^{-3}$ psi $\sqrt{in}$	a in	$K \times 10^{-3}$ psi $\sqrt{in}$	a in	$K \times 10^{-3}$ psi $\sqrt{in}$
1×10^{-6}	0·24	1·79						
2×10^{-6}	0·35	2·17	0·27	1·92				
4×10^{-6}	0·49	2·65	0·38	2·30				
6×10^{-6}	0·61	3·03	0·49	2·66				
8×10^{-6}	0·69	3·34	0·62	3·06	0·23	3·57		
1×10^{-5}	0·76	3·57	0·71	3·38	0·26	3·79		
2×10^{-5}	0·92	4·27	0·90	4·17	0·35	4·47	0·40	4·81
4×10^{-5}	1·05	4·95	1·04	5·29	0·46	5·18	0·52	5·58
6×10^{-5}	1·11	5·36	1·13	5·59	0·52	5·61	0·58	6·01
8×10^{-5}	1·14	5·66	1·16	5·83	0·57	5·92	0·63	6·31
1×10^{-4}	1·17	5·90			0·61	6·16	0·66	6·54
2×10^{-4}	1·24	6·69			0·71	6·92	0·76	7·27
4×10^{-4}					0·81	7·69	0·85	8·02
6×10^{-4}					0·86	8·14	0·90	8·47
8×10^{-4}					0·90	8·47	0·93	8·80
1×10^{-3}					0·93	8·72	0·96	9·05

Table 8

EFFECT OF d/b ON THE CRACK PROPAGATION RATE OF 3" WIDE PANELS

(iii) $\underline{d/b = 2{\cdot}1}$

Alternating stress	3600 psi				7200 psi			
Test No.	290		291		287		288	
$\frac{da}{dN}$ inches per cycle	a in	$K \times 10^{-3}$ psi $\sqrt{in}$	a in	$K \times 10^{-3}$ psi $\sqrt{in}$	a in	$K \times 10^{-3}$ psi $\sqrt{in}$	a in	$K \times 10^{-3}$ psi $\sqrt{in}$
2×10^{-6}	0·36	2·21	0·32	2·09				
4×10^{-6}	0·55	2·86	0·45	2·53				
6×10^{-6}	0·67	3·25	0·58	2·94				
8×10^{-6}	0·74	3·52	0·68	3·30	0·27	3·83		
1×10^{-5}	0·80	3·72	0·76	3·56	0·29	4·02	0·29	4·04
2×10^{-5}	0·94	4·36	0·93	4·29	0·38	4·68	0·42	4·90
4×10^{-5}	1·06	5·03	1·05	4·98	0·51	5·51	0·51	5·55
6×10^{-5}	1·12	5·43	1·11	5·39	0·59	6·03	0·57	5·90
8×10^{-5}	1·15	5·73	1·15	5·70	0·64	6·39	0·60	6·15
1×10^{-4}	1·18	5·98	1·17	5·94	0·68	6·67	0·63	6·35
2×10^{-4}	1·24	6·77			0·79	7·49	0·72	6·97
4×10^{-4}					0·88	8·30	0·81	7·64
6×10^{-4}							0·85	8·08
8×10^{-4}							0·89	8·36
1×10^{-3}							0·91	8·60
2×10^{-3}							0·99	9·38

Table 9

EFFECT OF d/b ON THE CRACK PROPAGATION RATE OF 3" WIDE PANELS

(iv) d/b = 3·2

Alternating stress	3600 psi				7200 psi			
Test No.	283		284		285		286	
$\frac{da}{dN}$ inches per cycle	a in	$K \times 10^{-3}$ psi $\sqrt{in}$	a in	$K \times 10^{-3}$ psi $\sqrt{in}$	a in	$K \times 10^{-3}$ psi $\sqrt{in}$	a in	$K \times 10^{-3}$ psi $\sqrt{in}$
2×10^{-6}	0·29	1·97	0·29	1·99				
4×10^{-6}	0·42	2·42	0·51	2·72				
6×10^{-6}	0·54	2·81	0·63	3·11				
8×10^{-6}	0·64	3·14	0·71	3·38	0·27	3·89		
1×10^{-5}	0·71	3·40	0·76	3·58	0·32	4·24		
2×10^{-5}	0·89	4·13	0·91	4·21	0·44	5·05		
4×10^{-5}	1·03	4·81	1·03	4·86	0·54	5·74		
6×10^{-5}	1·09	5·22	1·09	5·26	0·60	6·13	0·57	5·95
8×10^{-5}	1·13	5·51	1·13	5·55	0·64	6·42	0·61	6·18
1×10^{-4}	1·15	5·75	1·16	5·78	0·67	6·64	0·63	6·36
2×10^{-4}			1·23	6·56	0·77	7·34	0·71	6·93
4×10^{-4}			1·28	7·42	0·86	8·08	0·79	7·55
6×10^{-4}					0·91	8·53	0·84	7·93
8×10^{-4}					0·94	8·85	0·87	8·22
1×10^{-3}					0·96	9·11	0·90	8·44
2×10^{-3}							0·97	9·19

Table 10

EFFECT OF d/b ON THE CRACK PROPAGATION RATE OF 3" WIDE PANELS

(v) $d/b = 4 \cdot 75$

Alternating stress	3600 psi				7200 psi			
Test No.	311		314		316		317	
$\frac{da}{dN}$ inches per cycle	a in	$K \times 10^{-3}$ psi $\sqrt{in}$	a in	$K \times 10^{-3}$ psi $\sqrt{in}$	a in	$K \times 10^{-3}$ psi $\sqrt{in}$	a in	$K \times 10^{-3}$ psi $\sqrt{in}$
2×10^{-6}	0·25	1·83	0·25	1·81				
4×10^{-6}	0·57	2·91	0·47	2·59				
6×10^{-6}	0·72	3·44	0·63	3·10	0·24	3·65	0·25	3·67
8×10^{-6}	0·81	3·76	0·72	3·42	0·27	3·83	0·28	3·97
1×10^{-5}	0·86	3·99	0·78	3·65	0·29	3·98	0·31	4·19
2×10^{-5}	1·00	4·67	0·94	4·34	0·35	4·45	0·41	4·87
4×10^{-5}	1·11	5·37	1·06	5·01	0·44	5·05	0·51	5·54
6×10^{-5}	1·16	5·80	1·11	5·42	0·51	5·53	0·57	5·95
8×10^{-5}	1·19	6·11	1·15	5·72	0·57	5·91	0·62	6·24
1×10^{-4}	1·21	6·36	1·17	5·96	0·61	6·21	0·65	6·47
2×10^{-4}					0·74	7·11	0·75	7·20
4×10^{-4}					0·84	7·94	0·84	7.95
6×10^{-4}					0·89	8·41	0·89	8·40
8×10^{-4}					0·93	8·75	0·93	8·72

Table 11

EFFECT OF PANEL WIDTH ON THE CRACK PROPAGATION RATE

(1) Width = 1½".

Alternating stress	3600 psi										7200 psi							
Test No.	20		21		22		24		25		17		18		19		23	
$\frac{da}{dN}$ inches per cycle	a in	K x 10^{-3} psi $\sqrt{in}$	a in	K x 10^{-3} psi $\sqrt{in}$	a in	K x 10^{-3} psi $\sqrt{in}$	a in	K x 10^{-3} psi $\sqrt{in}$	a in	K x 10^{-3} psi $\sqrt{in}$	a in	K x 10^{-3} psi $\sqrt{in}$	a in	K x 10^{-3} psi $\sqrt{in}$	a in	K x 10^{-3} psi $\sqrt{in}$	a in	K x 10^{-3} psi $\sqrt{in}$
0.39×10^{-6}					0.11	1.22	0.11	1.24	0.11	1.21								
0.79×10^{-6}	0.15	1.44	0.15	1.43	0.15	1.45	0.15	1.47	0.15	1.44								
1.58×10^{-6}	0.23	1.85	0.21	1.74	0.21	1.77	0.25	1.94	0.23	1.82								
2.36×10^{-6}	0.30	2.21	0.26	2.01	0.27	2.08	0.32	2.32	0.30	2.19	0.07	1.88	0.07	1.90	0.06	1.75	0.07	1.97
3.15×10^{-6}	0.34	2.43	0.30	2.23	0.32	2.30	0.35	2.54	0.33	2.41	0.08	2.11	0.08	2.12	0.08	2.07	0.12	2.59
0.39×10^{-5}	0.36	2.59	0.33	2.39	0.34	2.47	0.38	2.70	0.36	2.57	0.10	2.39	0.10	2.35	0.11	2.44	0.15	2.92
0.79×10^{-5}	0.42	3.04	0.40	2.85	0.41	2.93	0.43	3.15	0.42	3.03	0.22	3.62	0.21	3.55	0.21	3.55	0.22	3.65
1.58×10^{-5}	0.46	3.50									0.28	4.28	0.28	4.23	0.27	4.20	0.28	4.23
2.36×10^{-5}															0.30	4.53	0.30	4.55
3.15×10^{-5}															0.32	4.75	0.32	4.77
0.39×10^{-4}															0.33	4.92	0.34	4.93

Table 12

EFFECT OF PANEL WIDTH ON THE CRACK PROPAGATION RATE

(ii) Width = 3"

Alternating stress	3600 psi						7200 psi					
Test No.	350		352		355		351		353		354	
$\frac{da}{dN}$ inches per cycle	a in	$K \times 10^{-3}$ psi $\sqrt{in}$	a in	$K \times 10^{-3}$ psi $\sqrt{in}$	a in	$K \times 10^{-3}$ psi $\sqrt{in}$	a in	$K \times 10^{-3}$ psi $\sqrt{in}$	a in	$K \times 10^{-3}$ psi $\sqrt{in}$	a in	$K \times 10^{-3}$ psi $\sqrt{in}$
2×10^{-6}			0·29	1·97	0·27	1·90						
4×10^{-6}	0·42	2·44	0·45	2·51	0·40	2·34						
6×10^{-6}	0·54	2·81	0·55	2·85	0·51	2·70						
8×10^{-6}	0·61	3·06	0·62	3·10	0·60	3·03			0·23	3·54		
1×10^{-5}	0·67	3·25	0·68	3·29	0·68	3·29	0·25	3·71	0·25	3·72	0·22	3·46
2×10^{-5}	0·82	3·83	0·85	3·91	0·87	4·03	0·37	4·56	0·33	4 27	0·34	4·40
4×10^{-5}	0·96	4·43	0·98	4·55	1·01	4·71	0·46	5·17	0·41	4·83	0·44	5·06
6×10^{-5}	1·02	4·81	1·05	4·93	1·07	5·11	0·51	5·49	0·46	5·19	0·49	5·42
8×10^{-5}	1·07	5·08	1·09	5·22	1·11	5·41	0·54	5·72	0·50	5·46	0·53	5·66
1×10^{-4}	1·10	5·30	1·12	5·44	1·14	5·64	0·57	5·89	0·54	5·68	0·56	5·80
2×10^{-4}			1·20	6·19	1·22	6·41	0·64	6·42	0·64	6·40	0·65	6·45
4×10^{-4}							0·72	6·98	0·75	7·16	0·73	7·08
6×10^{-4}							0·77	7·33	0·80	7·60	0·79	7·47
8×10^{-4}							0·80	7·59	0·84	7·93	0·82	7·75
1×10^{-3}							0·83	7·80	0·87	8·18	0·85	7·98

Table 13

EFFECT OF PANEL WIDTH ON THE CRACK PROPAGATION RATE

(iii) Width = $4\frac{1}{2}$"

Alternating stress	3600 psi						7200 psi					
Test No.	359		360		361		362		363		364	
$\frac{da}{dN}$ inches per cycle	a in	$K \times 10^{-3}$ psi $\sqrt{in}$	a in	$K \times 10^{-3}$ psi $\sqrt{in}$	a in	$K \times 10^{-3}$ psi $\sqrt{in}$	a in	$K \times 10^{-3}$ psi $\sqrt{in}$	a in	$K \times 10^{-3}$ psi $\sqrt{in}$	a in	$K \times 10^{-3}$ psi $\sqrt{in}$
4×10^{-6}	0·40	2·33	0·41	2·35	0·43	2·40						
6×10^{-6}	0·55	2·75	0·57	2·81	0·58	2·83						
8×10^{-6}	0·65	3·03	0·67	3·08	0·69	3·12						
1×10^{-5}	0·73	3·24	0·75	3·28	0·77	3·35						
2×10^{-5}	0·97	3·88	0·97	3·87	1·03	4·05	0·36	4·46	0·35	4·37		
4×10^{-5}	1·20	4·56	1·17	4·47	1·26	4·77	0·46	5·08	0·46	5·08	0·46	5·08
6×10^{-5}	1·32	4·97	1·28	4·85	1·38	5·20	0·53	5·46	0·54	5·55	0·55	5·58
8×10^{-5}	1·40	5·27	1·36	5·12	1·46	5·52	0·58	5·75	0·61	5·92	0·61	5·89
1×10^{-4}	1·46	5·51	1·42	5·35	1·51	5·77	0·63	6·00	0·67	6·24	0·65	6·11
2×10^{-4}	1·62	6·31	1·58	6·10	1·66	6·60	0·79	6·89	0·87	7·32	0·76	6·73
4×10^{-4}			1·71	6·92	1·78	7·50	0·97	7·89	1·05	8·37	0·86	7·29
6×10^{-4}							1·07	8·48	1·15	8·96	0·92	7·61
8×10^{-4}							1·14	8·90	1·21	9·37	0·96	7·83
1×10^{-3}							1·19	9·21			0·99	8·00
2×10^{-3}							1·33	10·2			1·08	8·54
4×10^{-3}											1·17	9·10

Table 14.

EFFECT OF PANEL WIDTH ON THE CRACK PROPAGATION RATE

(iv) Width = $6\frac{1}{2}$"

Alternating stress	3600 psi						7200 psi					
Test No.	365		366		369		367		368		370	
$\frac{da}{dN}$ inches per cycle	a in	$K \times 10^{-3}$ psi $\sqrt{in}$	a in	$K \times 10^{-3}$ psi $\sqrt{in}$	a in	$K \times 10^{-3}$ psi $\sqrt{in}$	a in	$K \times 10^{-3}$ psi $\sqrt{in}$	a in	$K \times 10^{-3}$ psi $\sqrt{in}$	a in	$K \times 10^{-3}$ psi $\sqrt{in}$
4×10^{-6}	0·49	2·54	0·44	2·43	0·43	2·40						
6×10^{-6}	0·62	2·89	0·61	2·86	0·63	2·92						
8×10^{-6}	0·72	3·14	0·73	3·15	0·77	3·25						
1×10^{-5}	0·81	3·34	0·82	3·37	0·88	3·50						
2×10^{-5}	1·14	4·08	1·13	4·06	1·22	4·26						
4×10^{-5}	1·56	5·05	1·45	4·79	1·56	5·04	0·46	5·01	0·46	5·01	0·48	5·11
6×10^{-5}	1·79	5·63	1·64	5·25	1·74	5·52	0·55	5·48	0·55	5·48	0·57	5·63
8×10^{-5}	1·93	6·04	1·77	5·59	1·87	5·87	0·61	5·81	0·61	5·83	0·65	5·99
1×10^{-4}	2·03	6·36	1·87	5·86	1·96	6·15	0·66	6·07	0·67	6·11	0·70	6·27
2×10^{-4}	2·28	7·35	2·14	6·75	2·21	7·06	0·84	6·90	0·88	7·08	0·89	7·13
4×10^{-4}							1·04	7·83	1·14	8·28	1·09	8·05
6×10^{-4}							1·17	8·43	1·30	9·02	1·21	8·61
8×10^{-4}							1·27	8·88	1·41	9·54	1·30	9·02
1×10^{-3}							1·35	9·23	1·50	9·94	1·37	9·35
2×10^{-3}							1·58	10·4			1·59	10·4
4×10^{-3}							1·79	11·5				

Table 15

EFFECT OF PANEL WIDTH ON THE CRACK PROPAGATION RATE

(v) Width = 10"

Alternating stress	3600 psi						7200 psi					
Test No.	382		383		384		385		386		387	
$\frac{da}{dN}$ inches per cycle	a in	$K \times 10^{-3}$ psi $\sqrt{in}$	a in	$K \times 10^{-3}$ psi $\sqrt{in}$	a in	$K \times 10^{-3}$ psi $\sqrt{in}$	a in	$K \times 10^{-3}$ psi $\sqrt{in}$	a in	$K \times 10^{-3}$ psi $\sqrt{in}$	a in	$K \times 10^{-3}$ psi $\sqrt{in}$
4×10^{-6}	0·42	2·35	0·33	2·08	0·43	2·37						
6×10^{-6}	0·58	2·77	0·55	2·70	0·60	2·83						
8×10^{-6}	0·70	3·04	0·70	3·06	0·73	3·11						
1×10^{-5}	0·78	3·24	0·82	3·32	0·83	3·32						
2×10^{-5}	1·07	3·81	1·18	4·02	1·14	3·94					0·30	4·03
4×10^{-5}	1·41	4·45	1·53	4·66	1·48	4·57	0·45	4·87			0·47	5·05
6×10^{-5}	1·69	4·95	1·73	5·01	1·71	4·98	0·54	5·42	0·48	5·10	0·57	5·56
8×10^{-5}	1·97	5·46	1·86	5·26	1·89	5·31	0·61	5·78	0·58	5·60	0·64	5·90
1×10^{-4}	2·23	5·94	1·97	5·45	2·05	5·60	0·67	6·04	0·66	5·98	0·69	6·15
2×10^{-4}	2·92	7·38	2·30	6·06	2·60	6·67	0·86	6·86	0·93	7·18	0·87	6·92
4×10^{-4}			2·62	6·70	3·10	7·85	1·08	7·78	1·30	8·60	1·09	7·80
6×10^{-4}			2·80	7·11			1·28	8·52	1·56	9·57	1·28	8·54
8×10^{-4}			2·93	7·41			1·48	9·27	1·75	10·3	1·52	9·40
1×10^{-3}							1·68	9·99	1·90	10·8	1·75	10·2
2×10^{-3}											2·30	12·3

Table 16

EFFECT OF PANEL WIDTH ON THE CRACK PROPAGATION RATE

(vi) . Width = 20"

Alternating stress	3600 psi						7200 psi					
Test No.	391		409		410		406		411		412	
$\frac{da}{dN}$ inches per cycle	a in	$K \times 10^{-3}$ psi $\sqrt{in}$	a in	$K \times 10^{-3}$ psi $\sqrt{in}$	a in	$K \times 10^{-3}$ psi $\sqrt{in}$	a in	$K \times 10^{-3}$ psi $\sqrt{in}$	a in	$K \times 10^{-3}$ psi $\sqrt{in}$	a in	$K \times 10^{-3}$ psi $\sqrt{in}$
4×10^{-6}					0·32	2·05						
6×10^{-6}			0·60	2·80	0·63	2·87						
8×10^{-6}	0·62	2·86	0·81	3·26	0·83	3·31						
1×10^{-5}	0·80	3·25	0·97	3·57	0·99	3·61						
2×10^{-5}	1·34	4·21	1·43	4·37	1·46	4·40						
4×10^{-5}	1·84	5·00	1·86	5·01	1·89	5·05	0·59	5·64	0·41	4·70	0·46	4·95
6×10^{-5}	2·11	5·36	2·10	5·34	2·14	5·39	0·74	6·33	0·57	5·52	0·60	5·70
8×10^{-5}	2·31	5·62	2·26	5·55	2·31	5·63	0·84	6·76	0·67	6·01	0·70	6·16
1×10^{-4}	2·45	5·81	2·38	5·71	2·45	5·81	0·92	7·05	0·75	6·35	0·78	6·47
2×10^{-4}	2·90	6·39	2·74	6·19	2·93	6·42	1·13	7·84	0·97	7·24	0·99	7·30
4×10^{-4}	3·34	6·95	3·12	6·66	4·23	8·08	1·31	8·45	1·16	7·94	1·17	7·96
6×10^{-4}	3·62	7·29	3·37	6·98	5·72	10·25	1·40	8·74	1·26	8·28	1·26	8·27
8×10^{-4}	3·82	7·56	3·61	7·28			1·46	8·92	1·33	8·50	1·32	8·48
1×10^{-3}	4·00	7·78	3·99	7·77			1·49	9·05	1·38	8·66		
2×10^{-3}	4·73	8·76										

Table 17

EFFECT OF ROLLING DIRECTION ON THE CRACK PROPAGATION RATE OF $4\frac{1}{2}$" WIDE PANELS

(i) Alternating stress = 3600 psi

Rolling direction	Longitudinal						Transverse					
Test No.	359		360		361		376		377		378	
$\frac{da}{dN}$ inches per cycle	a in	$K \times 10^{-3}$ psi $\sqrt{in}$	a in	$K \times 10^{-3}$ psi $\sqrt{in}$	a in	$K \times 10^{-3}$ psi $\sqrt{in}$	a in	$K \times 10^{-3}$ psi $\sqrt{in}$	a in	$K \times 10^{-3}$ psi $\sqrt{in}$	a in	$K \times 10^{-3}$ psi $\sqrt{in}$
4×10^{-6}	0·40	2·33	0·41	2·35	0·43	2·40			0·41	2·36	0·40	2·32
6×10^{-6}	0·55	2·75	0·57	2·81	0·58	2·83	0·51	2·63	0·53	2·69	0·56	2·78
8×10^{-6}	0·65	3·03	0·67	3·08	0·69	3·12	0·61	2·90	0·61	2·93	0·66	3·06
1×10^{-5}	0·73	3·24	0·75	3·28	0·77	3·35	0·68	3·11	0·68	3·12	0·74	3·26
2×10^{-5}	0·97	3·88	0·97	3·87	1·03	4·05	0·91	3·73	0·92	3·73	0·96	3·85
4×10^{-5}	1·20	4·56	1·17	4·47	1·26	4·77	1·14	4·37	1·15	4·42	1·16	4·45
6×10^{-5}	1·32	4·97	1·28	4·85	1·38	5·20	1·26	4·77	1·28	4·84	1·27	4·82
8×10^{-5}	1·40	5·27	1·36	5·12	1·46	5·52	1·34	5·06	1·37	5·15	1·35	5·10
1×10^{-4}	1·46	5·51	1·42	5·35	1·51	5·77	1·40	5·30	1·43	5·39	1·41	5·32
2×10^{-4}	1·62	6·31	1·58	6·10	1·66	6·60	1·57	6·06	1·59	6·19	1·57	6·06
4×10^{-4}			1·71	6·92	1·78	7·50	1·71	6·91			1·71	6·89

Table 18

EFFECT OF ROLLING DIRECTION ON THE CRACK PROPAGATION RATE OF 4½" WIDE PANELS

(ii) Alternating stress = 7200 psi

Rolling direction	Longitudinal						Transverse					
Test No.	362		363		364		379		380		381	
$\frac{da}{dN}$ inches per cycle	a in	$K \times 10^{-3}$ psi $\sqrt{in}$	a in	$K \times 10^{-3}$ psi $\sqrt{in}$	a in	$K \times 10^{-3}$ psi $\sqrt{in}$	a in	$K \times 10^{-3}$ psi $\sqrt{in}$	a in	$K \times 10^{-3}$ psi $\sqrt{in}$	a in	$K \times 10^{-3}$ psi $\sqrt{in}$
2×10^{-5}	0·36	4·46	0·35	4·37							0·33	4·25
4×10^{-5}	0·46	5·08	0·46	5·08	0·46	5·08	0·44	4·97	0·42	4·81	0·44	4·97
6×10^{-5}	0·53	5·46	0·54	5·55	0·55	5·58	0·52	5·43	0·51	5·38	0·52	5·39
8×10^{-5}	0·58	5·75	0·61	5·92	0·61	5·89	0·58	5·74	0·59	5·80	0·57	5·69
1×10^{-4}	0·63	6·00	0·67	6·24	0·65	6·11	0·62	5·98	0·65	6·13	0·61	5·93
2×10^{-4}	0·79	6·89	0·87	7·32	0·76	6·73	0·76	6·75	0·84	7·18	0·75	6·70
4×10^{-4}	0·97	7·89	1·05	8·37	0·86	7·29	0·91	7·54	1·02	8·20	0·90	7·53
6×10^{-4}	1·07	8·48	1·15	8·96	0·92	7·61	0·99	8·02	1·12	8·78	0·99	8·04
8×10^{-4}	1·14	8·90	1·21	9·37	0·96	7·83	1·05	8·38	1·18	9·18	1·06	8·41
1×10^{-3}	1·19	9·21			0·99	8·00	1·10	8·66	1·23	9·50	1·10	8·70
2×10^{-3}	1·33	10·2			1·08	8·54	1·24	9·55			1·25	9·62
4×10^{-3}					1·17	9·10						

Table 19

EFFECT OF ANTI-BUCKLING BARS ON THE CRACK PROPAGATION OF 20" PANELS

Alternating stress = 3600 psi

Test condition	Without anti-buckle bars						With anti-buckle bars			
Test No.	391		409		410		388			405
$\frac{da}{dN}$ inches per cycle	a in	$K \times 10^{-3}$ psi $\sqrt{in}$	a in	$K \times 10^{-3}$ psi $\sqrt{in}$	a in	$K \times 10^{-3}$ psi $\sqrt{in}$	a in	$K \times 10^{-3}$ psi $\sqrt{in}$	a in	$K \times 10^{-3}$ psi $\sqrt{in}$
4×10^{-6}					0·32	2·05				
6×10^{-6}			0·60	2·80	0·63	2·87				
8×10^{-6}	0·62	2·86	0·81	3·26	0·83	3·31	0·75	3·14		
1×10^{-5}	0·80	3·25	0·97	3·57	0·99	3·61	0·92	3·47		
2×10^{-5}	1·34	4·21	1·43	4·37	1·46	4·40	1·40	4·32	1·18	3·96
4×10^{-5}	1·84	5·00	1·86	5·01	1·89	5·05	1·86	5·01	1·58	4·59
6×10^{-5}	2·11	5·36	2·10	5·34	2·14	5·39	2·13	5·37	1·82	4·95
8×10^{-5}	2·31	5·62	2·26	5·55	2·31	5·63	2·31	5·62	2·02	5·24
1×10^{-4}	2·45	5·81	2·38	5·71	2·45	5·81	2·45	5·81	2·22	5·51
2×10^{-4}	2·90	6·39	2·74	6·19	2·93	6·42	2·94	6·43		
4×10^{-4}	3·34	6·95	3·12	6·66	4·23	8·08	3·65	7·34		
6×10^{-4}	3·62	7·29	3·37	6·98	5·72	10·25	4·87	8·95		
8×10^{-4}	3·82	7·56	3·61	7·28			5·64	10·11		
1×10^{-3}	4·00	7·78	3·99	7·77			6·06	10·83		
2×10^{-3}	4·73	8·76					6·98	12·77		
4×10^{-3}							7·63	14·67		

Table 20

CRACK PROPAGATION RATES OF 3" WIDE PANELS WITH CLADDING REMOVED

Alternating stress	3600 psi						7200 psi					
Test No.	320		321		326		322		323		327	
$\frac{da}{dN}$ inches per cycle	a in	$K \times 10^{-3}$ psi $\sqrt{in}$	a in	$K \times 10^{-3}$ psi $\sqrt{in}$	a in	$K \times 10^{-3}$ psi $\sqrt{in}$	a in	$K \times 10^{-3}$ psi $\sqrt{in}$	a in	$K \times 10^{-3}$ psi $\sqrt{in}$	a in	$K \times 10^{-3}$ psi $\sqrt{in}$
8×10^{-7}	0·19	1·66										
1×10^{-6}	0·22	1·77										
2×10^{-6}	0·31	2·11	0·26	1·99	0·22	1·92						
4×10^{-6}	0·41	2·47	0·39	2·47	0·33	2·34						
6×10^{-6}	0·49	2·75	0·52	2·94	0·40	2·64						
8×10^{-6}	0·58	3·04	0·65	3·37	0·48	2·91						
1×10^{-5}	0·66	3·32	0·73	3·68	0·55	3·18			0·21	3·84	0·20	3·72
2×10^{-5}	0·87	4·14	0·91	4·48	0·79	4·10	0·30	4·37	0·29	4·53	0·27	4·27
4×10^{-5}	1·01	4·87	1·04	5·22	0·95	4·89	0·44	5·43	0·37	5·18	0·34	4·89
6×10^{-5}	1·07	5·29	1·10	5·66	1·02	5·34	0·51	5·93	0·42	5·55	0·40	5·34
8×10^{-5}	1·11	5·60	1·14	5·98	1·07	5·66	0·56	6·27	0·45	5·82	0·45	5·73
1×10^{-4}	1·14	5·85	1·16	6·24	1·10	5·91	0·60	6·54	0·48	6·03	0·50	6·08
2×10^{-4}	1·22	6·64	1·23	7·08	1·18	6·74	0·70	7·34	0·57	6·70	0·64	7·16
4×10^{-4}	1·27	7·52			1·25	7·65	0·80	8·15	0·66	7·42	0·76	8·14
6×10^{-4}							0·85	8·63	0·72	7·86	0·82	8·68
8×10^{-4}							0·89	8·98	0·75	8·19	0·86	9·06
1×10^{-3}							0·92	9·25	0·78	8·44	0·89	9·35
2×10^{-3}									0·87	9·28		
4×10^{-3}									0·95	10·16		

SYMBOLS

a, a_o	- crack half-length
a_1	- crack half-length corrected for plasticity
A	- a constant
A_j	- a constant coefficient
b	- sheet half-width
B	- a constant
C_1, C_2, C_3	- constants
d	- half the free length of a sheet
E	- Young's Modulus
E_s	- secant modulus
j	- index (= 0, 1, 2, 3)
k	- strain concentration factor
K	- stress intensity factor (based on σ_a)
$K_C, K_N, K_T, K_{TN}, K_F$	- stress concentration factors (section 3)
K_W	- a finite width correction (equation 55)
m	- constant exponent in stress-strain law (section 3.3.1)
N, N_o	- number of cycles
r	- polar co-ordinates
r_o	- length of plastic zone ahead of the crack
R	- ratio of minimum stress to maximum stress (= 0·1)
R_o	- r_o/a
s	- a constant
t	- sheet thickness
X	- $\exp(C_1 N)$
Y	- $(1 - a/b)^{s+1}$
Z	- ratio of operating stress to yield stress
α_D	- Dixon's finite width correction
α_G	- Greenspan's finite width correction
α_W	- Westergaard's finite width correction
β	- dimensionless parameter (defined in (33))
γ	- dimensionless parameter (defined in (53))
γ_F	- dimensionless parameter (defined in (56))

SYMBOLS (CONTD)

ε	- strain
$\varepsilon_o, \varepsilon'_o$	- reference points on the stress-strain curve
ε_c	- critical strain (section 3.3.1)
ε_n	- average strain on net section
θ	- polar co-ordinate
λ	- a constant
ρ	- radius of crack tip
ρ'	- a material constant
σ	- a stress
σ_a	- amplitude of alternating stress on gross area
σ_n	- maximum average stress on net-section
σ_p	- peak stress on gross area
σ_∞	- stress applied at infinity
σ_y	- yield stress
σ_o, σ'_o	- reference points on the stress-strain curve
σ_b	- buckling stress

REFERENCES

No.	Author	Title, etc
1	J. Schijve, D. Broek, P. de Rijk	The effect of the frequency of an alternating load on the crack rate in a light alloy sheet. NLR-TN M.2092, Nationaal Luchtvaartlaboratorium, Amsterdam (1961)
2	W. Barrois	Critical study on fatigue crack propagation. A.R.C. 25623 (1964)
3	P.C. Paris	A note on variables affecting the rate of crack growth due to cyclic loading. Boeing Report D-17867, Boeing Aircraft Co., (1957)
4	D.R. Donaldson, W.E. Anderson	Crack propagation behaviour of some airframe materials. Proceedings of the Crack Propagation Symposium, 2, 375, Cranfield, (1961)
5	H.F. Hardrath, A.J. McEvily	Engineering aspects of fatigue crack propagation. Cranfield Symposium, 1, 231, (1961)
6	P. Kuhn I.E. Figge	Unified notch-strength analysis for wrought aluminum alloys. NASA TN D-1259, (1962)
7	E.R. Welbourne	The correlation of unstable crack length data for sheet materials. Aeronaut Q, XII, pp 395-408, (1961)
8	F.J. Bradshaw, C. Wheeler	The effect of environment on the crack propagation in aluminium alloys. To be published
9	E.H. Mansfield	On theoretical plasticity and crack propagation. A.R.C. C.P. 688, (1962)
10	N.J.F. Gunn	Fatigue cracking rates and residual strengths of eight aluminium sheet alloys. R.A.E. TR 64024, (1964)
11	N.E. Frost D.S. Dugdale	The propagation of fatigue cracks in sheet specimens. J. Mech Phys Solids, 6, 92, (1958)
12	H.W. Liu	Crack propagation in thin metal sheet under repeated loading. Trans A.S.M.E., Series D, J. Basic Engineering, 83, 23, (1961)

REFERENCES (CONTD)

No.	Author	Title, etc.
13	A.K. Head	The growth of fatigue cracks. Phil Mag., 44, 925, (1953)
14	W. Weibull	The effect of size and stress history on fatigue crack initiation and propagation. Cranfield Symposium, 2, 271, (1961)
15	G.R. Irwin	Analysis of stress and strain near the end of a crack traversing a plate. J. Appl.Mech., 24, pp 361-364 (1957)
16	G.R. Irwin	Fracture. Handbach der Physik 16, (Elasticity and Plasticity), Springer-Verlag, (1958)
17	H.M. Westergaard	Bearing pressures and cracks. J. Appl.Mech., 6, A-49, (1939)
18	G.R. Irwin, J.A. Kies	Fracturing and fracture dynamics. Welding Journal, 31, 95-s, (1952)
19	G.R. Irwin, J.A. Kies	Critical energy rate analysis of fracture strength. Welding Research (Suppl. Welding Journal), 19, 193, (1954)
20	M. Greenspan	Axial rigidity of perforated structural members. J. Research Nat. Bur. of Standards, 31, 305, (1943)
21	J.R. Dixon	Stress distribution around edge slits in a plate loaded in tension - the effect of finite width of plate. J. Roy. Aero. Soc., 66, 320, (1962)
22	A.S.T.M. Bulletin 243	Fracture testing of high strength sheet materials (1960)
23	D.P. Rooke	Elastic yield zones round a crack tip. (Comparison of exact and approximate theories. A.R.C. 25443 (1963)
24	Royal Aeronautical Society	Fatigue crack propagation in aluminium alloy sheet materials. Data Sheet, Fatigue A.06.04
25	H. Neuber	Theory of notch stresses. (Trans By D. Taylor) J.W. Edwards, Michigan, (1946)

REFERENCES (CONTD)

No.	Author	Title, etc.
26	Royal Aeronautical Society	Information on the use of Data Sheets 00.02, Data Sheet, Structures 1, 00.02.00
27	R.C.J. Howland	On the stresses in the neighbourhood of a circular hold in a strip under tension. Phil. Trans. Roy. Soc., A.229, 49, (1930)
28	Royal Aeronautical Society	Effective strain concentration factors for cracks in unreinforced sheets under tension. Data Sheet, Fatigue, A.06.02
29	P. Kuhn	Notch effects on fatigue and static strength. Symposium on Aeronautical fatigue (ICAF and AGARD) Rome, (1963)
30	D.G. Ford, D.G. Graff, A.O. Payne	Some statistical aspects of fatigue life variation. Fatigue of Aircraft Structures, p.179, Pergamon (1962)
31	P.J.E. Forsythe	A two stage process of fatigue crack growth. Cranfield Symposium, 1, 76, (1961)
32	H.A. Lipsitt, F.W. Forbes, R.B. Baird	Crack propagation in cold-rolled aluminum sheet. Proc. A.S.T.M., 59, 734, (1959)
33	H.W. Liu	Discussion. Cranfield Symposium, 2, 514, (1961)
34	H.W. Liu	Size effects on fatigue crack propagation. CALCIT SM 63-7, California Institute of Technology, (1963)
35	W. Weibull	A theory of fatigue crack propagation in sheet specimens. Int. Conf. on Mechanisms of Fatigue in Crystalline Solids, 1962
36	D.A. Bateman, F.J. Bradshaw, D.P. Rooke	Some observations on surface deformation round cracks in stressed sheets. R.A.E. Tech Note CPM 63, 1964

REFERENCES (CONTD)

No.	Author	Title, etc.
37	N.E. Frost	Effect of mean stress on the rate of growth of fatigue cracks in sheet materials. J. Mech. Engineering Sci., 4, 22, (1962)
38	A.J. McEvily W. Illg	The rate of fatigue crack propagation in two aluminum alloys. NACA TN 4394, (1958)
39	G.R. Irwin	Theoretical aspects of fracture failure analysis. Metals Eng. Quart., 3, 25, (1963)

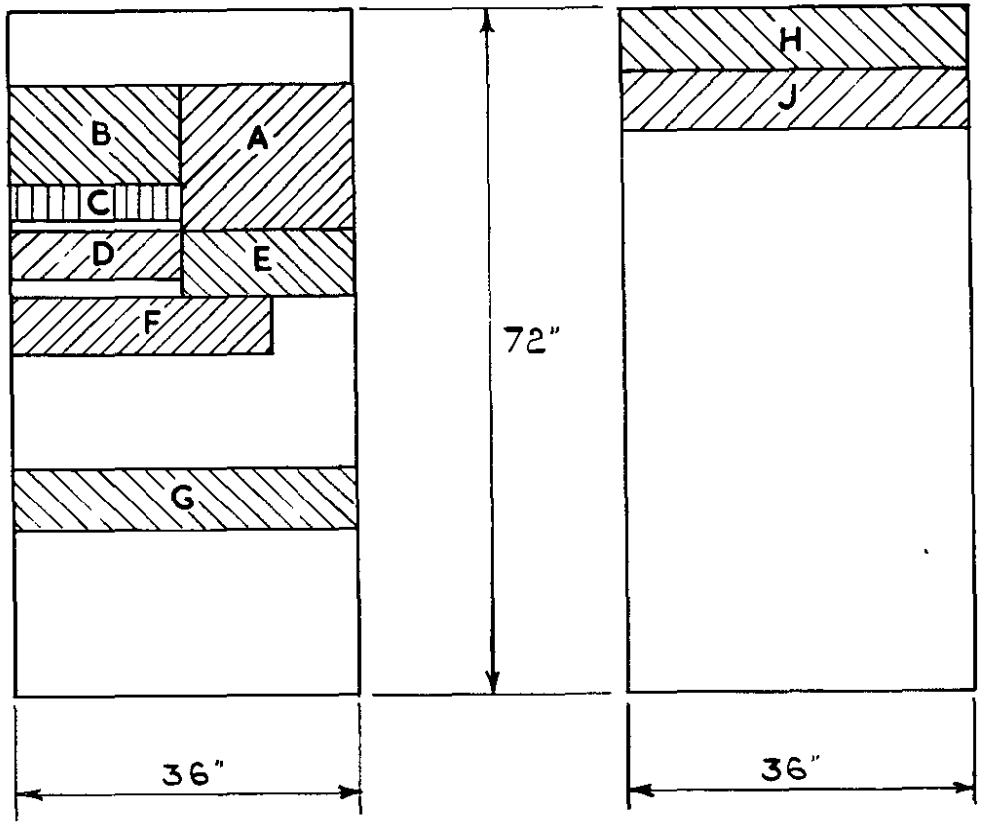

POSITION	EXPERIMENT
A	EFFECT OF d/b
B	
C	
D	
E	
F	EFFECT OF WIDTH
G	EFFECT OF CLADDING
H	SCATTER IN 3" PANELS
J	

FIG. 1 POSITIONS OF CRACK PROPAGATION PANELS FROM SHEETS IN CAST 'A'

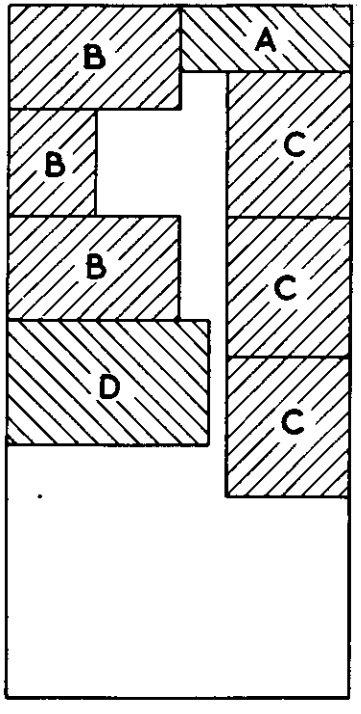

SHEET 18

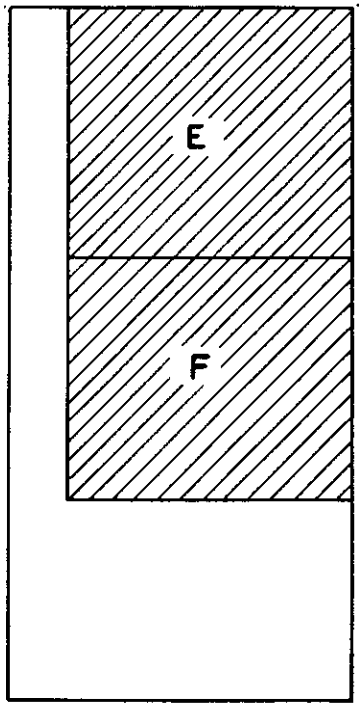

SHEET 23

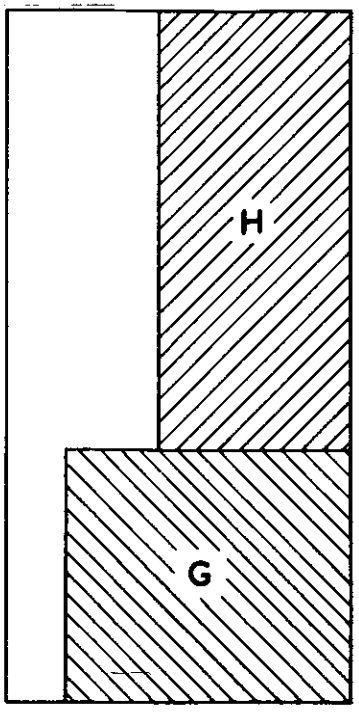

SHEETS 26, 27, & 29

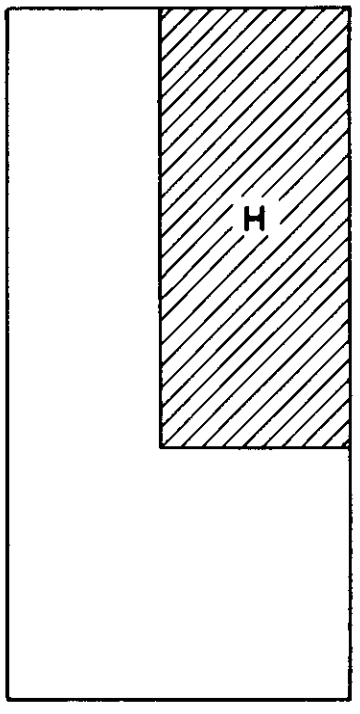

SHEETS 19, 20, 24, 25, 34, 35 & 40

POSITION	EXPERIMENT	
A	3" PANELS	EFFECT OF PANEL WIDTH
B	4½" PANELS	
C	6½" PANELS	
E & F	10" PANELS	
H	20" PANELS	
D	DIRECTIONALITY	
F & G	SCATTER IN 10" PANELS	

FIG.2. POSITIONS OF CRACK PROPAGATION PANELS FROM SHEETS IN CAST 'B'

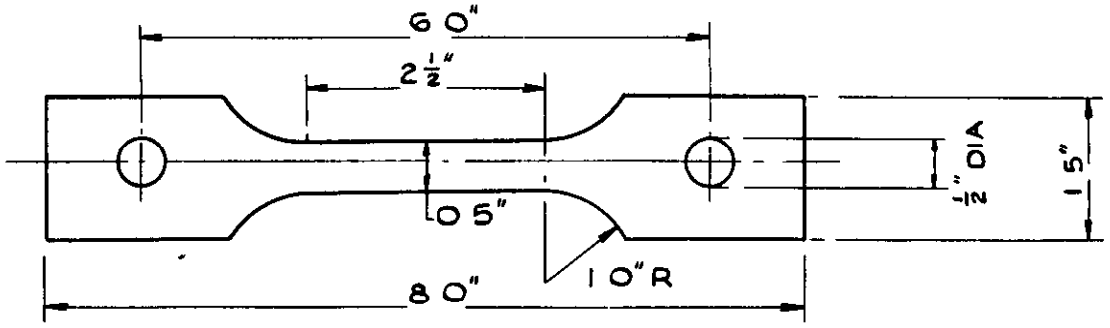

TENSILE TEST PIECE
1/2 SCALE

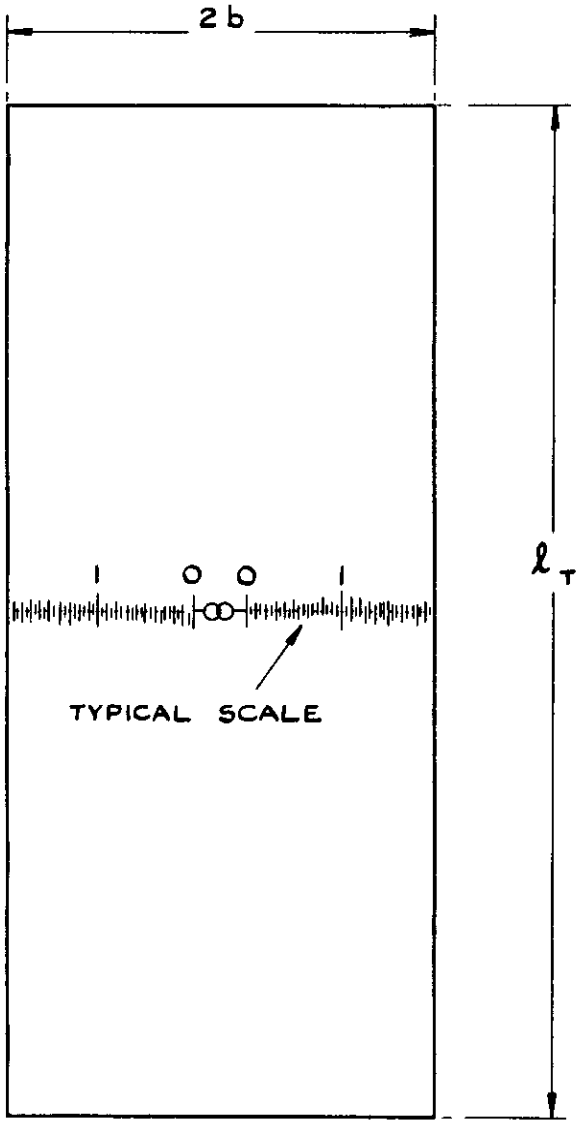

WIDTH 2b"	OVERALL LENGTH l_T"	FREE LENGTH 2d"	d/b
3	3 8	3·6	1 2
	5 1	4 8	1 6
	6 8	6 3	2 1
	10 0	9 6	3 2
	14 6	14 25	4 75
3	6 4	6	2
4 1/2	10 6	9	2
6 1/2	14 6	13	2
10	25 5	20	2
20	45 5	40	2

CRACK PROPAGATION PANEL
1/2 SCALE

FIG 3. TEST SPECIMENS

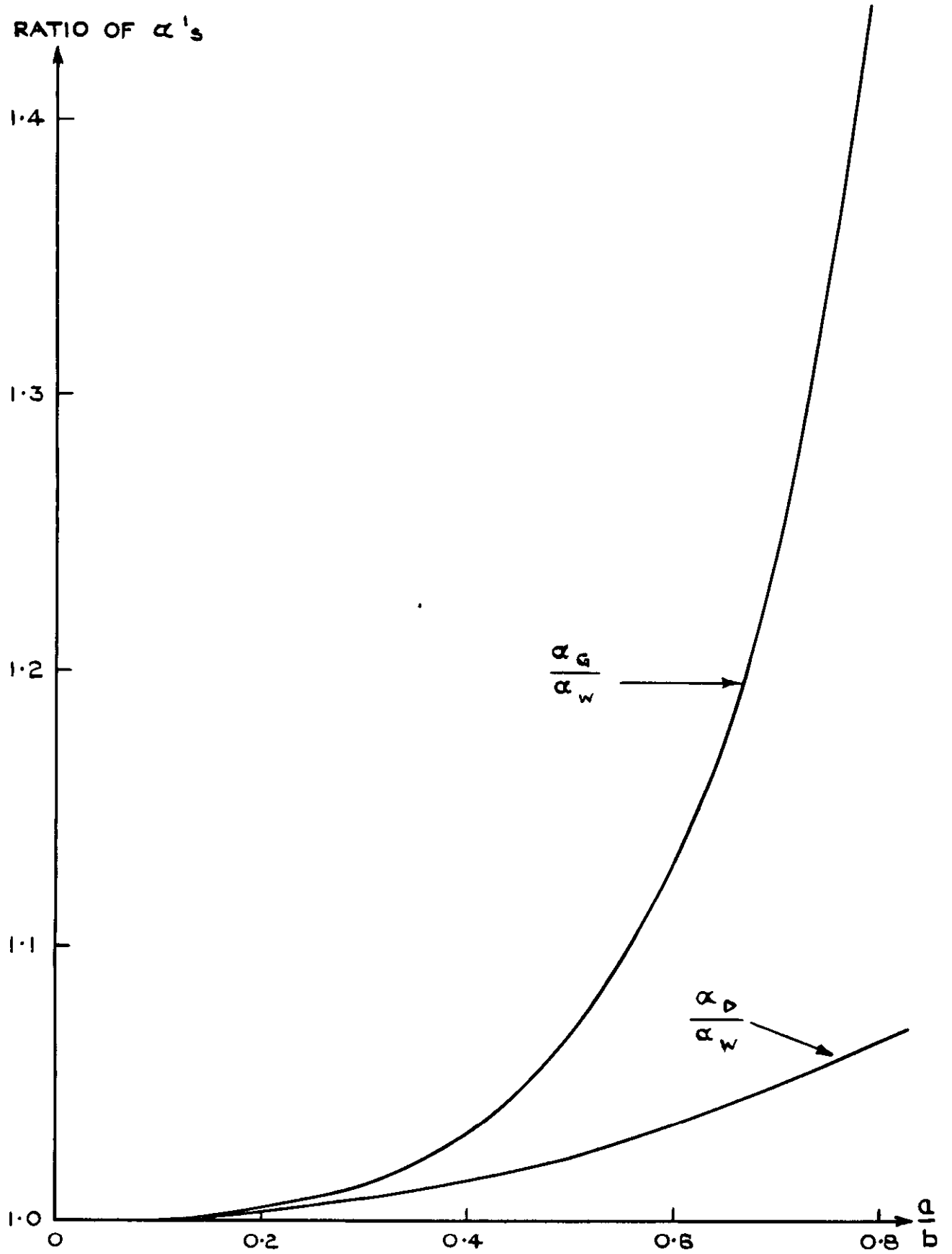

FIG. 4 COMPARISON OF VARIOUS FINITE WIDTH CORRECTIONS
(α_W WESTERGAARD, α_G GREENSPAN, α_D DIXON)

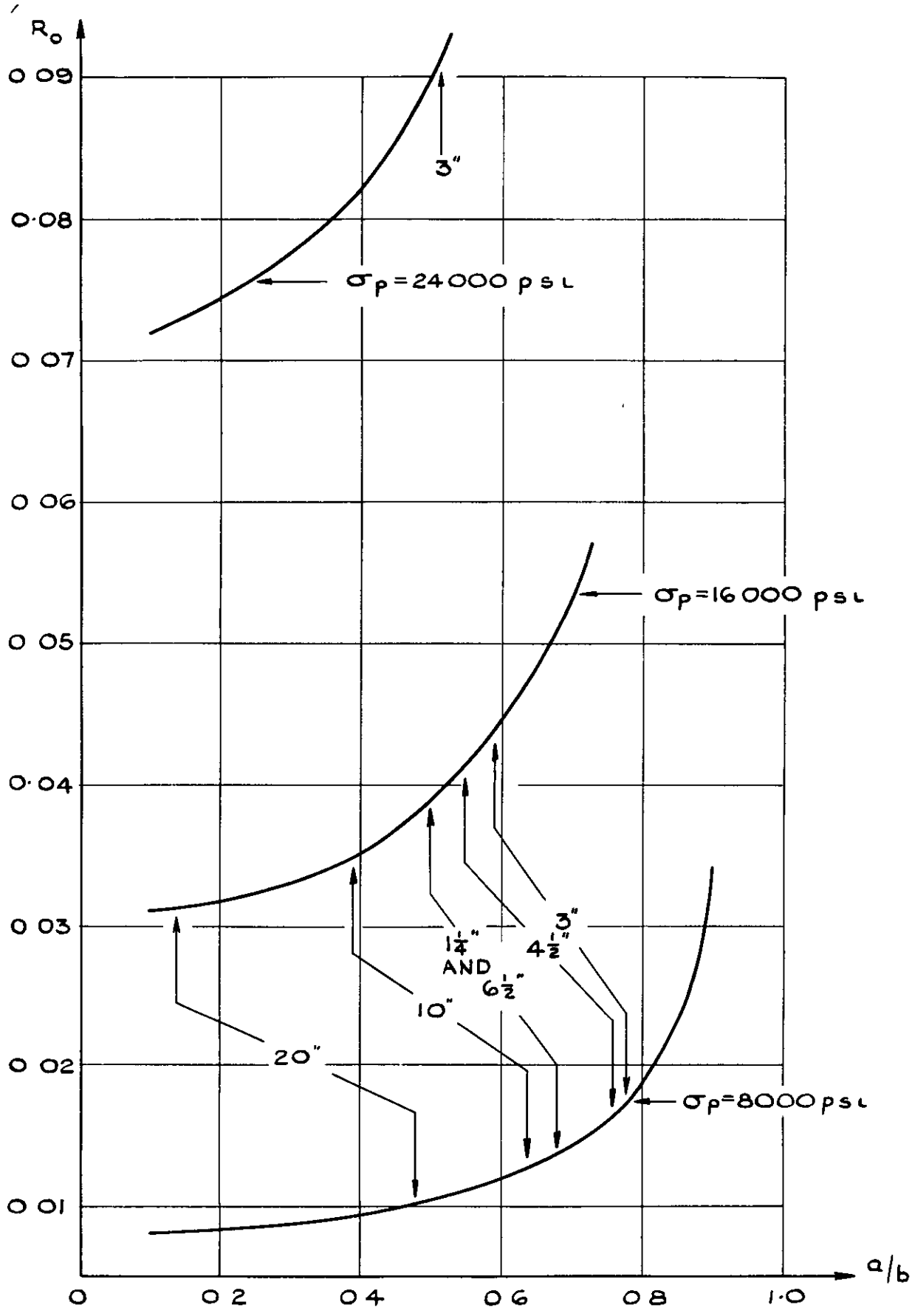

FIG.5. RATIO OF VON MISES YIELD ZONE AHEAD OF CRACK TO CRACK HALF-LENGTH VS. a/b
(ARROWS INDICATE AVERAGE MAXIMUM EXPERIMENTAL CRACK-LENGTHS)

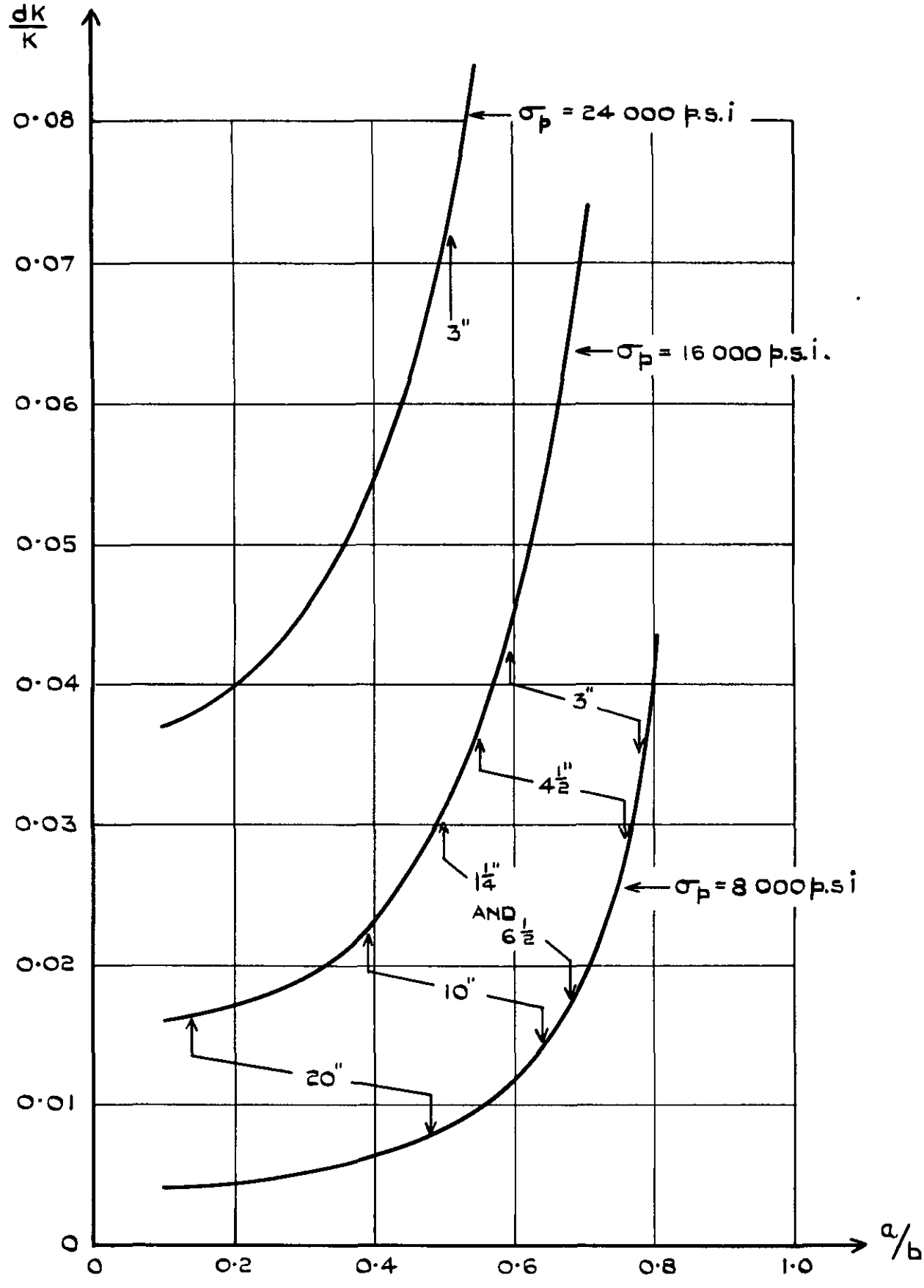

FIG. 6. CORRECTION TO K DUE TO PLASTICITY vs a/b
(ARROWS INDICATE AVERAGE MAXIMUM EXPERIMENTAL CRACK LENGTHS)

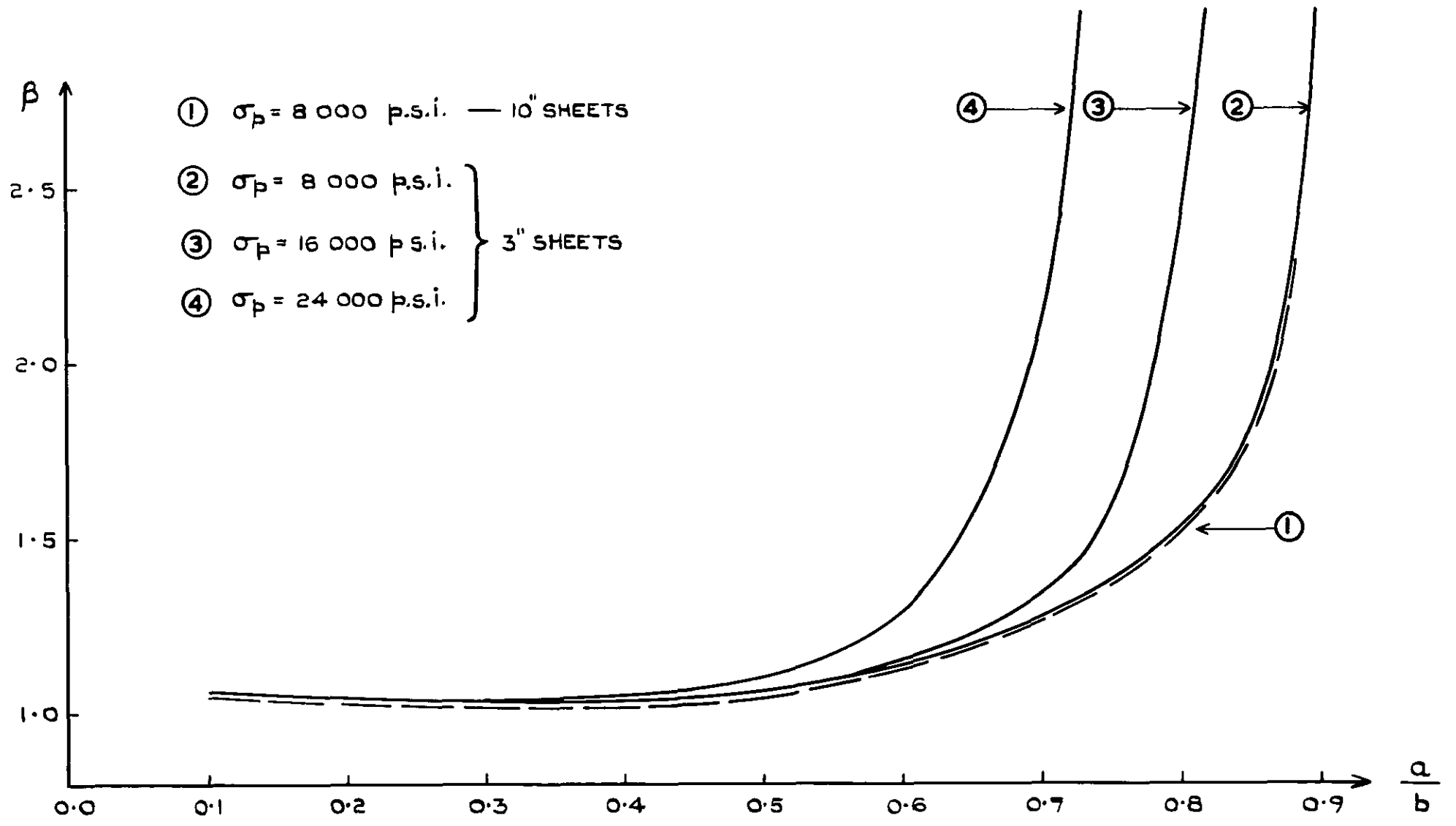

FIG. 7 COMPARISON OF ϵ_c WITH K AS A FUNCTION OF CRACK - LENGTH

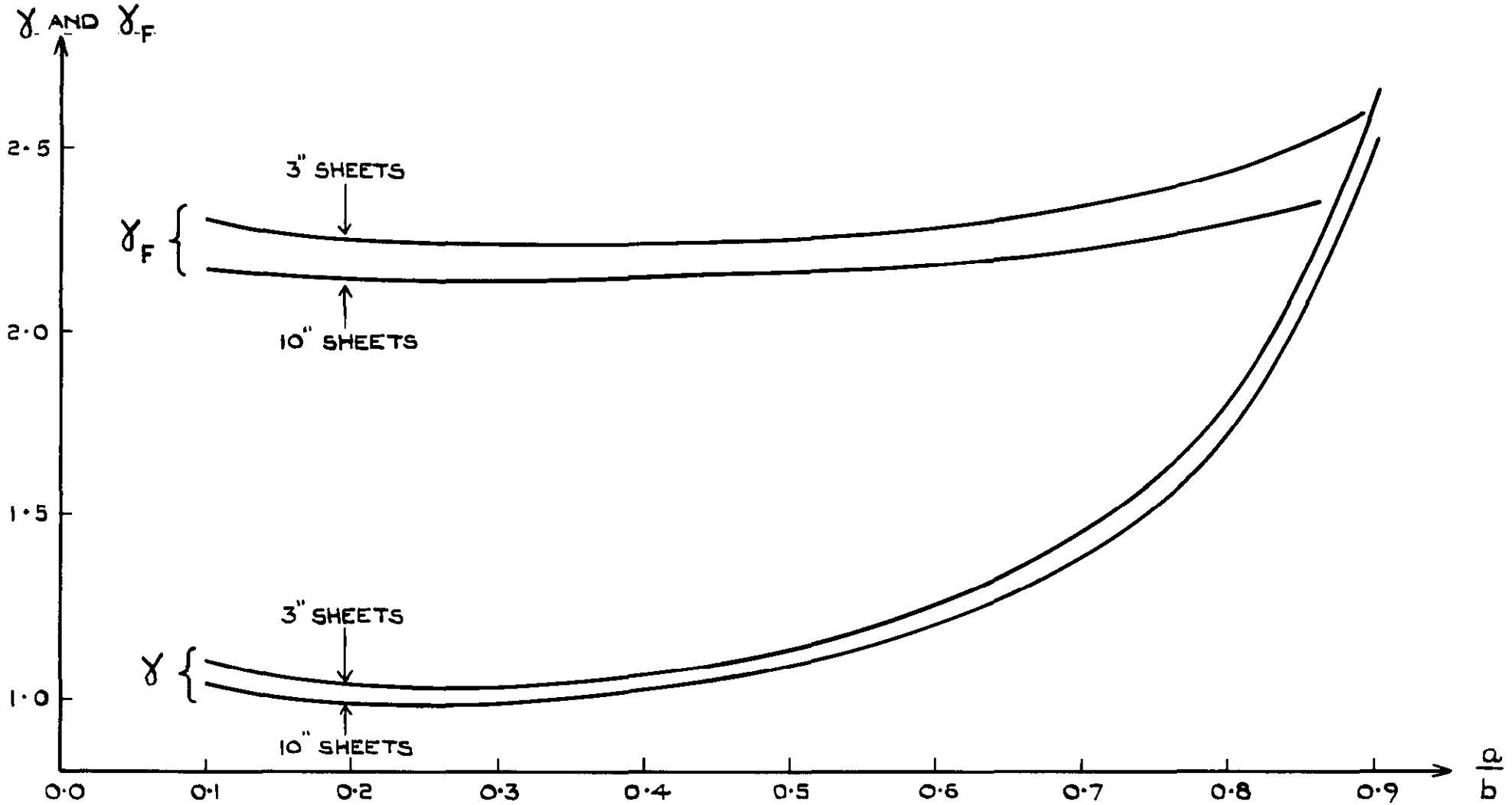

FIG. 8. COMPARISON OF $(K_{TN}\,\sigma_n)$ WITH K AS A FUNCTION OF CRACK-LENGTH

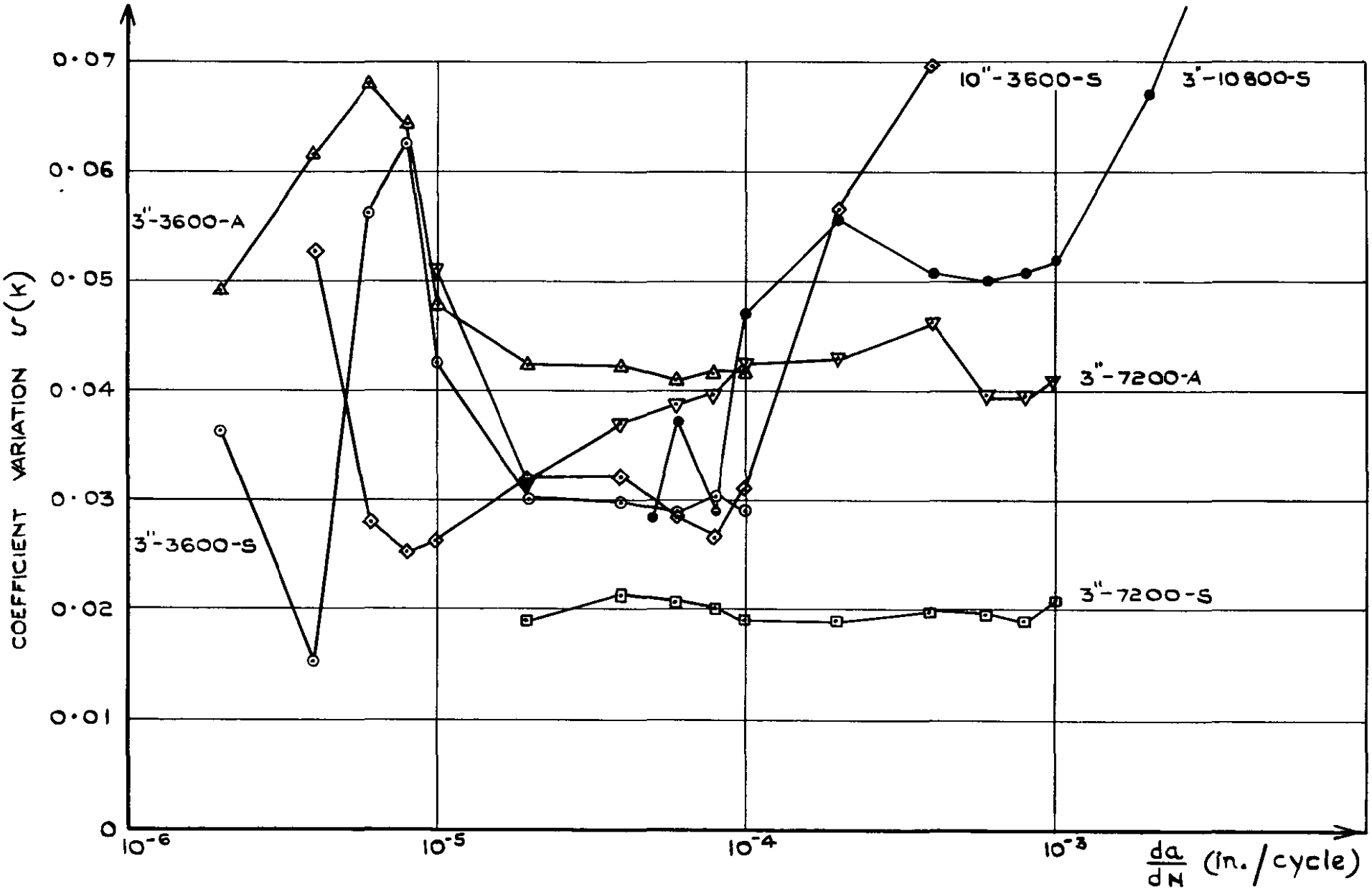

FIG. 9. VARIATION IN K AT DIFFERENT CRACK GROWTH RATES
THE CURVES ARE LABELLED (PANEL WIDTH ALTERNATING STRESS p.s.i - RESULTS ANALYSED)
S = SCATTER TESTS A = ALL TESTS

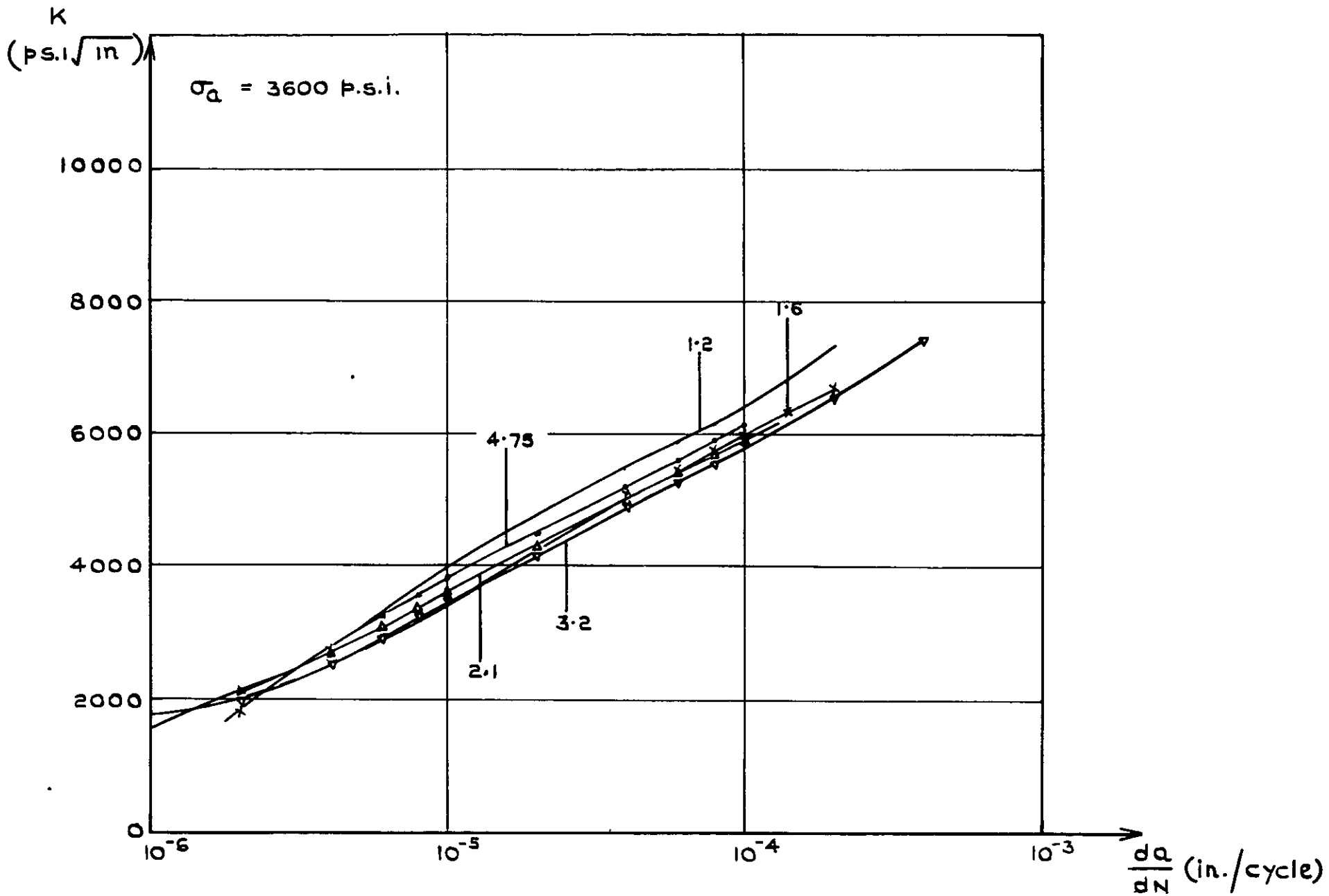

FIG. 10. EFFECT OF LENGTH / WIDTH RATIO IN 3" WIDE PANELS

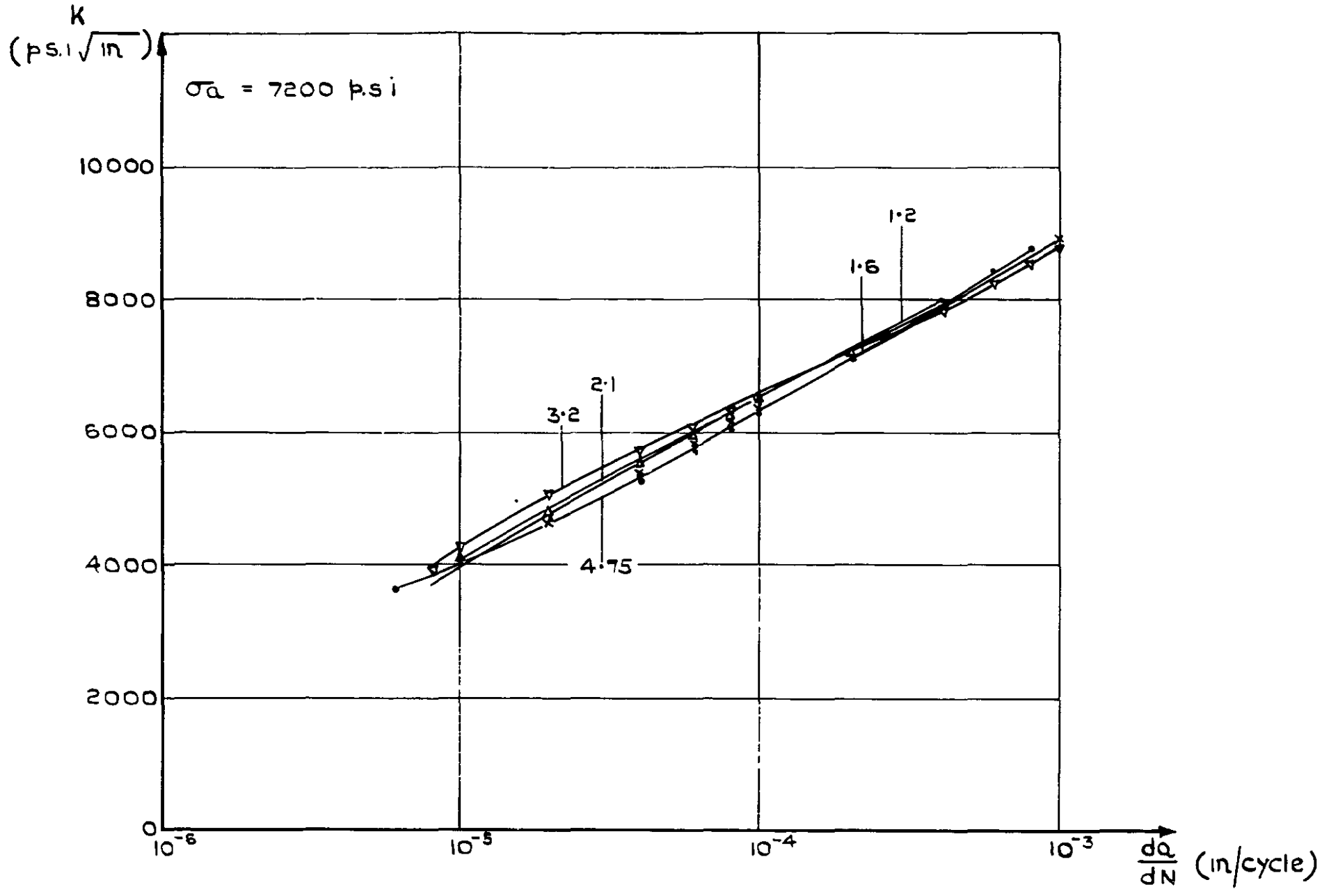

FIG. 11. EFFECT OF LENGTH/WIDTH RATIO IN 3" WIDE PANELS

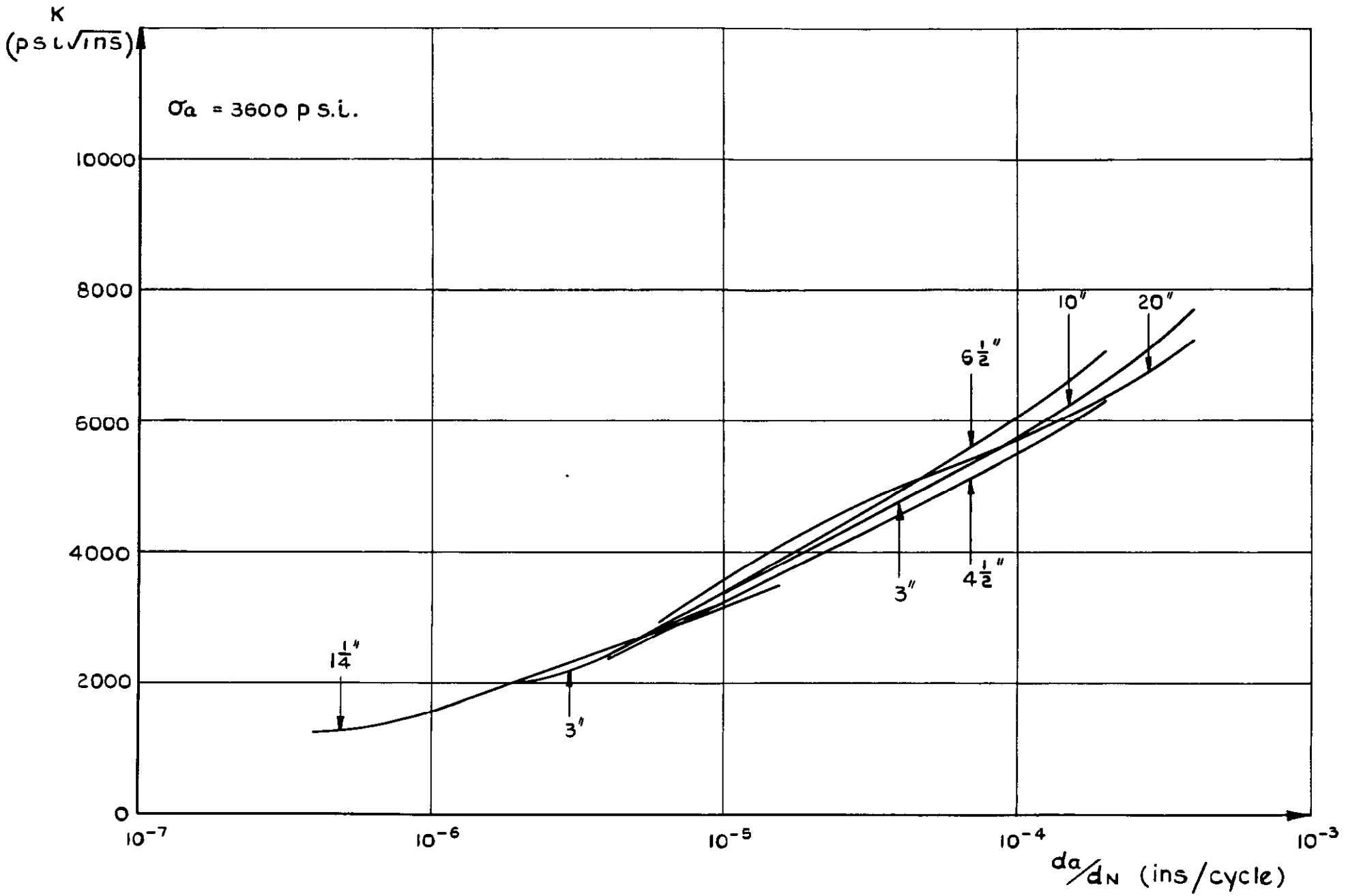

FIG. 12 EFFECT OF PANEL WIDTH

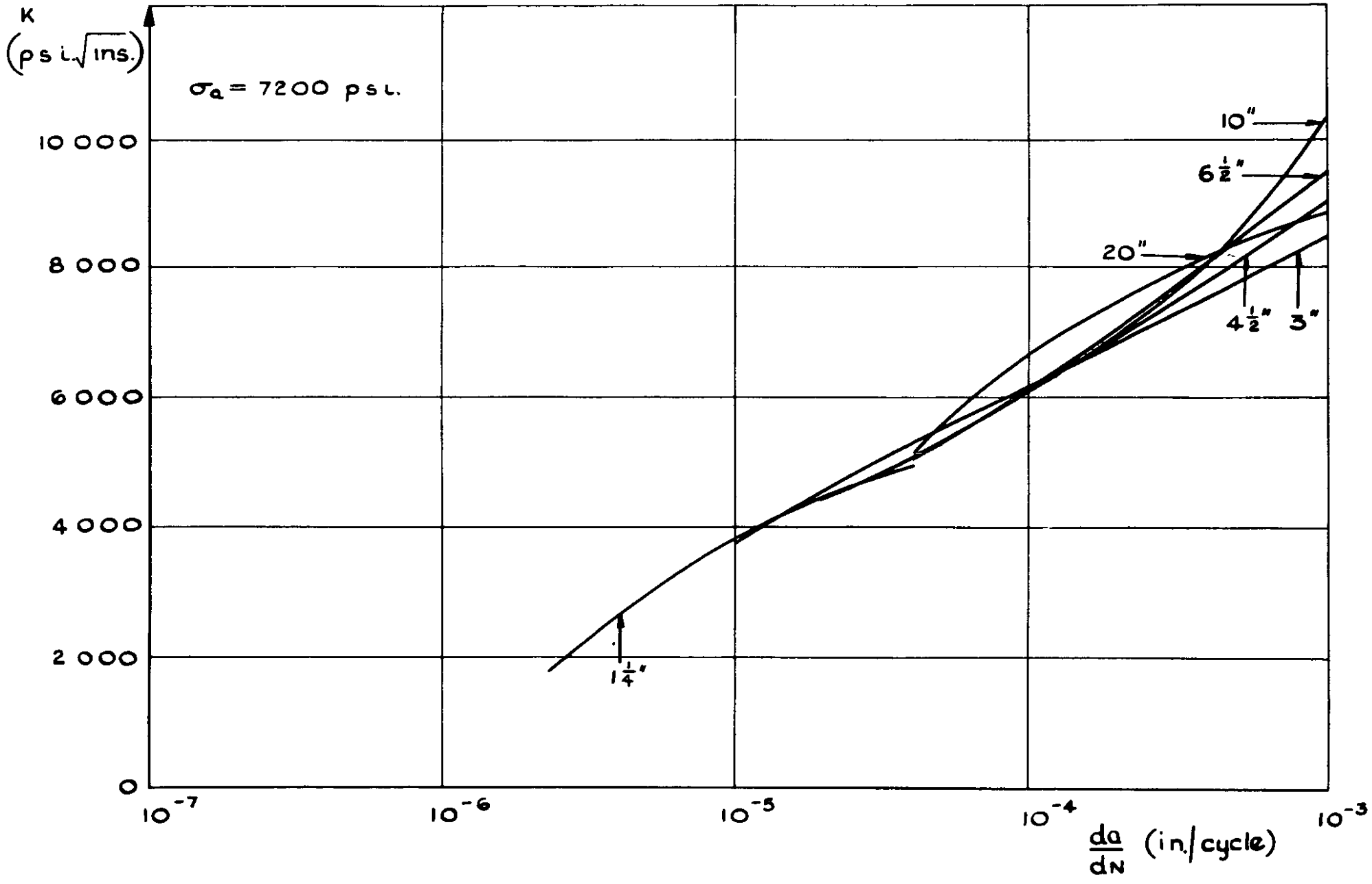

FIG.13. EFFECT OF PANEL WIDTH

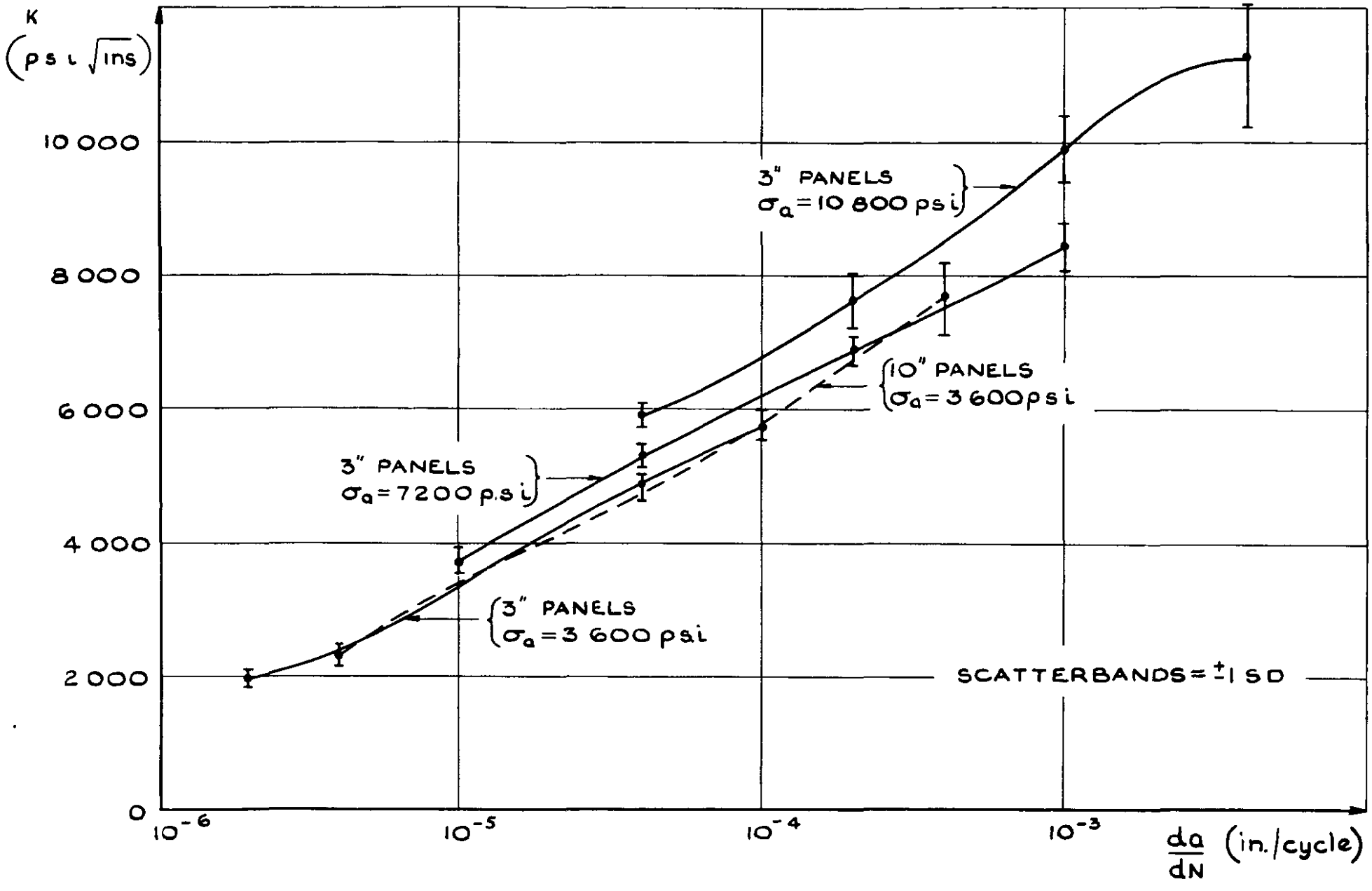

FIG. 14. K vs. da/dN FOR 3" AND 10" PANELS

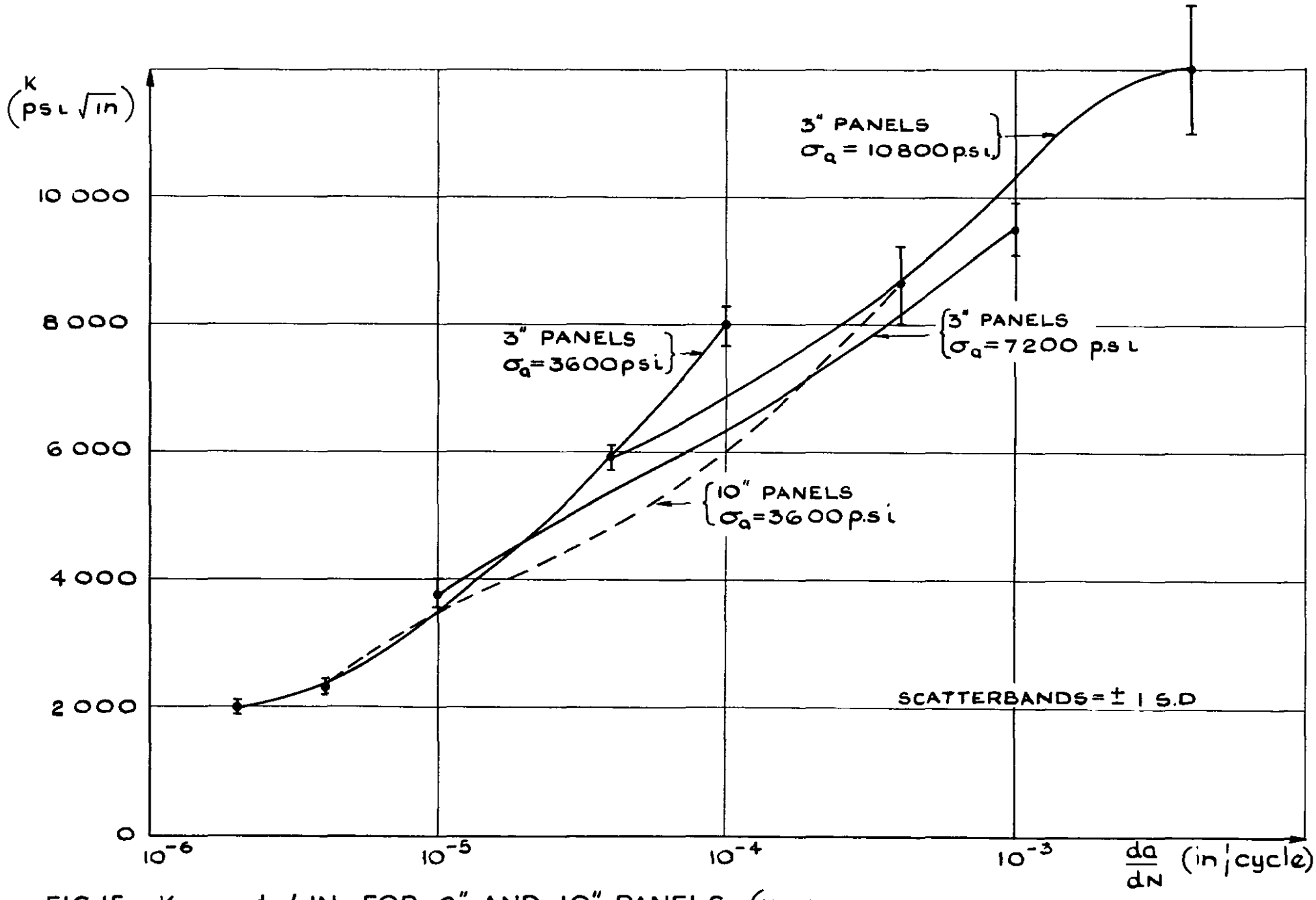

FIG. 15. K vs. da/dN FOR 3" AND 10" PANELS (USING THE α_G FINITE WIDTH CORRECTION)

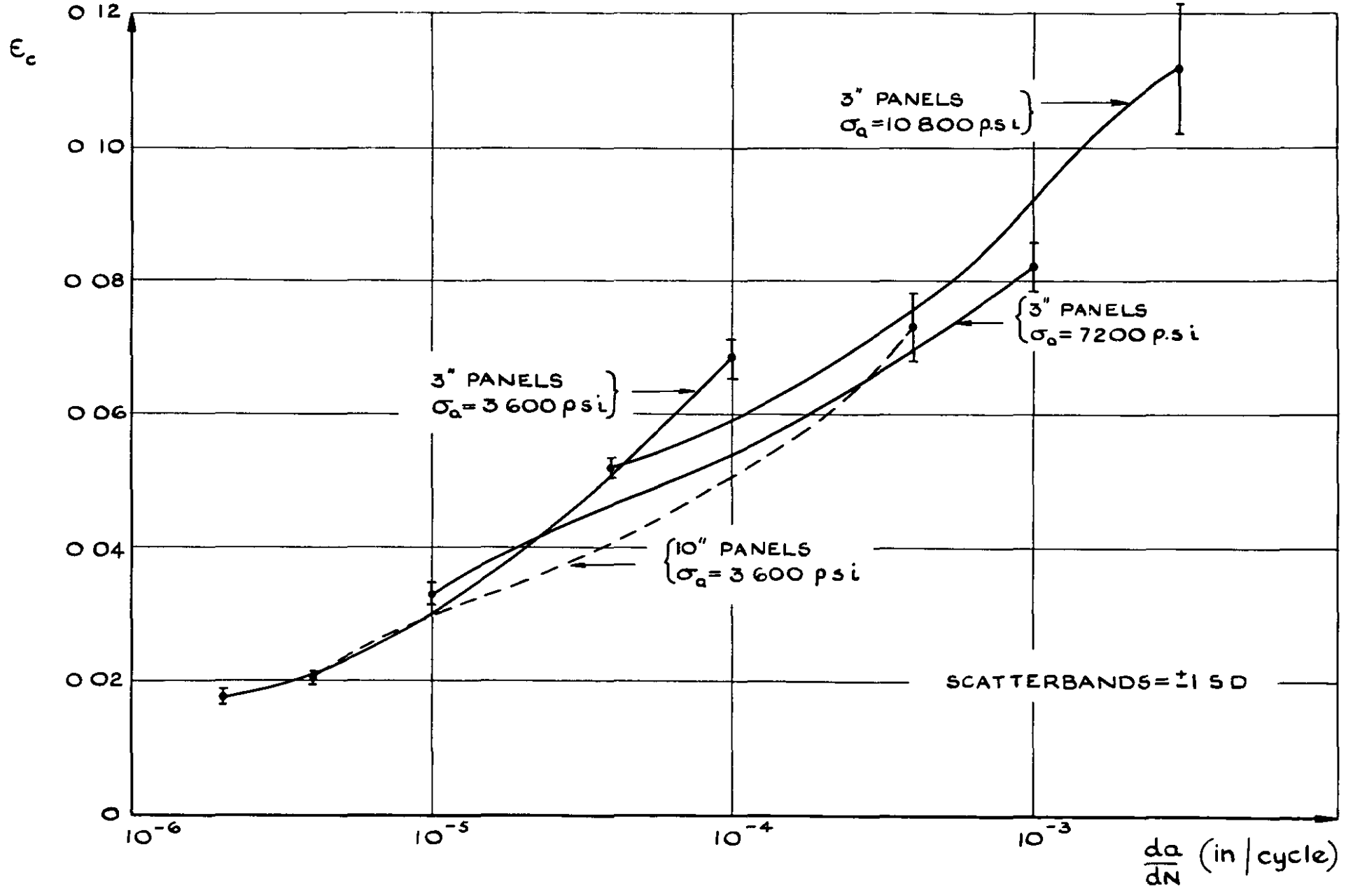

FIG.16. ϵ_c vs. da/dN FOR 3" AND 10" PANELS

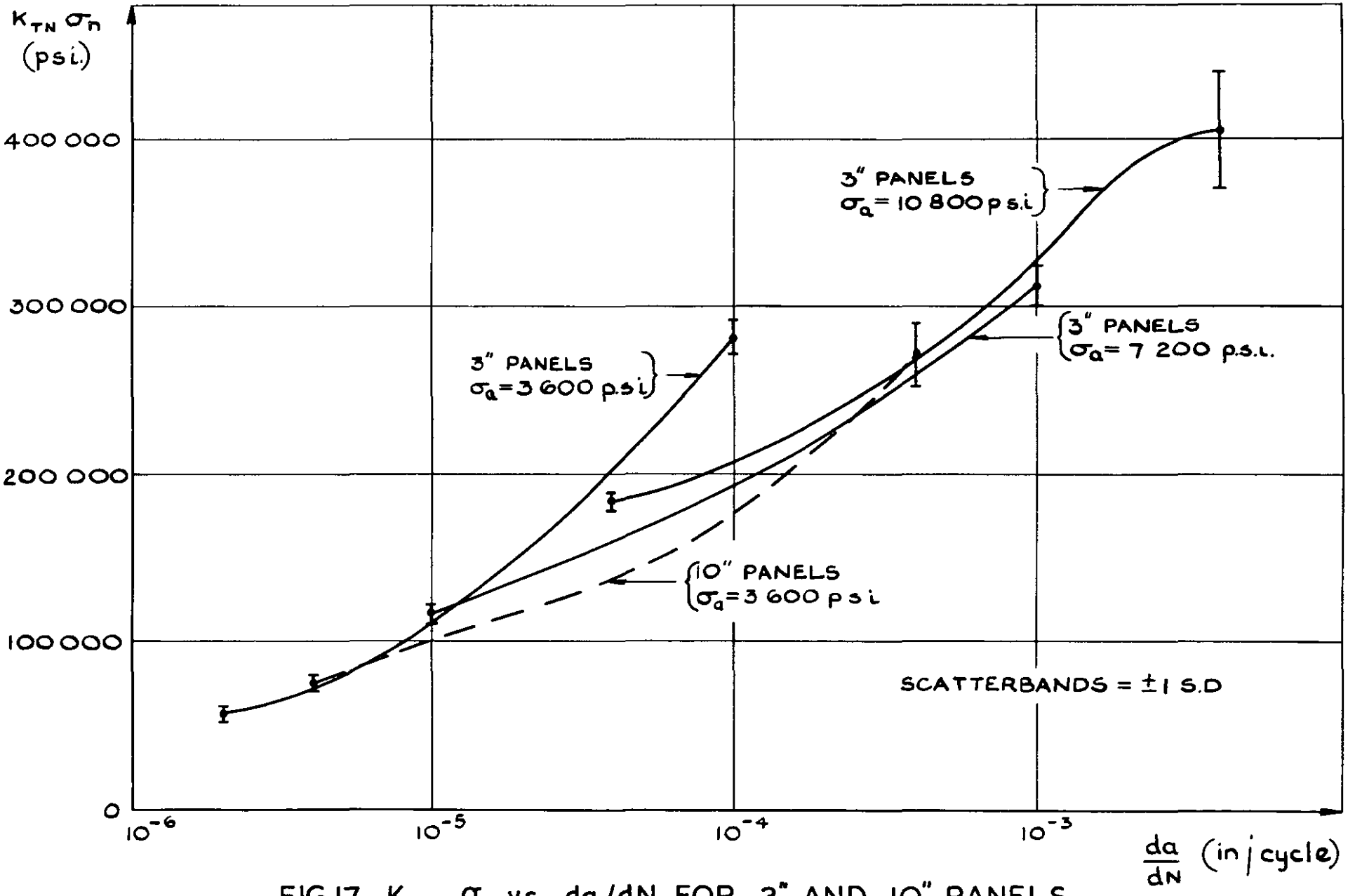

FIG.17. $K_{TN}\,\sigma_n$ vs. da/dN FOR 3" AND 10" PANELS

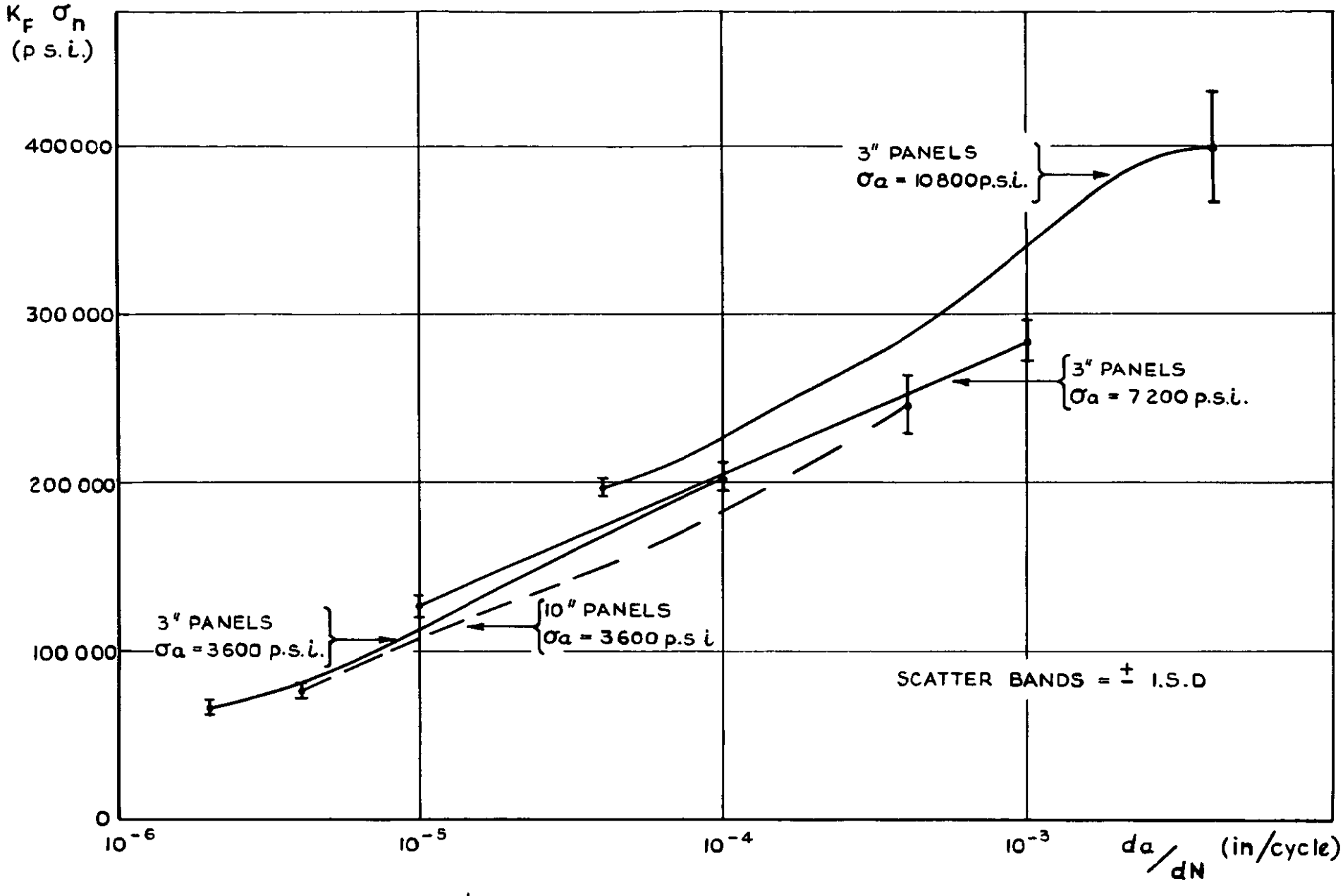

FIG. 18 $K_F\ \sigma_n$ vs. da/dN FOR 3" AND 10" PANELS

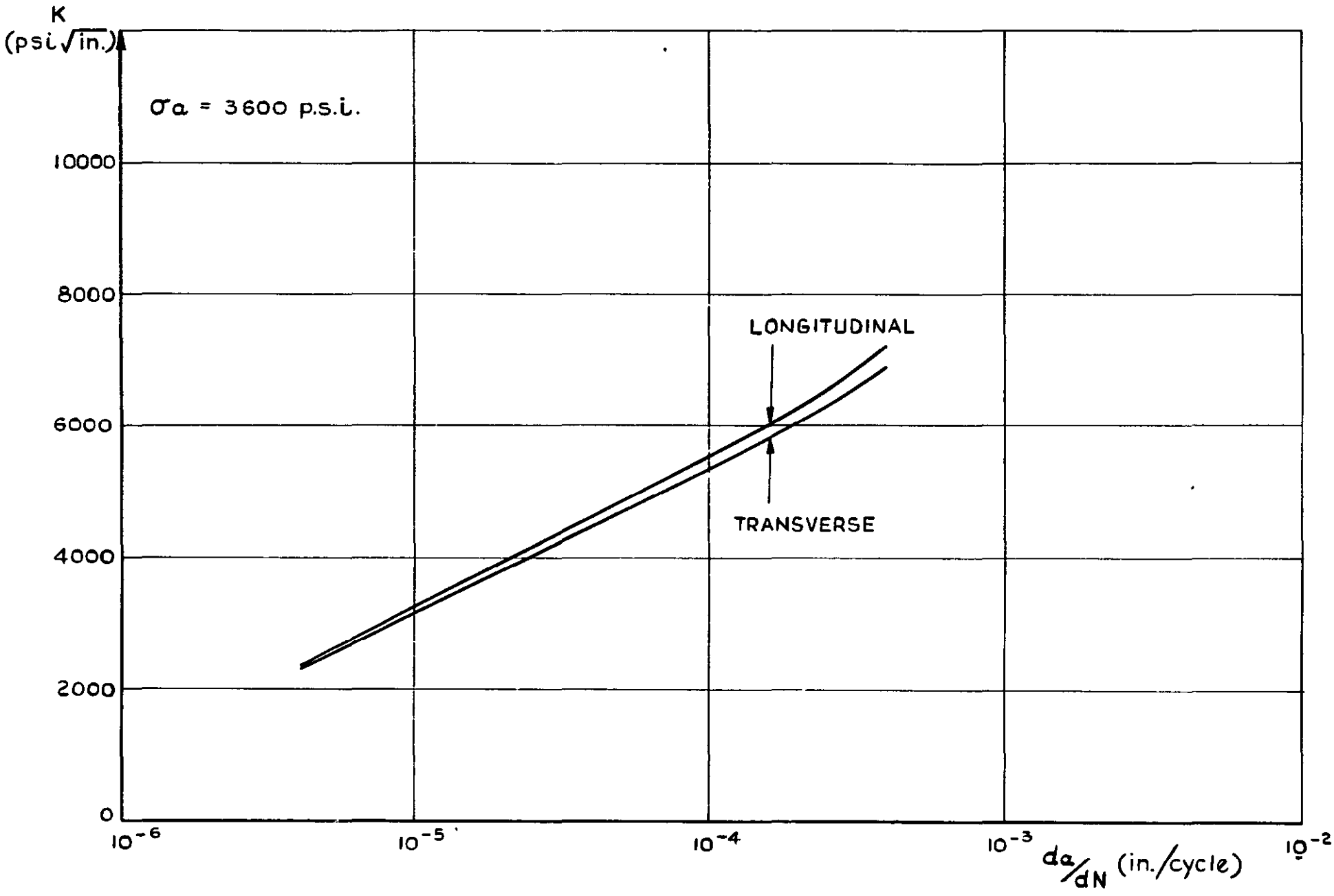

FIG. 19 EFFECT OF DIRECTION OF CRACK PROPOGATION IN $4\frac{1}{2}$" WIDE PANELS

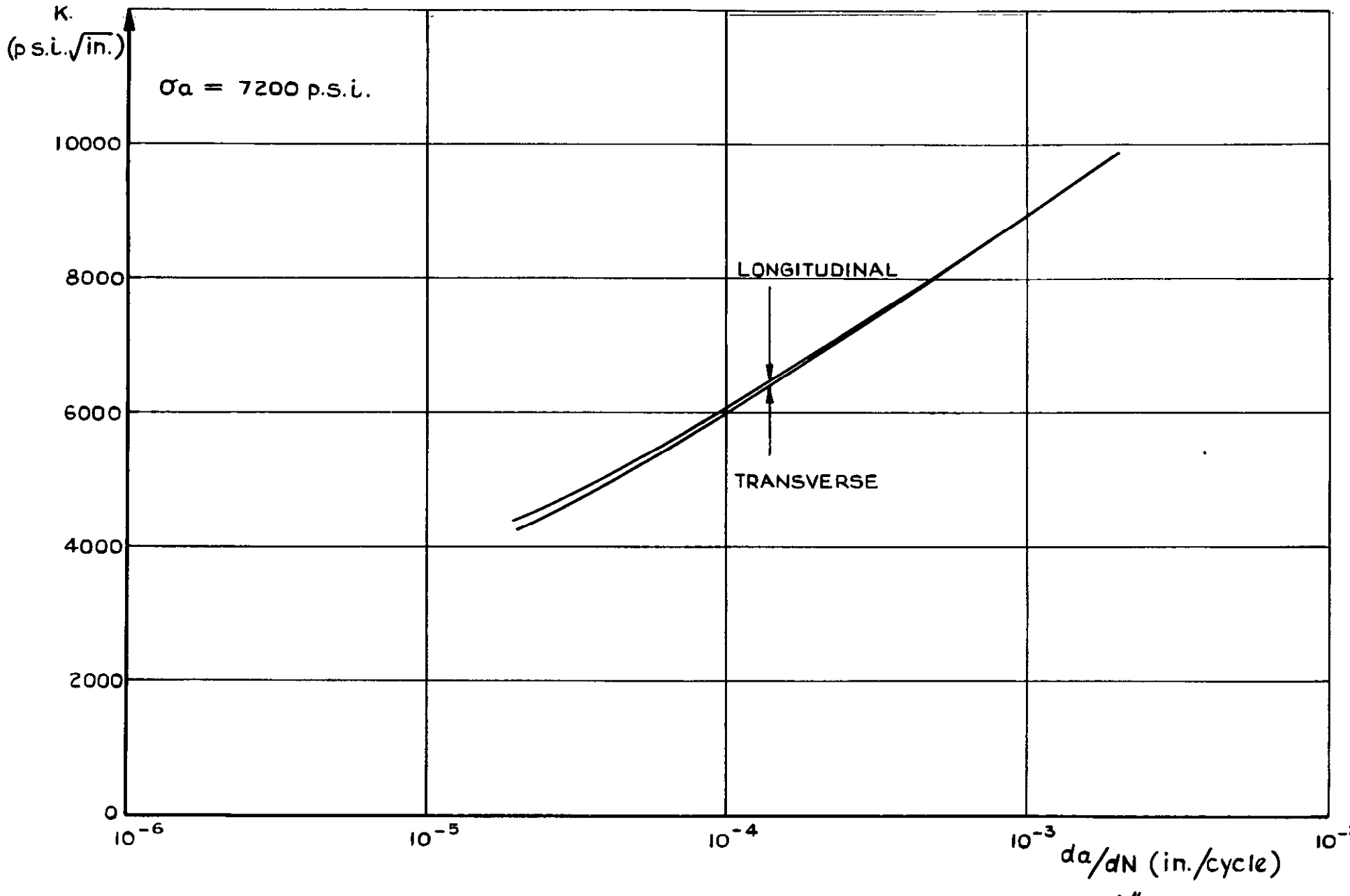

FIG. 20 EFFECT OF DIRECTION OF CRACK PROPAGATION IN $4\frac{1}{2}$" WIDE PANELS

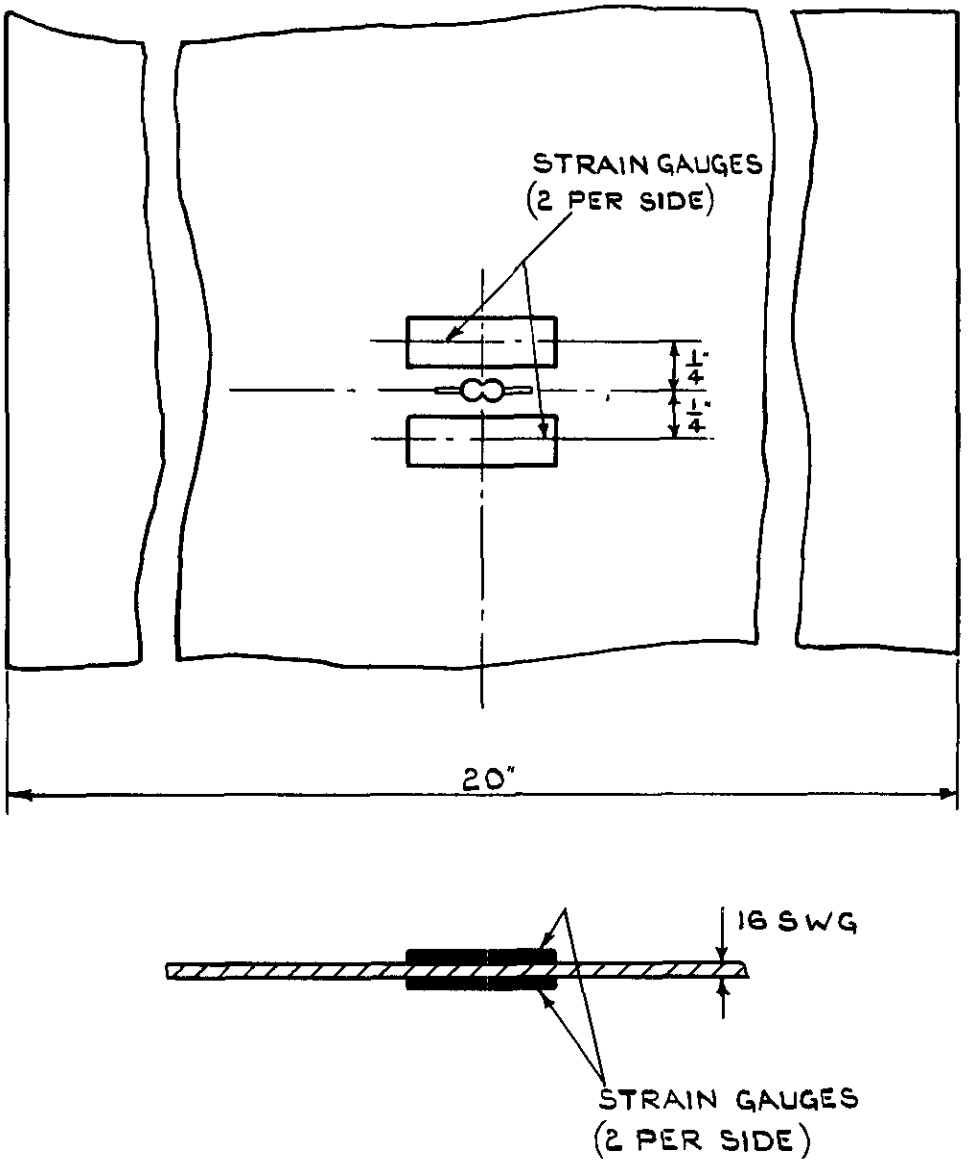

FIG. 21 POSITION OF THE 4 STRAIN GAUGES TO MEASURE BUCKLING IN A 20" WIDE PANEL

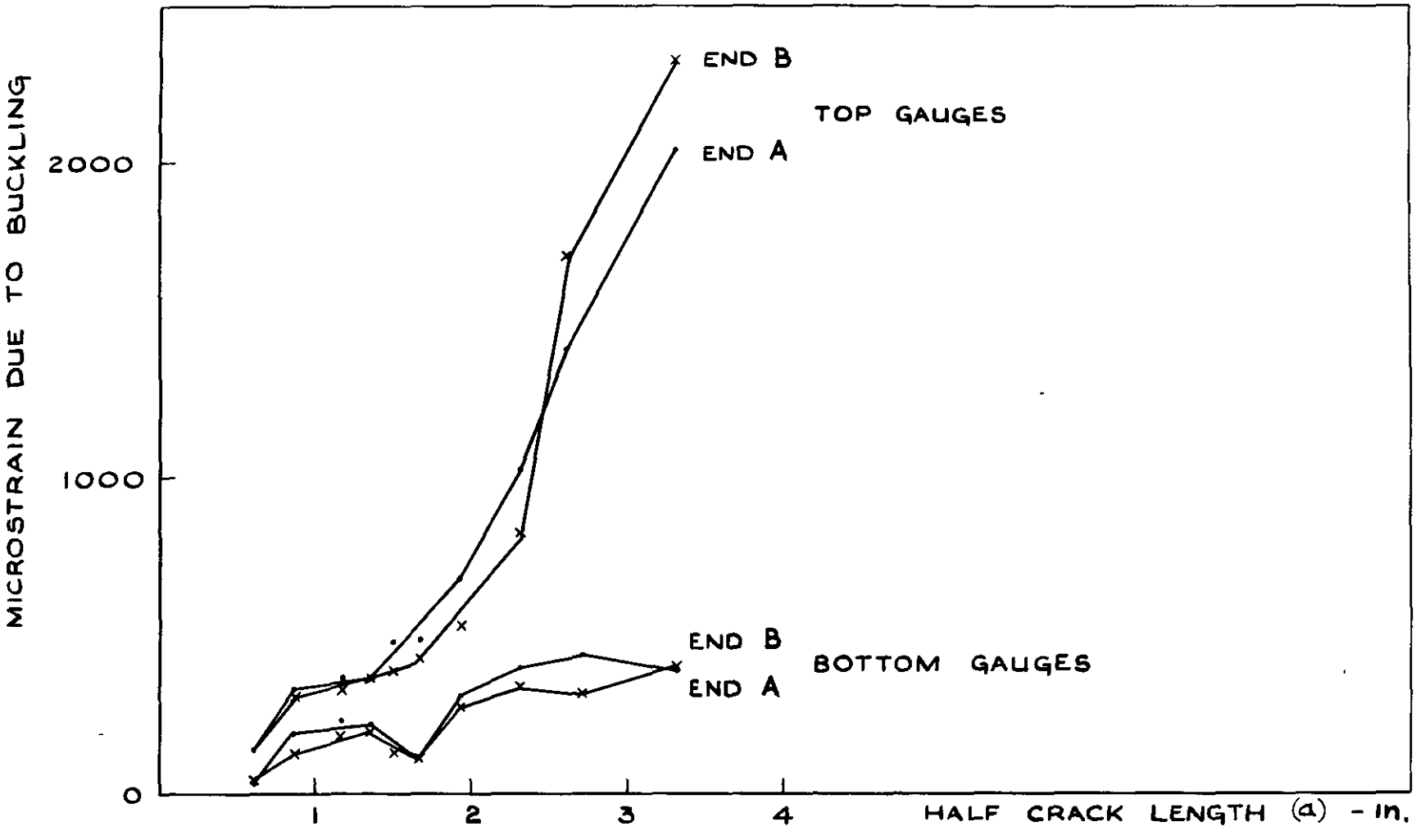

FIG. 22. BUCKLING STRAIN IN A 20" PANEL WITHOUT ANTI-BUCKLE BARS

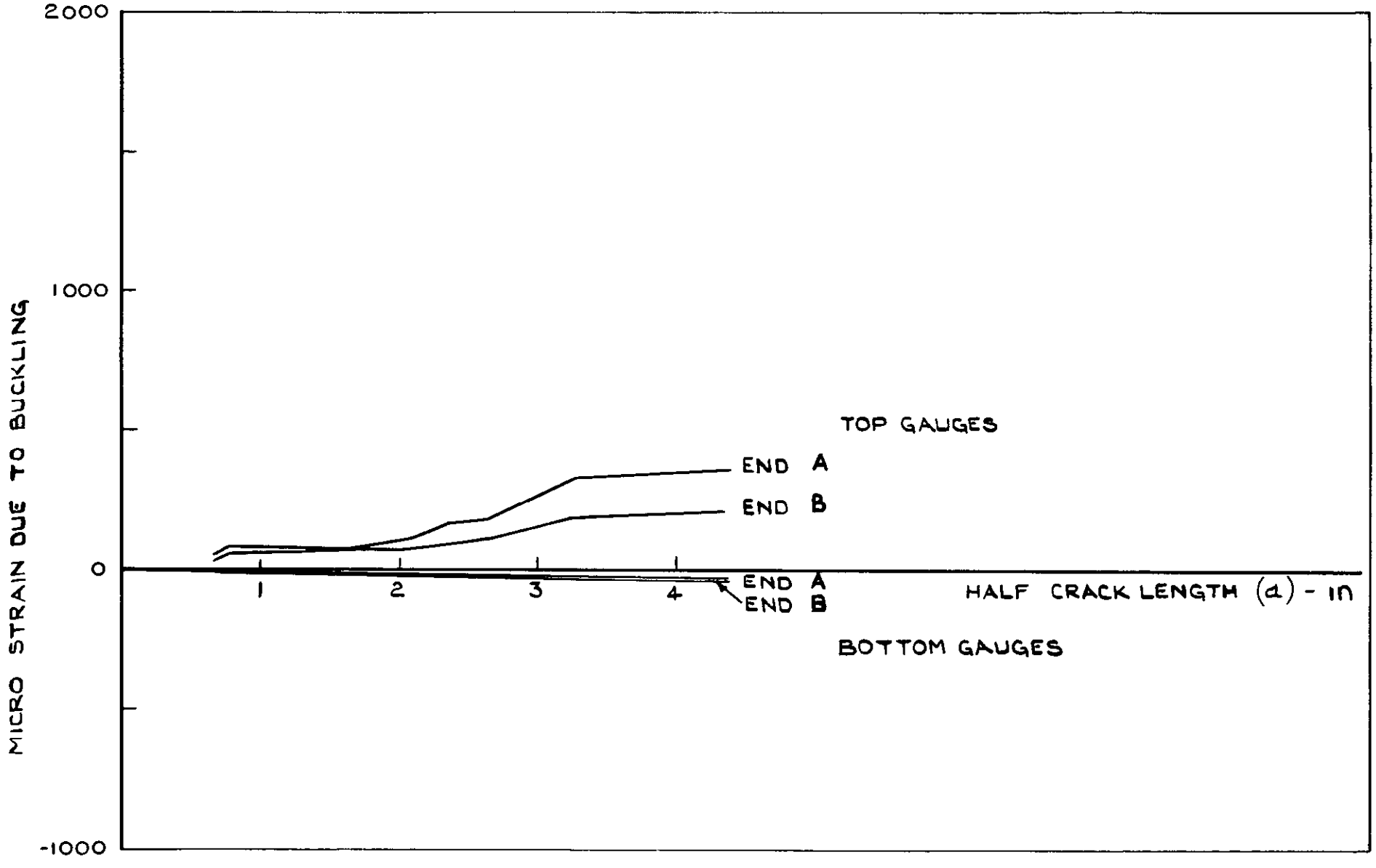

FIG. 23 BUCKLING STRAIN IN A 20" PANEL WITH ANTI-BUCKLE BARS

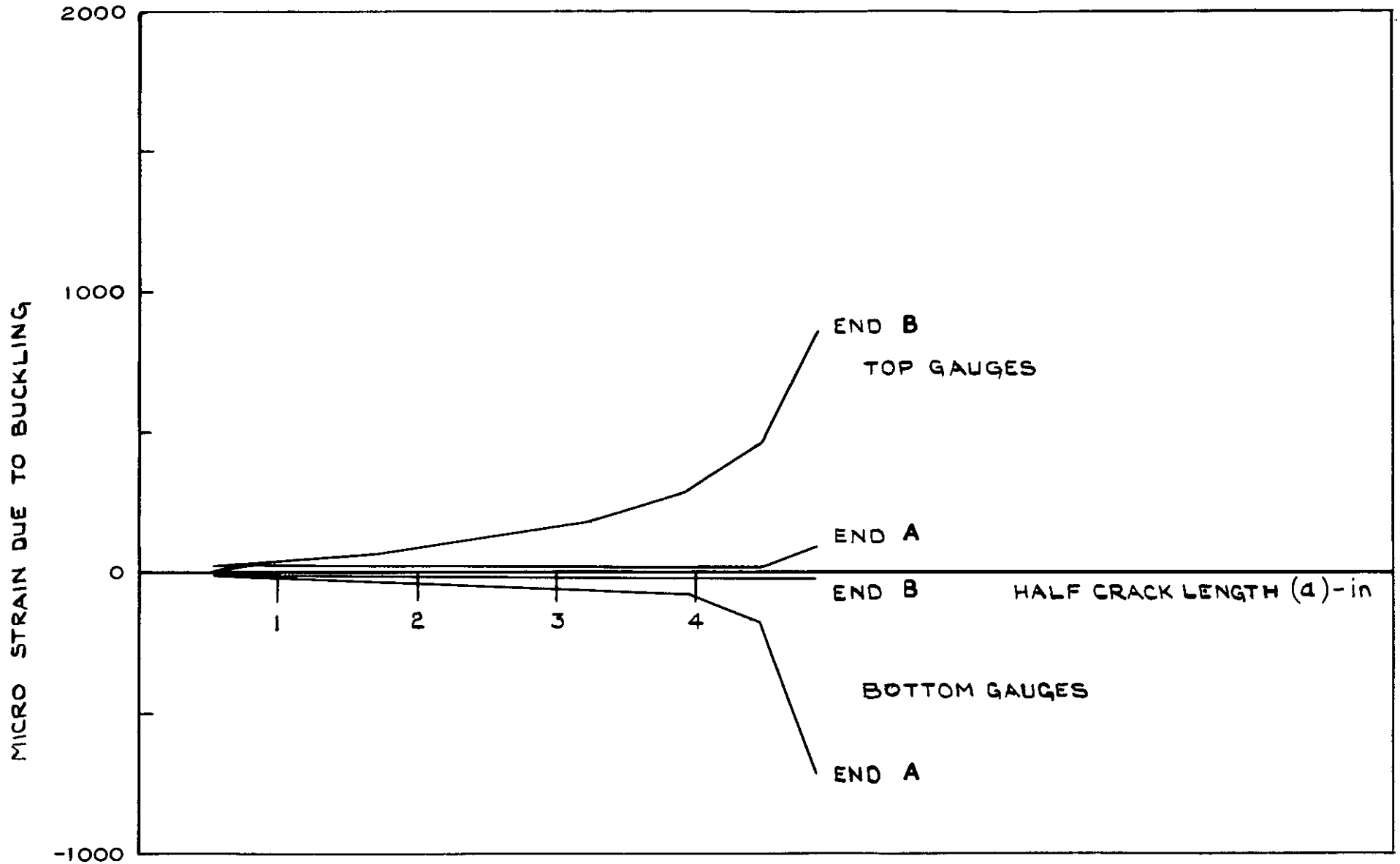

FIG 24 BUCKLING STRAIN IN A 20" PANEL WITH ANTI-BUCKLE BARS

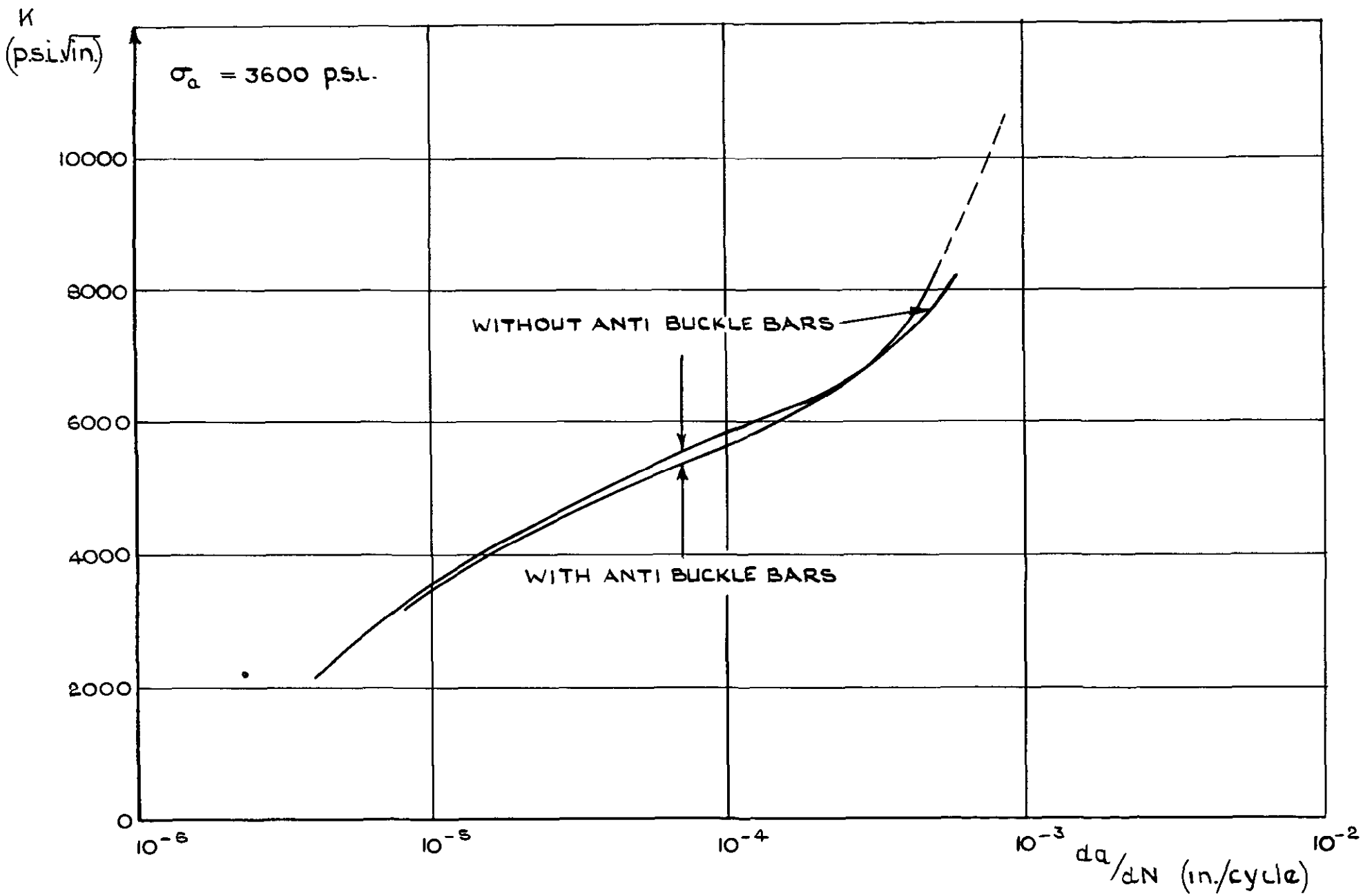

FIG 25 EFFECT OF BUCKLING IN 20" WIDE PANELS

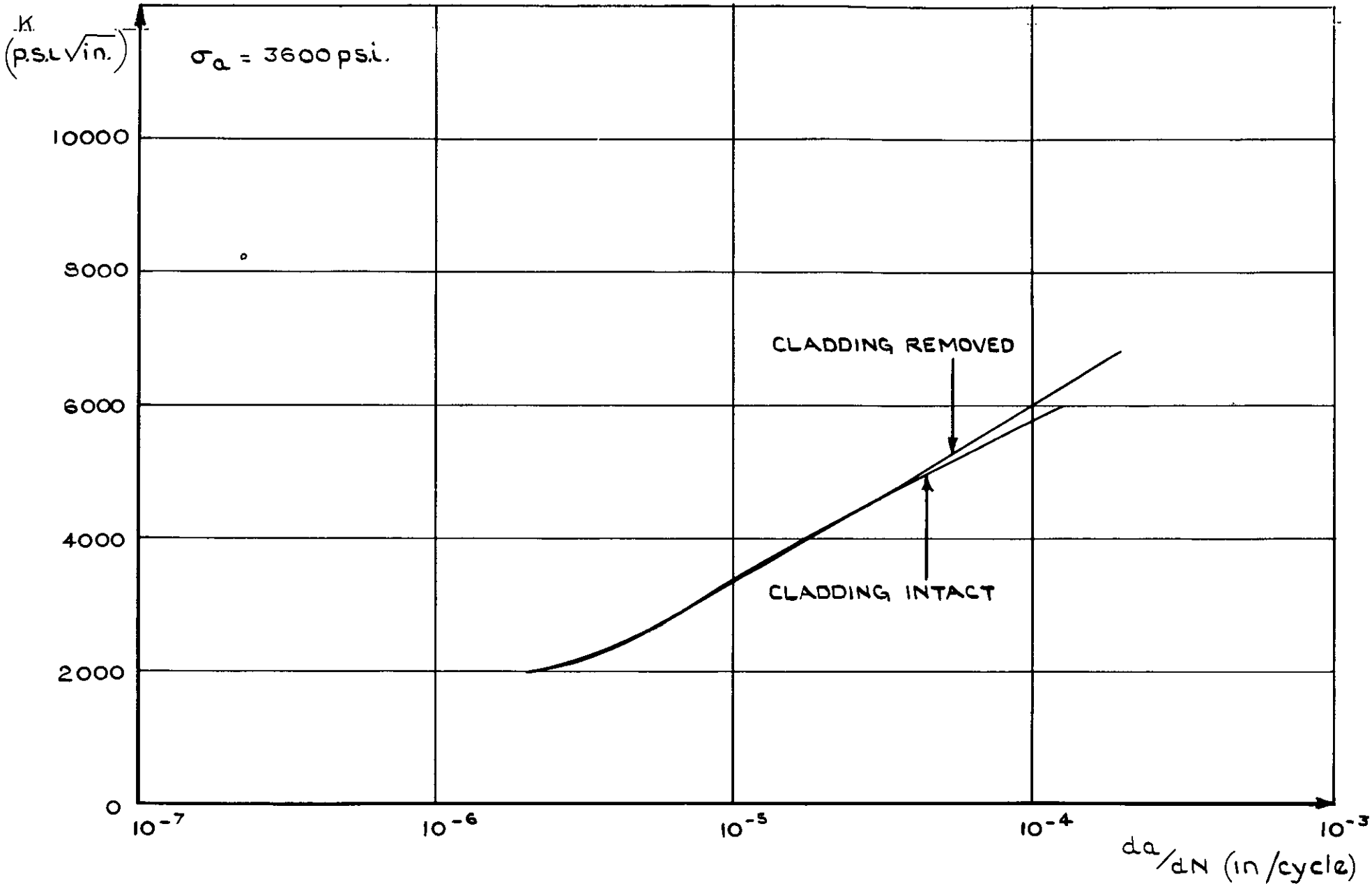

FIG 26 EFFECT OF CLADDING ON 3″ WIDE PANELS

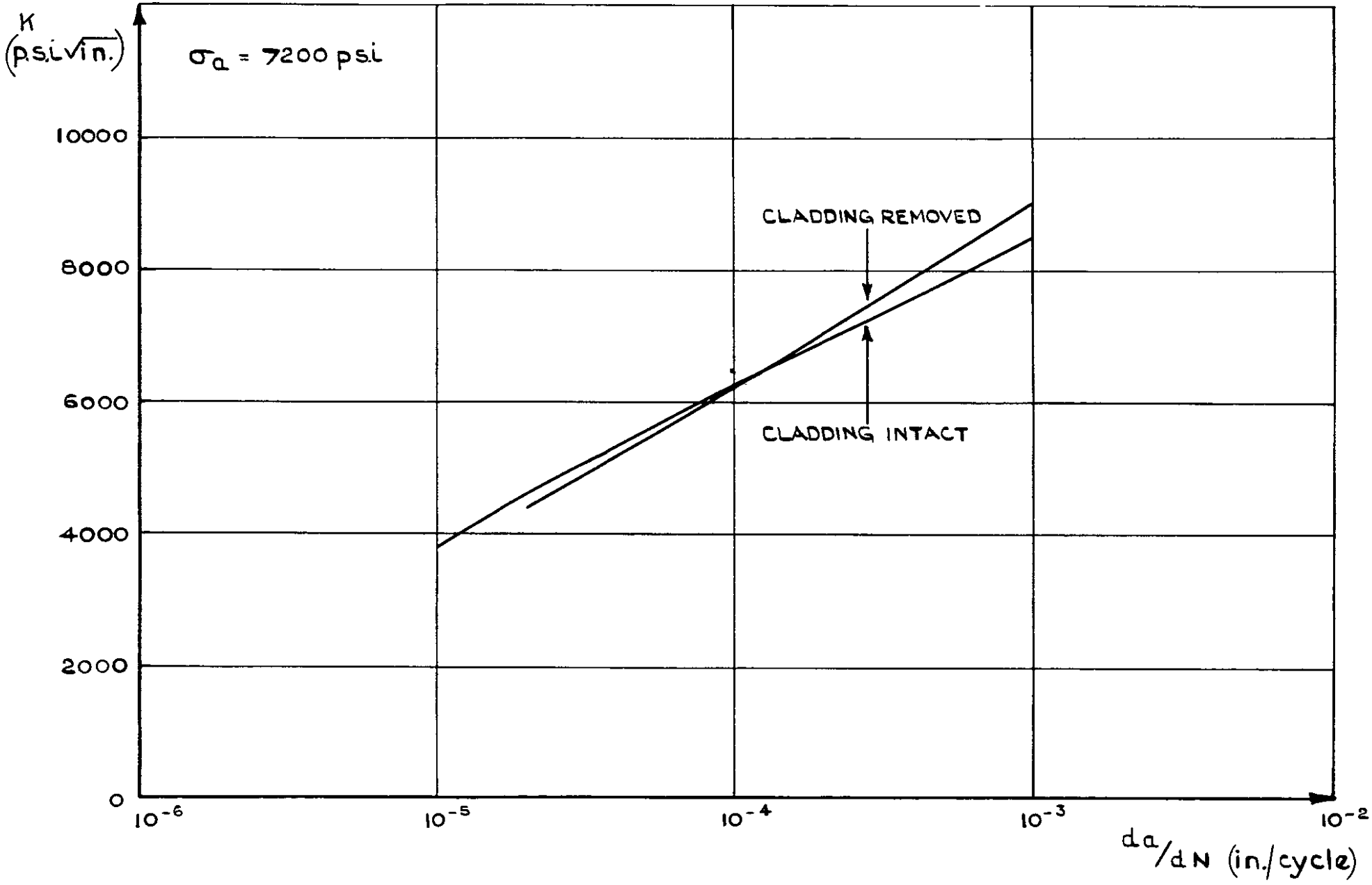

FIG 27 EFFECT OF CLADDING ON 3"WIDE PANELS

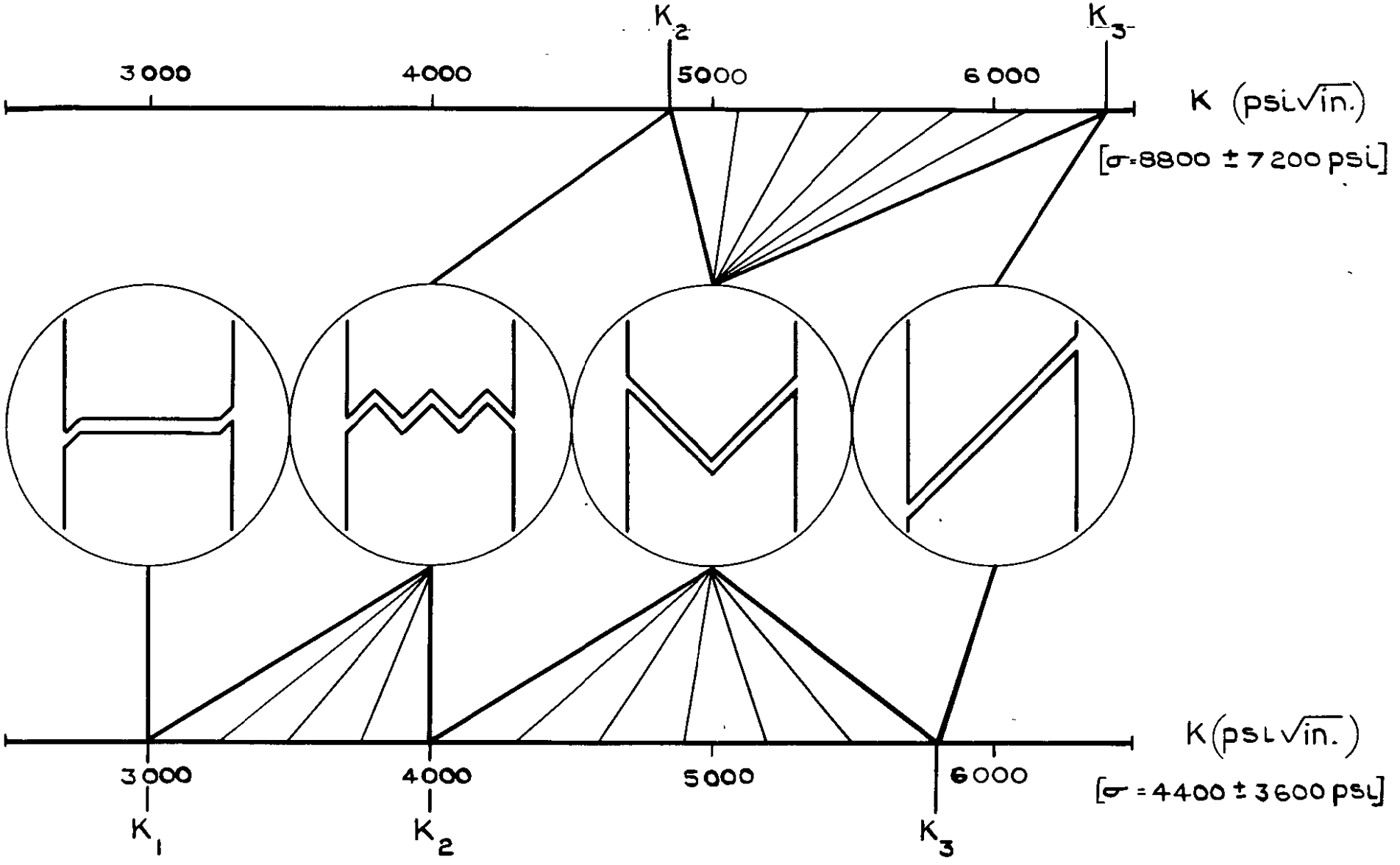

FIG 28 SCHEMATIC REPRESENTATION OF FRACTURE SURFACE

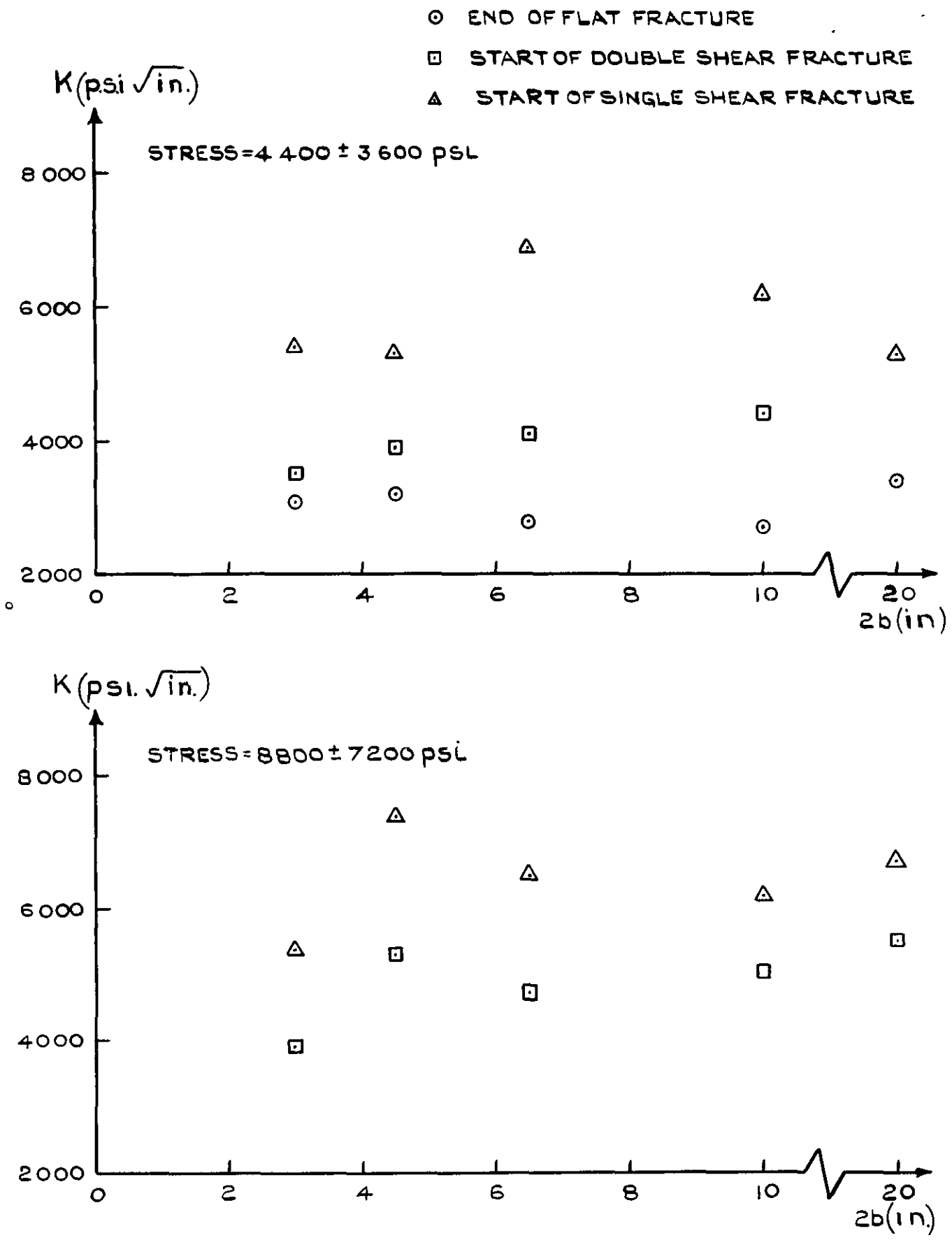

FIG 29 K-VALUES AT WHICH FRACTURE MODE TRANSITIONS OCCUR AT VARIOUS PANEL WIDTHS

Printed in England for Her Majesty's Stationery Office by the Royal Aircraft Establishment, Farnborough Dd 125875 K.4.

Published by
HER MAJESTY'S STATIONERY OFFICE
To be purchased from
49 High Holborn, London W.C 1
423 Oxford Street, London W 1
13A Castle Street, Edinburgh 2
109 St Mary Street, Cardiff
Brazennose Street, Manchester 2
50 Fairfax Street, Bristol 1
35 Smallbrook, Ringway, Birmingham 5
80 Chichester Street, Belfast 1
or through any bookseller

S.O. CODE No. 23-9016-96